DEVELOPMENT AND CHARACTERIZATION OF MICROSCALE SAMPLERS COUPLED TO HPLC FOR NEAR REAL-TIME REACTION MONITORING

by

Claire Nichole Chisolm

A dissertation submitted in partial fulfillment
of the requirements for the degree of
Doctor of Philosophy
(Chemistry)
in The University of Michigan
2010

Doctoral Committee:

Professor Robert T. Kennedy, Chair
Professor Michael D. Morris
Professor Edward T. Zellers
Associate Professor Shuichi Takayama

To my family, for your support and encouragement
through all the vicissitudes of life

ACKNOWLEDGMENTS

I would first like to thank my advisor, Dr. Robert T. Kennedy, for his support and guidance over the last six years. I would also like to thank Dr. Michael Morris, Dr. Ted Zellers, Dr. Shuichi Takayama, and Dr. Brian Coppola, for their willingness to serve on my committee as well as their advice and encouragement. This dissertation would have not been completed without the assistance of my lab mates. I am grateful to them for always being willing to brainstorm ideas, provide encouragement, and commiserate when things did not go as planned. I would like to especially thank Dr. Kendra Reid Evans for her incredible patience in answering all my questions when I first joined the lab, and her continued friendship.

While completing this dissertation, I have enjoyed several fruitful collaborations. I would like to thank our collaborators at Pfizer Global Research for their input and ideas. I would like to particularly thank Dr. Frederick Antosz for his assistance in editing this manuscript and his insight into the pharmaceutical industry. I would also like to extend my appreciation to my collaborators in Dr. Gary Smith and Dr. Shuichi Takayama's lab, particularly Dr. Charles Bormann. I would also like to thank my colleagues at Assay Designs, particularly Rory Olson, for teaching me about immunoassay development.

Finally, I am incredibly grateful for the love and support of my friends and family. I am thankful for the never-ending support from my parents, Brannan Chisolm and Dr. Stephanie Chisolm, and from my sisters, Kate Chisolm and Caroline Chisolm. I would also like to thank my friends, particularly Dr. Jason Spruell, Beth Bigelow and Dara Strickland, for their understanding and support while I completed graduate school.

TABLE OF CONTENTS

LIST OF FIGURES

Figure

LIST OF TABLES

Table

LIST OF APPENDICES

Appendix

LIST OF ABBREVIATIONS

API	Active pharmaceutical ingredient
BFC	Blue food color
CE	Capillary electrophoresis
cGMP	Current good manufacturing practices
DBP	Dibutyl phthalate
FDA	United States Food & Drug Administration
FIA	Flow injection analysis
GC	Gas chromatography
HPLC	High-performance liquid chromatography
HRP	Horseradish peroxidase
HTLC	High-temperature liquid chromatography
ID	Inner diameter
kg	Kilogram
L	Liter
MD	Microdialysis
m	Meter
mL	Milliliter
mm	Millimeter
mM	Millimolar

mU	Milliunits
NEFA	Non-esterified fatty acid
OD	Outer diameter
Pa	Pascal
PAT	Process analytical technology
PDMS	Polydimethylsiloxane
PEEK	Polyether ether ketone
PFA	Perfluoroalkoxy
PFD	Perfluorodecalin
PFO	Perfluorooctanol
RP-HPLC	Reversed-phase high pressure liquid chromatography
s	Second
SIA	Sequential injection analysis
SIC	Sequential injection chromatography
µL	Microliter
µm	Micrometer
µM	Micromolar
UPLC	Ultra performance liquid chromatography
µSI-LOV	Micro sequential injection lab-on-valve
USP	United States Pharmacopeia
UV	Ultraviolet
YFC	Yellow food color

ABSTRACT

The ability to sample a chemical reaction mixture on-line and on a continuous basis can lead to a better understanding of the chemical process, resulting in improved yield and quality of product. This is particularly important for the development of active pharmaceutical ingredients (APIs). Two primary areas of improvement needed for near real-time sampling in the pharmaceutical industry are sampling from small-scale reactions (several milliliters), such as may be used during research and development, and sampling from heterogeneous reactions that contain solid particles. For small-scale reactions, a sampling device that removes microliters of the reaction mixture is required. A "push-pull" sampler was constructed from coaxial fused silica capillaries that continuously removes sample from a reactor at low flow rates (μL/min) and mixes the sample rapidly with a quenchant to preserve the reaction conditions before analysis. Finite element analysis showed that reducing the pull capillary ID resulted in faster mixing, while flow rate had a minimal effect on mixing time. This sampler was used with samples spanning a range of viscosities (1.5 – 4.8 Pa•s), and with samples containing spherical polystyrene beads 10 – 500 μm in diameter. The sampler was demonstrated by monitoring an aqueous enzymatic reaction as well as an organic reaction. A "droplet" sampler was then developed that uses segmented flow to remove sample from a reactor on demand. This sampler can remove and run very small (0.1 – 2 μL) samples with on-demand sampling. A third device was developed specifically for

heterogeneous samples that contain solid particles. This “soup pot” sampler was a custom-built borosilicate glass chamber for mixing sample with quenchant and diluent. A syringe was used to obtain sample and to mix the sample with quenchant/diluent in the chamber. A Teflon stopcock was modified to allow access to the reactor vessel while also providing a leak-free seal during mixing. The sampler was coupled to an analytical-scale HPLC and was demonstrated for monitoring dibutyl phthalate hydrolysis. These samplers represent several prototypes for further development of automated process monitoring of small reaction volumes and reactions containing particulates.

CHAPTER 1

INTRODUCTION

Background

A trend in the pharmaceutical industry is to combine real-time chemical measurements with statistical analysis to improve pharmaceutical manufacturing. These techniques, collectively known as Process Analytical Technologies (PAT), are designed to ensure timely feedback so the drug manufacturing process may be controlled and improved, with the ultimate goal of real-time release of product.[1-3] The United States Food & Drug Administration (FDA) holds the pharmaceutical industry strictly accountable in all aspects of drug product manufacturing, under its mandate to protect consumers. Before they may be released to the market, batches of drug product must be assayed to insure they fall within specifications for active pharmaceutical ingredient (API) quantity and bioavailability, as well as verifying that levels of impurities fall below maximum allowable limits. The tests required for each drug product are standardized across the industry, often through the United States Pharmacopeia (USP). As it is not cost-effective to test every unit (tablet, caplet, etc.) of a batch, only a small portion of the final batch undergoes testing. This assumes that the distribution of properties within a batch is Gaussian and that there is minimal variation throughout the batch.[1] When this is not true, "unit to unit variability causes sampling procedures to become a matter of luck as to whether or not the specification is met, thus creating a kind of sampling roulette.

This sampling roulette will cause the failure of some batches that are literally the same as batches that are released."[1] This method of testing may result in wasted product or in product being released to the market that does not meet the required specifications.

Variability in the final drug product may result from variability in the raw materials, variability in the quality of the intermediates in the synthesis of the API, and mixing the API with inactive ingredients to form the final product. Under a traditional production regime, strict process standards are maintained in an effort to control each of these possible sources of variability. For example, temperature and reaction time may be very carefully controlled during API synthesis, but without monitoring the progress of the reaction itself, small variations in the raw materials may result in large variability in the quality of the API. Monitoring the API synthesis on the time scale of the reaction allows for improved understanding of the process (and what factors increase variability within a batch) as well as the opportunity to change the reaction conditions to insure the final product falls within the necessary parameters.

Prior to 2002, there was little incentive for the pharmaceutical industry to implement real-time monitoring of API synthesis, because while it might improve their understanding of the process, it also added an additional layer of testing to that already required by the FDA. Additionally, it was not clear if they would be held accountable for the results of additional testing if those results indicated additional impurities or other problems not detected by standard testing. The FDA has acknowledged that this perception that the regulatory environment is "rigid and unfavorable to the introduction of innovative systems"[2] has been cited as a primary reason that real-time process monitoring and control was not receiving more attention within the industry.

This hesitancy toward innovation concerned the FDA. In 2002, they launched an initiative titled, "Pharmaceutical cGMPs for the 21st Century: A Risk-Based Approach," which sought to emphasize real-time understanding and control of drug manufacturing as a priority for ensuring a stream of safe, effective and inexpensive drug products[2] (cGMPS are Current Good Manufacturing Practices). In 2004 they released "Guidance for Industry: PAT — A Framework for Innovative Pharmaceutical Development, Manufacturing, and Quality Assurance", which outlined their support for voluntary innovation in the industry.[2] Most importantly, the FDA offered support and flexibility, allowing the industry to rely on previous testing requirements while developing new testing methodology. While pharmaceutical PAT is still very much in its infancy, PAT is becoming more commonplace and the FDA has approved a number of new drug applications that implement PAT, rather than traditional methods, for quality control.[4]

In order to control a reaction, testing needs to be performed within the time frame of the reaction. Traditionally, when a reaction is studied, samples are manually removed from a reactor, quenched and diluted, and sent to a central analytical laboratory for analysis. Depending on the workload, samples may take hours or days to be processed using this method. When sampling and analysis occur at the source of the process, using fast analysis techniques, information gained about the reaction process may be used for real-time decision making, changing reaction conditions to insure the desired final product is produced.[3]

The focus of this work is on at-line (sample is removed from the process stream and analyzed nearby) monitoring of API synthesis, enabling better process understanding and control. APIs may be synthesized biologically or chemically, and each synthesis

reaction presents its own challenges for sampling and analysis. Reactions may vary in temperature or viscosity, and may contain particulates such as cell debris or solid catalysts that introduce challenges for sample preparation and analysis. The scale of the reaction may also complicate at-line monitoring. At the research stage (pre-manufacturing), API synthesis reactions range from small-scale (< 10 mL) up to large-scale (20-30 L). At the small-scale, very small (μL) sampling volumes must be removed to avoid perturbing the reaction. At the large-scale, interfacing a sampling device with the reactor and ensuring that sampling is representative of the bulk reaction is a challenge.

We focused our sampler development on reaction volumes of < 1 L. Desired performance parameters for at-line sampling of a medium-scale reaction (50-500 mL), as defined by a major pharmaceutical company, are given in Table 1-1. The designed device should be capable of removing samples of 20-50 μL at a set sampling interval over a period of 2-48 hours. The sampler should rapidly quench the removed reaction aliquot (within 2 seconds) and be capable of sampling from a reactor containing 30-50% of solid particles, with viscosities ranging from 0.2-6 Pa•s. The sampler should be made from materials that are resistant to a range of chemicals, including organic solvents and corrosives. Additionally, the sampler should be easily interfaced with the reactor, and transfer of sample to an analytical instrument after quenching and any additional sample processing should be automated. When developing sampler designs, we used these desired performance parameters as guidelines and attempted to meet as many of them as possible.

Table 1-1. Performance parameters for at-line sampling of a medium-scale research reaction.

Performance Parameter	Desired Range
Reactor Vessel Size	50 - 500 mL
Percent Solids (Heterogeneous Reaction)	30% - 50%
Particle Size (Heterogeneous Reaction)	10 - 500 μm
Sampling time	2 - 48 hours
Sampling interval	5 minutes - 1 hour
Sample size	20-50 μL
Quench time	2 seconds
Quench volume	Up to 10x sample volume
Delivery to analytical instrumentation	Automated
Compatibilities	Organic solvents, corrosive materials
Viscosity	0.2 to 6 Pa•s
Temperature	20-130 °C; -80 to over 130 °C desired
Sample carryover	Less than 1%
Compatibility with reactor vessel	Must not interfere with operation of reactor; must not require additional safety precautions

Analytical Techniques for PAT

Real-time monitoring of drug product manufacturing has been dominated by vibrational spectroscopy because it is fast and can provide chemical information;[5] however, spectrometric methods are not ideal for all samples, particularly complex samples for which spectrometric analysis would be complicated by contaminants whose

spectra are similar to those of the desired analytes.[6] Chromatographic techniques are powerful tools to gain information about chemical and biological processes in complex mixtures. Gas chromatography (GC), the workhorse instrument of traditional online analysis, is less suited to water-based analysis[3] for the increasing number of biologics. High-pressure liquid chromatography (HPLC) (without coupled mass spectrometry) represented 53% of analysis of impurities in drugs from 1995-2001. The majority of these used reverse phase HPLC (RP-HPLC) with ultraviolet (UV) absorbance detection.[7] Developments in fast liquid chromatography,[8, 9] such as ultra high pressure liquid chromatography (UPLC),[10] high-temperature liquid chromatography (HTLC),[11] and the use of monolithic columns,[12] led to assay turn-around of 3-5 minutes which makes HPLC increasingly capable of real-time process monitoring in the pharmaceutical industry.

Automated Reaction Monitoring

Sampling systems may be batch systems that remove a single sample of pre-set volume or continuous systems. Batch systems have been used for process monitoring of monoclonal antibody production in fermentation vats. A system that injects fermentation broth sample (including a small number of cells) directly onto an HPLC column, without filtration or dilution, was reported (Figure 1-1).[13] This system is illustrative of sampling systems that do not perform sample prep, but simply remove sample from a reactor and inject it directly to an analytical instrument, in this case, HPLC. A similar system was developed for monitoring production of ethanol from glucose in a fermentation reactor.[14] The system removes aliquots from the fermentation broth followed by automated filtration, dilution and injection onto the HPLC. This system uses a Zymarc BenchMate

II,[15] a robotic arm system that performs mixing by tilting vials. The fermentation monitoring system (Figure 1-2) illustrates a primary goal of PAT: information about glucose and ethanol content in the broth is used to adjust system inputs such as gas flow and pH to insure the most productive turnover of glucose to ethanol possible.

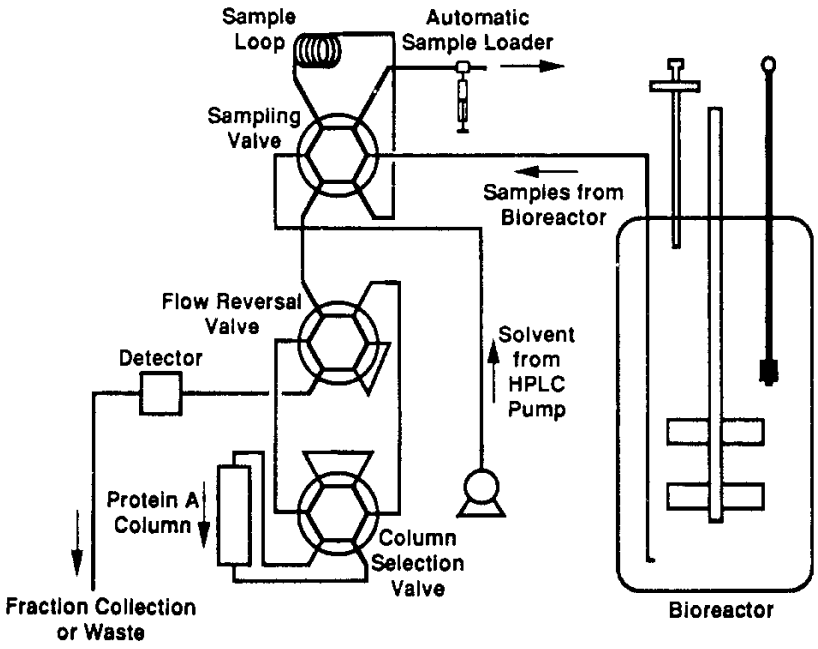

Figure 1-1. BioCAD HPLC system for fermentation broth monitoring. Used with permission from source.[13] This system removes aliquots of fermentation broth and directly injects them onto an HPLC column without sample dilution or filtration.

Microdialysis (MD) coupled to HPLC is an example of a continuous monitoring system. MD allows for selective sample collection, leaving particulate matter and proteins in the reaction vessel while transporting smaller analytes of interest for analysis via HPLC. MD coupled to HPLC has been used in many applications including monitoring in vivo,[16-18] sampling from whole blood,[19] and determination of metals in aqueous samples.[20] However, MD is not suitable for all applications of PAT because the membranes are not compatible with organic solvents, and solids or larger analytes of interest are excluded from the sample.

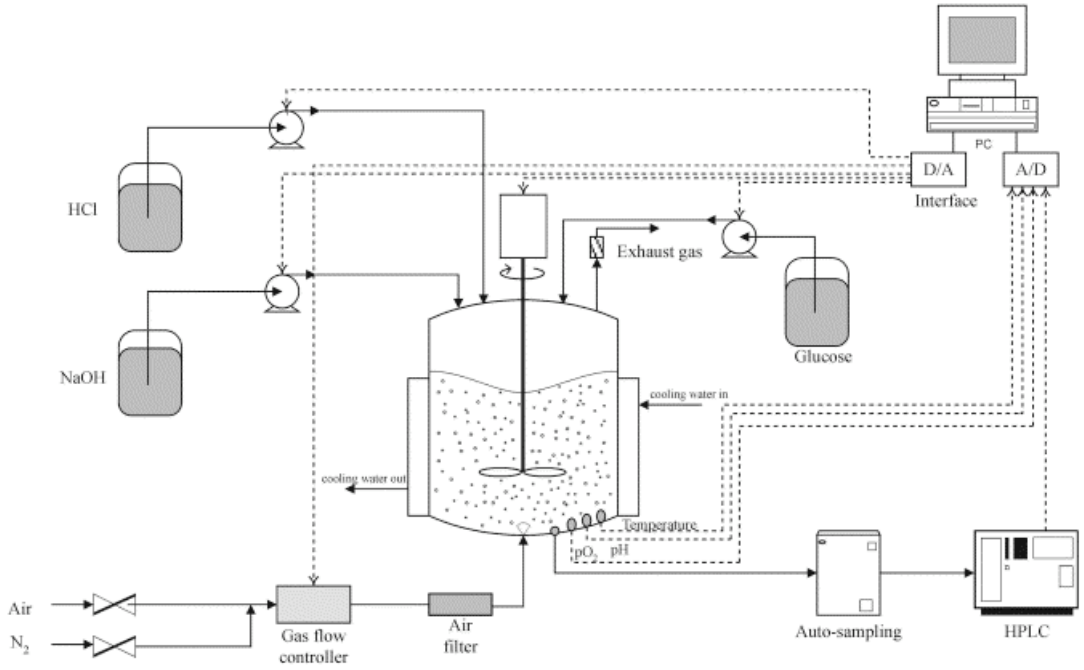

Figure 1-2. Automated monitoring system with feedback control. Used with permission from source.[14] This system uses computer control to monitor ethanol and glucose content in the reactor and adjust the system inputs to improve ethanol production.

Flow injection analysis and related techniques. Flow injection analysis (FIA) and its related techniques are powerful tools for automated sample processing that may be coupled to a collection of analytical methods for analysis of the processed sample. The evolution of FIA techniques has been recently reviewed,[21] and use in the pharmaceutical industry, as well as common detectors and detection limits achieved has also been reviewed.[22] FIA was first developed by Ruzicka[23] in 1975 and has been used extensively since that time. A typical FIA setup (Figure 1-3) consists of a peristaltic pump constantly pushing a carrier fluid through a two-position valve to a detector at a constant flow rate. The sample is pulled through the two-position valve, filling a sample loop of fixed volume. When the valve is triggered, the sample is injected into the flow stream, reacting with the carrier fluid as it moves through a holding coil. The length of

the holding coil and the carrier fluid flow rate control the amount of the time that the sample reacts before flowing past the detector.[23]

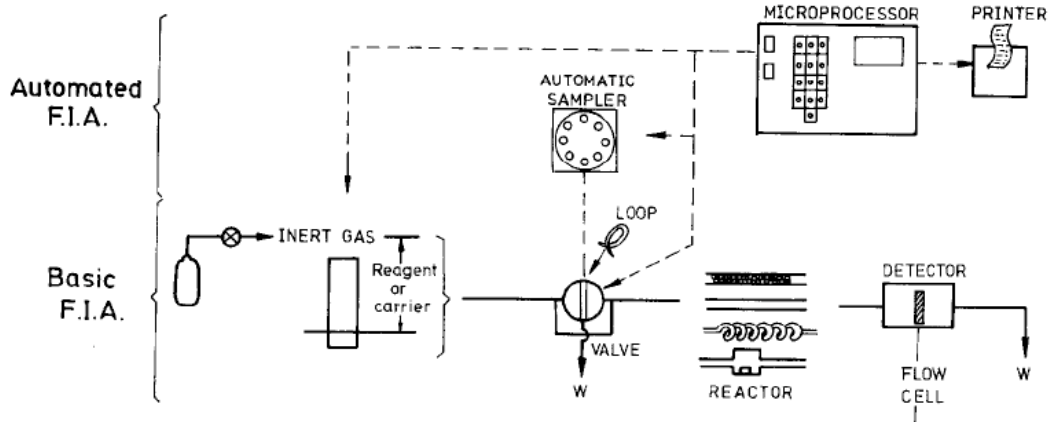

Figure 1-3. Flow injection analysis (FIA). Adapted from source[24] with permission.

Sequential injection analysis (SIA), first developed in 1990, uses bi-directional, programmable flow rates to improve mixing and decrease reagent consumption.[25] In contrast to FIA, where the carrier fluid is constantly flowing, SIA aspirates sample and reagents sequentially into a mixing coil. Reagents are flowed through the mixing coil, reversing direction and changing flow rates to enhance mixing. Once the reaction is complete, the fluid flows past a detector for analysis (Figure 1-4). SIA has been used for monitoring of analytes of interest in bioprocesses, such as L-cysteine[26] and glycerol.[27]

SIA has been used for online monitoring without chromatography to determine hydrogen peroxide content in lens cleaning solution with UV detection using an enzymatic reaction.[28] One paper uses a combination of techniques to monitor a bioprocess. Tubing with a filter on the tip is placed in the broth, continuously removing sample from the reactor. Fluid is removed from the analysis stream to be analyzed using FIA (ammonia), SIA (formaldehyde) and HPLC (1-3de1 I-TAC, the desired reaction product).[29]

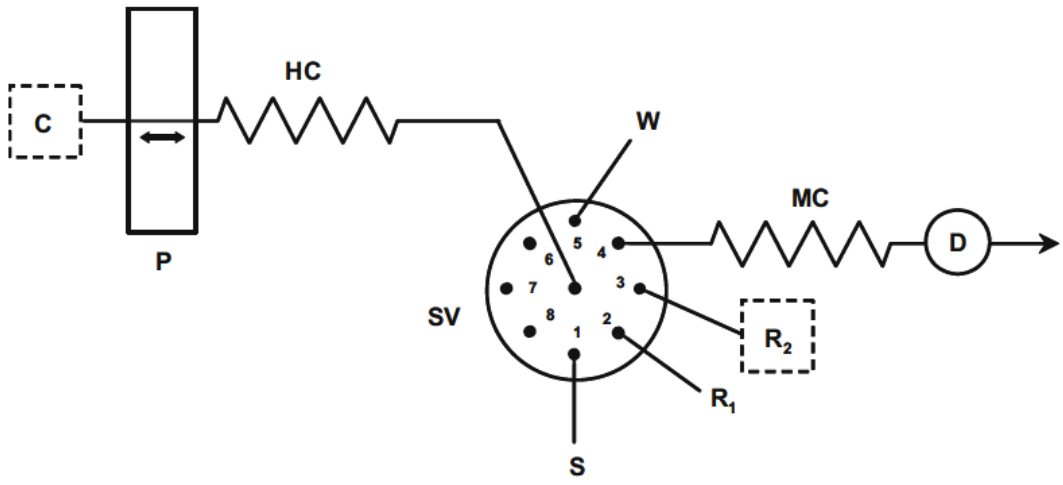

Figure 1-4. Sequential injection analysis (SIA). The SIA system consists of a selection valve (SV), peristaltic pump (P), holding coil (HC), knotted mixing coil (MC), spectrophotometric detection system (D), sample or standard (S), reagent (R), buffer/carrier stream (C), waste (W). Adapted from source.[27]

An improvement to the SIA design is the development of micro SIA lab-on-valve (μSI-LOV).[30] The system miniaturizes SIA so that the flow cell and analysis are performed on the valve (Figure 1-5). At the same time, the channels are large enough (500 μm) that small beads and other suspended matter (such as cells) can pass through the channels uninhibited. Fiber optic technology is used to perform absorbance and fluorescence measurements within a flow cell cut into the valve itself.[30] The μSI-LOV system has been used to monitor cell culture, using 60 μL of filtered sample for each assay. Assay controls were incorporated automatically using the μSI-LOV system. The system had some problems with clogging of the sample tubing,[31] a common problem for these types of systems. The μSI-LOV system was used for online monitoring of ammonia in E. Coli culture broth.[32] Broth was removed for analysis at a flow rate of 0.5 mL/min, with analysis of a portion of the sample every 6 minutes.[32] The uSI-LOV system has been demonstrated coupled to capillary electrophoresis (CE),[33, 34] adding the advantage of separations to the system.

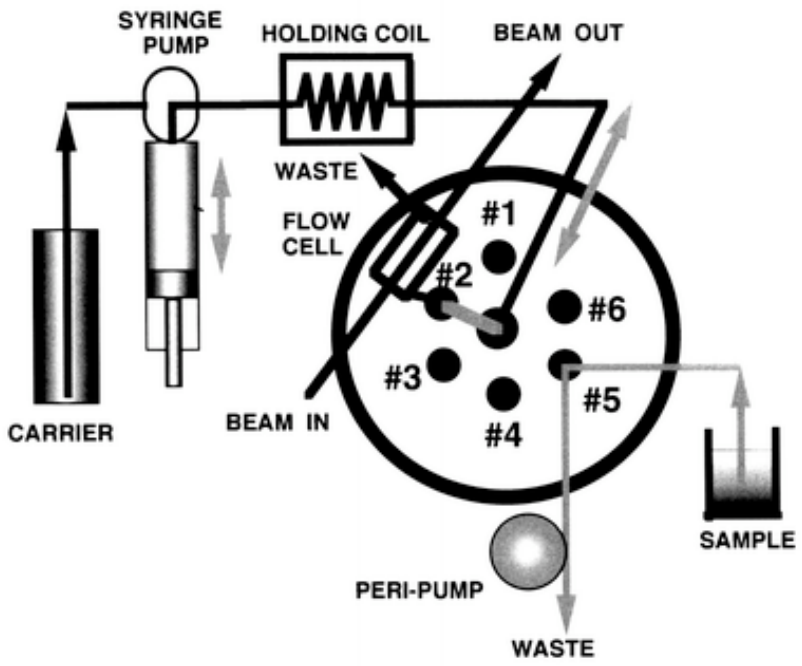

Figure 1-5. Micro-sequential injection lab-on-valve (μSI-LOV). Used with permission from source.[30]

Chromatographic systems. The addition of monolithic columns to SIA created sequential injection chromatography (SIC), which added the advantages of chromatography to the system for simultaneous detection of multiple analytes (Figure 1-6). The first system to incorporate a monolithic column[35] separated four components (methylparaben, propylparaben, sodium diclofenac and butylparaben), all detected using UV absorbance. Subsequent systems have been used to detect a variety of analytes, including food and cosmetic additives,[36] and pesticides.[37] This family of techniques, particularly μSI-LOV and SIC, are very promising for pharmaceutical applications. The systems can be easily automated, are amenable to sample sizes in the μL range, and have been demonstrated with solids (beads and cells) in the samples when a suitably wide-bore is used in the valve. The majority of research and development for these systems has been performed by FIAlab Instruments (Bellevue, WA).

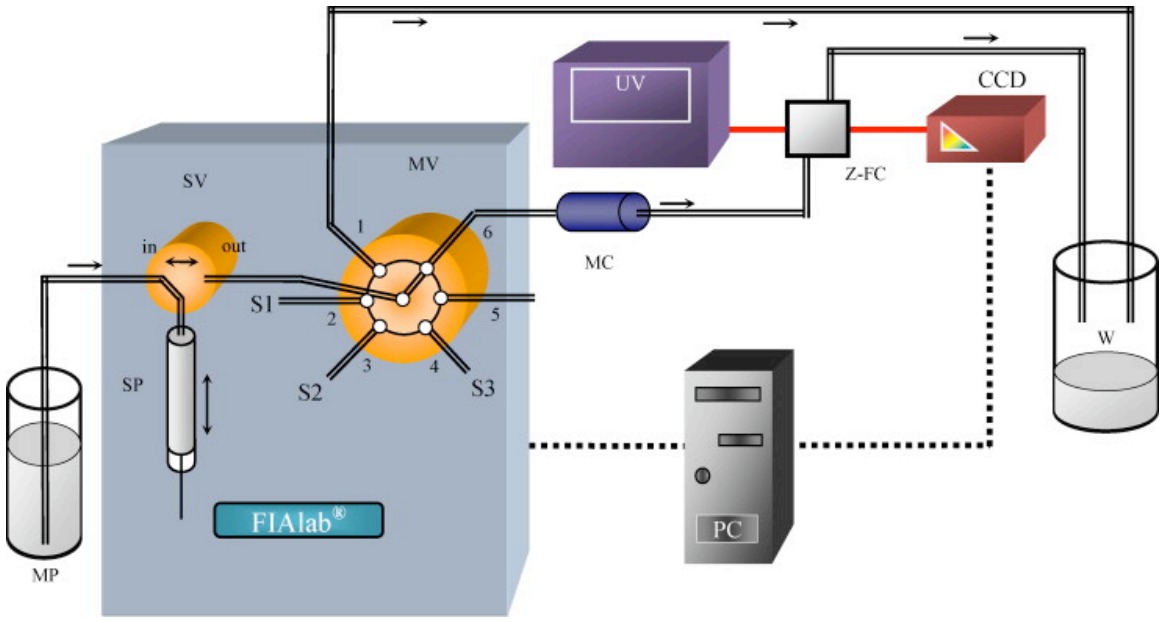

Figure 1-6. Sequential injection chromatography (SIC). Scheme of SIC set-up: CCD UV–vis detector (CCD); monolithic column (MC); mobile phase (MP); 6-port multi-position valve (MV); computer (PC); syringe pump (SP); solenoid valve (SV); Sample lines 1, 2, 3 (S1, S2, S3); UV lamp (UV); waste (W), Z-flow cell (Z-FC). Used with permission from source.[37]

The ExpressRT-100 reaction monitoring system (Eksigent, Dublin, CA, US) is based on Eksigent's previous development of capillary liquid chromatography systems for rapid analysis. The reaction monitoring system utilizes a sampling module (10 cm wide x 15 cm deep x 20 cm high) that is placed next to a reactor located in a hood. The sampling module is connected to a capillary LC system which sits on a separate cart, allowing easy access to multiple reactors. Sampling and analysis can take place as quickly as every three minutes. It can pull up sample volumes as small as 20 µL and dilute the sample to a pre-programmed dilution factor from 1-1000 in a dilution chamber. All wetted parts are chemically-resistant (fluoropolymers, fused silica, stainless steel). Clogging was observed when sampling from heterogenous samples. A filter was added at the tip of the sampling capillary to alleviate clogging in some solutions.[6] A

subsequent paper demonstrates use of the sampling system with flow chemistry (continuous flow reactor).[38]

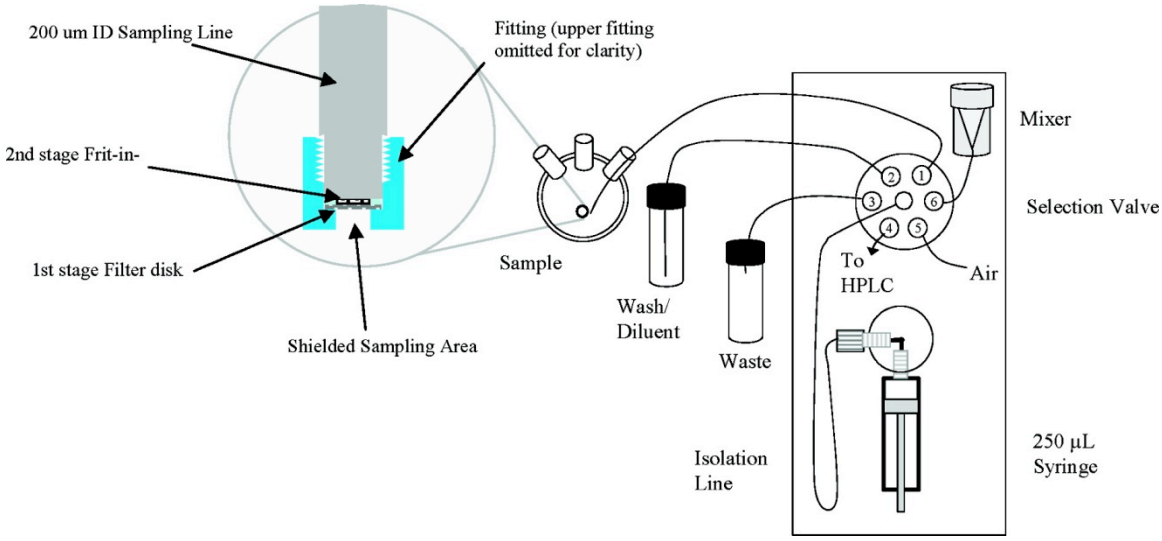

Figure 1-7. ExpressRT-100 reaction monitoring system. Used with permission from source.[6]

Waters (Milford, MA, US) has developed the PATROL UPLC Process Analyzer for rapid analysis using UPLC. They have demonstrated the ability to monitor the hydrolysis of acetylsalicylic acid by directly injecting the sample.[39] While they have demonstrated that UPLC is sufficiently fast to monitor reactions, they have not developed any system for sample quenching or processing before injection.

Groton Biosystems (Boxborough, MA, US) has developed a stand-alone process analyzer (GPA1000) that is capable of removing samples from a reactor, and performing sample preparation steps in approximately 15 minutes. Prepared samples are analyzed with a capillary electrophoresis (CE) system built in to the unit. Total sample preparation and analysis time is estimated at 45 minutes. While the system is automated and has been created specifically for process monitoring, it is only suitable for reactors larger than one liter, as each sample ranges from 0.5-5 mL in required volume.

Groton Biosystems has also created a sophisticated system for monitoring fermentation reactors, the ARS-M. This system pulls up aliquots of sample using either disposable needles or tubing (with our without filters, depending on the assay desired) and is able to perform dilution, filtration, cell lyzing and reagent addition automatically. The ARS-M system can be coupled to HPLC, cell-counting instruments, or to a sample collector if samples are to be analyzed at a later time. The system uses PEEK, stainless steel and fluoropolymers for all wetted surfaces to improve chemical compatibility. While the system is capable of quite a few operations, it is still primarily suitable for large-scale reactions as sample volumes are in the milliliter range based on the dead volume of the system.[40]

Dissertation Overview

While some systems have been developed for pharmaceutical PAT, they may be improved. Many of the systems require volumes of sample (tens of microliters up to milliliters per data point) that are not compatible with monitoring small-scale reactions. This inhibits the use of these systems with early development of an API synthesis where the reactor volume may only be a few milliliters total volume. As a result, initial HPLC analysis of a new reaction system would have to be performed manually. Automated analysis with samplers capable of removing very small volumes of fluid (sub-microliter) would provide considerable time and cost savings by not needing a researcher to manually remove samples over a period of hours. Additionally, being able to study the API synthesis prior to scaling up provides additional information so researchers may

determine if a particular API candidate should be considered for further investment or removed from the pipeline.

The other primary challenge in process monitoring systems is representative sampling from heterogeneous samples that contain solids. This is a particularly difficult challenge when removing small sample sizes. Several sampling systems have installed filters on intake tubing as a way to bypass this problem, while others only attempt to sample from homogeneous samples. Many API synthesis reactions contain solid particles. In biological reactions, cells and cell debris are present in the reactor. In organic reactions, reagents may be present at a concentration that they precipitate out of the solution, or solid catalysts may be used to speed up the process. We have attempted to directly sample from solutions with particles and investigated how solids may affect our sampling system.

The overall objective of this work was to develop sampling systems that could remove a small volume of sample (microliter range), quench the reaction, and perform at-line HPLC analysis. In chapter 2 we present a sampler design for continuous sampling using less than a microliter of sample for each minute of sampling. This "push-pull" was built from fused silica capillary and a PEEK tee and fittings, ensuring chemical compatibility with a wide range of reagents (although long-term use at high pH is not recommended). The design takes advantage of rapid passive mixing (seconds) characteristic of microfluidic systems. The sampler was characterized with samples of a varying viscosity and has been tested with heterogeneous samples containing polystyrene beads. The push-pull sampler was demonstrated monitoring both an enzymatic reaction without a chromatographic component, and monitoring the hydrolysis of acetylsalicylic

acid to salicylic acid while coupled to an analytical-scale HPLC instrument. Data and results from this chapter have been accepted for publication in the *Journal of Chromatography A*.

In chapter 3 we present a second sampler, capable of batch sampling with even smaller sample volumes (sub-microliter per data point). This "droplet" sampler takes advantage of the properties of segmented flow microfluidics to mix the sample and quenchant. As this sampler is connected to a movable stage, multiple reactions may be analyzed using the same system. This sample is coupled to the HPLC for analysis of the small sample volumes.

The final sampler, presented in chapter 4, directly tackles the challenge of heterogeneous samples. This "soup pot" sampler is a custom-built borosilicate glass chamber for mixing sample with quenchant and diluent. A syringe is used to obtain sample and is subsequently used for mixing the sample with quenchant/diluent in the chamber. A Teflon stopcock has been modified to allow access to the reactor vessel while also providing a leak-free seal during mixing. The sampler is coupled to an analytical-scale HPLC and has been demonstrated for reaction monitoring of dibutyl phthalate hydrolysis. These samplers represent prototypes for further development of automated process monitoring by HPLC.

CHAPTER 2

DEVELOPMENT AND CHARACTERIZATION OF "PUSH-PULL" SAMPLING DEVICE WITH FAST REACTION QUENCHING COUPLED TO HPLC FOR PHARMACEUTICAL PAT

Introduction

In this work, we describe a microscale sampling system suitable for near real-time monitoring of very small-scale reactions (several milliliters), inspired by push-pull perfusion systems used for neuroscience.[41, 42] As discussed previously, sampling from very small reactions requires the removal of very small volumes of sample so as not to affect the reaction system while in the process of monitoring the system. The development of an automated system for very small volume sampling provides considerable cost advantages for a pharmaceutical company because they are better able to understand the reaction early in the scale-up process, determining whether they should continue to develop the active pharmaceutical ingredient (API), and they are not required to pay for a researcher to perform manual sampling over a period of hours.

Microfluidics is a growing area of research and microfluidic systems have been extensively reviewed over the last year,[43-47] including advances in microfluidic separations,[48-51] detection methods for microfluidic systems,[52-55] and numerous applications.[56-76] Microfluidic systems have characteristic length on the order of micrometers to millimeters and are advantageous due to their very small reagent requirements, large surface-to-volume ratio that allows for rapid reactions, and rapid

dispersion of heat which aids in developing very fast separations techniques such as capillary electrophoresis (CE). Due to their small characteristic lengths, most microfludic systems have laminar flow properties unless operated at high flow rates. In a laminar system, mixing is controlled by diffusion across a channel or tube. This leads to unique devices that could not be created at a larger scale, such as the H-filter,[77] which extracts small molecules from one flow stream into a secondary flow stream, leaving larger proteins and particles behind. The push-pull device developed here used laminar flow for very predictable adjustment of flow properties, and used the rapid mixing at the microfluidic scale to perform rapid quenching of a sample as it is removed from a reactor.

The device performs automated sampling with rapid (seconds) passive mixing with a quenchant/diluent and downstream reaction monitoring. The small dimensions of the sampler body take advantage of the properties of microfluidic systems, including rapid passive mixing and minimal reagent consumption. Rapid mixing ensures that as sample is removed from the reactor, the reaction may be quenched so that reaction conditions are maintained until the sample may be analyzed downstream. The low (μL/min) reagent consumption reduces cost and waste for analysis, while also allowing the sampler to be used with small-scale (mL) reactions such as may be seen in a research and development environment. Under normal operating conditions, withdrawing sample from a reactor at 0.5 μL/min, only 0.72 mL of sample would be consumed after a full 24 hours of continuous sampling.

Unlike a microfluidic chip system, commonly made from glass or polymers such as polydimethylsiloxane (PDMS), the sampler body is made entirely from commercially available parts that are easily exchanged and do not need specialized facilities to produce.

The sampler body is constructed from fused silica capillary and polyether ether ketone (PEEK), materials that make it amenable to a wide variety of analytes. Both materials have low chemical reactivity, even with organic solvents and corrosives, and may be used over a range of temperatures. The main sampler body is connected to two syringe pumps to drive flow and mixing, minimizing the number of parts that have the potential to fail during sampling. The sampler was connected to three monitoring systems, and was computer-controlled with software written in LabVIEW, making operation simple for the end-user.

We have demonstrated the ability of the sampling system to monitor reactions with a temporal resolution of less than one minute, and a delay time of several minutes (limited by length of capillary from sample to detector) with automated data collection and system control. Finite element modeling of the sampler shows that it can rapidly dilute or quench reactions and quenching has been confirmed experimentally. We have investigated the effect of particulate matter and viscosity on the system. A modification to the system, stop-flow sampling, which would let sample consumption be minimized if samples were only needed infrequently, was considered. Finally, we monitored two separate reactions, with the sampler coupled to two different detection systems to demonstrate its utility for monitoring real reactions.

Experimental Section

Materials. Blue food color (water, propylene glycol, FD&C Blue 1, 0.1% propylparaben) was obtained from McCormick (Sparks, MD, US). Amplex Red (10-acetyl-3,7-dihydroxyphenoxazine) and Amplex Red Stop Reagent (proprietary) were

purchased from Invitrogen (Carlsbad, CA, US). Acetylsalicylic acid and salicylic acid were obtained from Acros Organics (Morristown, NJ, US). All water used was deionized to 18 MΩ resistivity with an E-pure 1090 series system from Barnstead Thermolyne Cooperation (Dubuque, IA, US). Unless otherwise noted, all other chemicals were purchased from Fisher Scientific (Chicago, IL, US).

Sampler assembly. The sampler was constructed using three fused silica capillaries (Polymicro Technologies, Phoenix, AZ, US) and a mixing tee (Valco Instruments, Houston, TX, US) as shown in Figure 2-1. One end of the push capillary (40 μm ID, 100 μm OD) was connected to a Fusion 400 (push) syringe pump (Chemyx, Inc., Stafford, TX, US) and the other end was inserted completely through the mixing tee and sheathed within the pull capillary (250 μm ID, 360 μm OD). The transfer capillary (150 μm ID, 360 μm OD) connected the tee sidearm to a PHD2000 (pull) syringe pump (Harvard Instruments, Holliston, MA, US). Fluid was continuously pulled up from the sample, mixed with quenchant/diluent from the push capillary in the mixing zone, and the mixed solution was pulled into the transfer capillary.

Mixed sample flow was monitored in one of three configurations: direct monitoring, FIA monitoring, and HPLC monitoring. In all three configurations, ultraviolet (UV) absorbance within a capillary was measured with a Spectra 100 variable wavelength detector (Spectra Physics, Mountain View, CA, US). The detector output was recorded with USB-6008 DAQ card combined with LabVIEW (National Instruments, Austin, TX, US) software written specifically for this application.

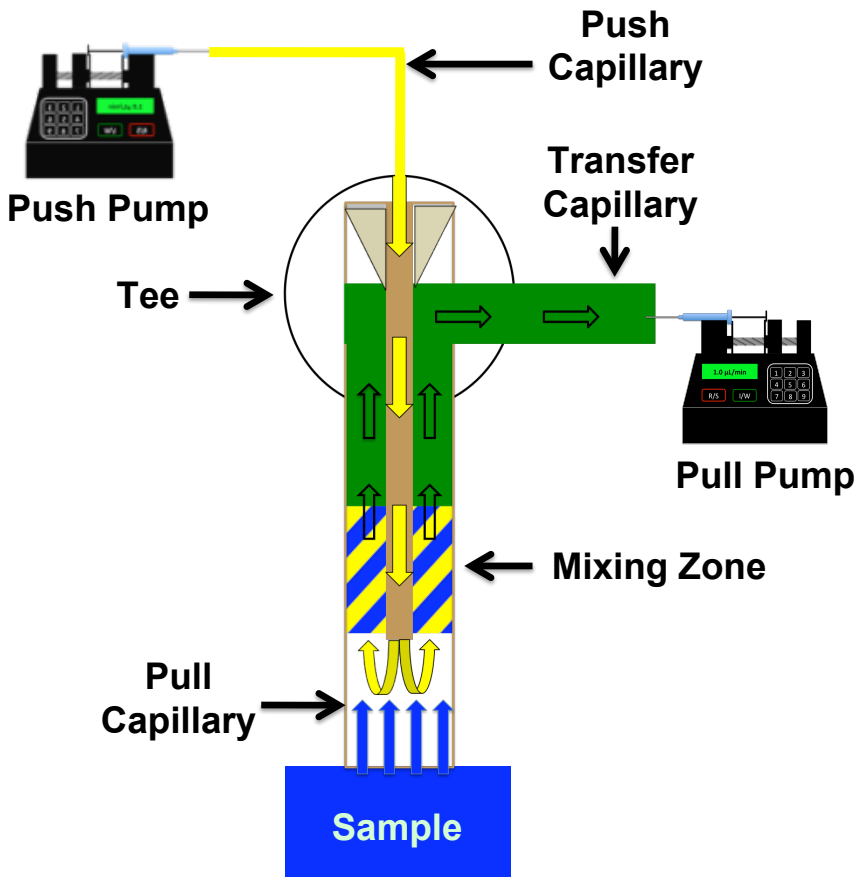

Figure 2-1. Illustration of the push-pull sampler (not to scale). Sample is continuously pulled into the sampler body with the pull syringe where it is rapidly mixed with fluid from the push pump upstream of the push capillary tip in the mixing zone. The mixed solution is pulled through the tee and out the transfer capillary, where it may be analyzed. See Appendix C for more details about push-pull sampler assembly.

For direct detection monitoring (Figure 2-2 A), a small area of polyimide coating was removed from the surface of the transfer capillary to allow for transmittance of UV-light through the capillary, and mixed sample was detected using the variable wavelength detector. For FIA monitoring, an 8-port 2-position switching valve (Valco Instruments) was added between the sampler body and the pull pump. The valve was fitted with two 0.5 µL fused silica capillary injection loops. A third (carrier) syringe pump was attached to the valve to provide carrier flow. Sample mixed with quenchant/diluent was pulled

through the valve to fill the injection loop and then injected every minute from the loop into the carrier flow stream. While one loop was being filled, the other loop was injected. A window was burned in the carrier capillary and injected sample was detected with the variable wavelength detector described previously.

For experiments using HPLC monitoring (Figure 2-2 C), 2 µL stainless steel sample loops were installed on the 8-port switching valve used for FIA. Sample was injected every 5 minutes onto a 150 long x 4.6 mm ID column packed with 5 µm Grace Prosphere HP C4 particles (Grace Davison Discovery Science, Deerfield, IL, US) installed on an Agilent 1100 HPLC (Agilent Technologies, Inc., Santa Clara, CA, US). The sample was separated isocratically with 35% methanol, 65% 10 mM monopotassium phosphate (pH 2.3) as the mobile phase. A variable wavelength detector, described previously, was placed post-column to monitor effluent absorbance was monitored at 254 nm.

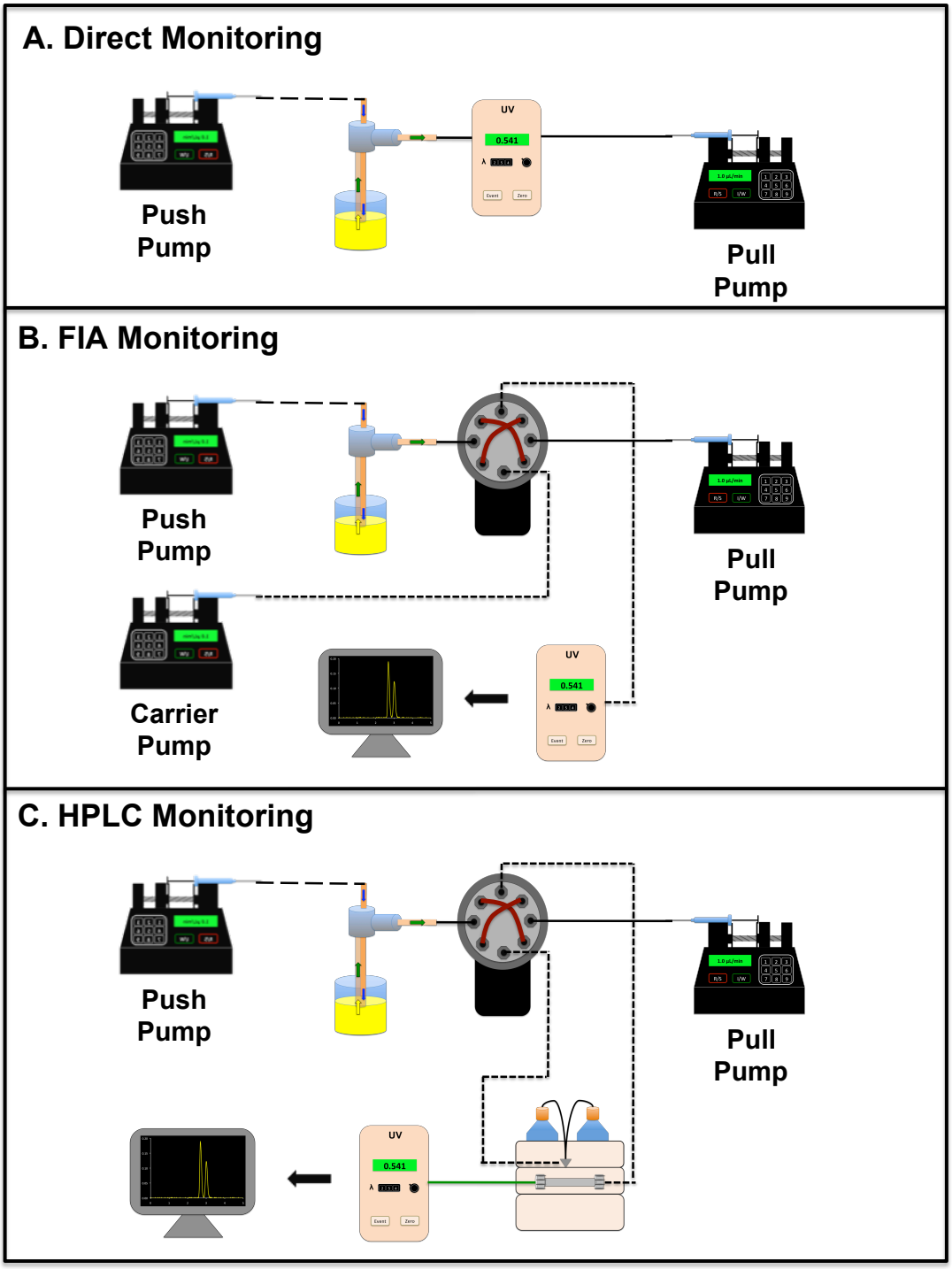

Figure 2-2. Illustration of the push-pull sampling system. Overview (not to scale) of A. direct monitoring, B. flow injection analysis (FIA) monitoring, and C. HPLC monitoring.

COMSOL Multiphysics Modeling. A finite element modeling program, COMSOL Multiphysics 3.5a (COMSOL, Inc., Burlington, MA, US), was used to model fluid flow and mixing within the nested capillary system. A 3 mm segment of the sampling tip was modeled in three dimensions, with the push capillary recessed 1 mm vertically from the tip of the pull capillary (Figure 2-3) and 15 μm horizontally from one side of the pull capillary to match the arrangement used for experiments. Area A is defined as an inlet with laminar volumetric flow and a concentration of 1 mM. Area B is defined as an open boundary for fluid flow with a concentration of 0 mM. Area C is defined as an outlet with laminar volumetric flow and an open boundary for convection and diffusion. Modules for incompressible, isothermal fluid flow and convection and diffusion were used. Constants for water at 20 °C (density of 998.207 kg/m^3 and viscosity of 1.002 x 10^{-3} Pa•s) were used for the model. The diffusion coefficient was set to 1.0 x 10^{-9} m^2/s to approximate a small molecule in water.[78]

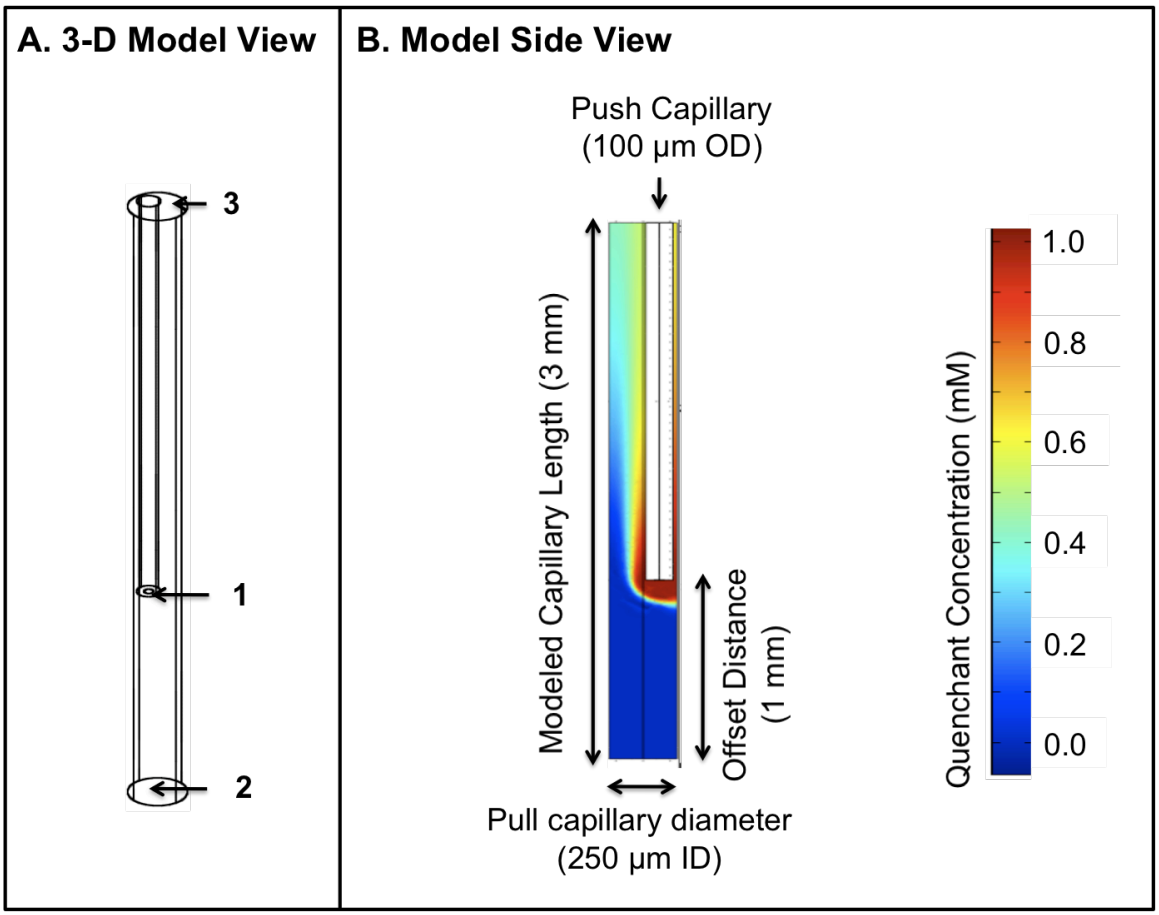

Figure 2-3. COMSOL model of the push-pull sampler. This model was used for determining the effect of sample capillary diameter on mixing time, the effect of flow rate on mixing time and the correct offset distance between the tip of the pull capillary and the tip of the recessed push capillary to ensure quenchant does not leak into the bulk sample. A. Three-dimensional view of a 3 mm segment of the sampling tip with nested push capillary offset by 1 mm. Area 1 is defined as an inlet with a volumetric flow rate of 0.5 µL/min and a quenchant concentration of 1.0 mM. Area 2 is defined as an open boundary with free flow of fluid and a defined quenchant concentration of 0.0 mM. Area 3 is defined as and outlet with a volumetric flow rate of 1.0 µL/min and an open boundary for mass transport. B. Side view of the modeled sampling tip showing sample (0.0 mM) mixing with quenchant/diluent (1.0 mM) at a pull flow rate of 1.0 µL/min and a push flow rate of 0.5 µL/min.

On-line Dilution. Dilute blue food color (in water) was sampled at a constant flow rate (1.0 or 2.0 µL/min). The flow rate of water through the push capillary

was varied to dilute the mixed sample to different degrees. FIA was used to monitor the degree of sample dilution.

Delay and Response Time. Delay and response times were determined using direct monitoring. Every 10 minutes, 100 μL of blue food color was added to a stirred vial containing a constant volume of water. The pull flow rate was set to 1.0, 2.0 or 3.0 μL/min. Water was pumped through the push capillary at 50% of the pull flow rate. Absorbance was recorded at 280 nm using direct monitoring. The experiment was repeated, directly dipping the transfer capillary (with the sampler removed) into the sample vial, isolating the contribution to delay and response times due to the length of transfer capillary only.

Stop-Flow Sampling. The system was modified by placing a six-port switching valve between the push syringe pump and the push capillary to enable rapid switching between two push flow rates. Syringes were filled with water and connected to the six-port valve adjacent to the push capillary. Two inlet capillaries, of equal dimension to the push capillary, were attached to the six-port valve adjacent to the inlet capillaries, equalizing the pressure drop when the valve was actuated. One syringe was set to 0.9 μL/min (sampling "off") and the other was set to 0.1 μL/min (sampling "on"), while the pull flow rate was set to 1.0 μL/min. Blue food color, diluted in water, was used as the sample. The resulting mixed sample/water solutions were monitored using FIA.

Particles. Solutions of blue food color diluted in ethanol were prepared with 10.0, 100 or 500 μm polystyrene beads. Each solution was sampled at 1, 2 and 4 μL/min pull flow rate with isopropanol flowing at a constant 0.5 μL/min through the push capillary. To determine the effect of bead concentration on reproducible sampling, serial

dilutions (1:10) of 10.0 μm particles were made in blue food color (diluted in ethanol). Each solution was sampled at 1, 2 and 4 μL/min pull flow rate with a constant 0.5 μL/min isopropanol push flow rate. All mixed solutions were monitored with FIA.

Viscosity. Samples of varying viscosity were prepared by mixing a constant volume of blue food color (diluted in ethanol) with isopropanol and glycerol. Isopropanol was pumped through the push capillary as a model quenchant/diluent. To determine the maximum pull flow rate for a given viscosity, the push flow rate was held constant at (0.1 μL/min). The pull flow rate was initialized at 1.0 μL/min and increased by 1.0 μL/min every 20 minutes until cavitation was observed in the pull syringe. To determine if sampling is reproducible across a range of viscosies, within the allowed flow rates for each viscosity, peak height reproducibility was monitored using FIA, with the push flow rate set to 50% of the pull flow rate.

Verification of quenching using an enzymatic reaction. Amplex Red was prepared in dimethylsulfoxide according to manufacturer directions. Amplex Red Stop Reagent was prepared with ethanol and water according to manufacturer directions. Samples of 200 μM Amplex Red were prepared in 50 mM phosphate buffer (pH 7.4) with 1, 2 or 4 milliunits per milliliter (mU/mL) horseradish peroxidase (HRP). An equal volume of 8.8 mM hydrogen peroxide in the same buffer was added to the sample to start the reaction (diluting all reagents by ½). Amplex Red Stop Reagent was used as a quenchant to stop the reaction. The pull flow rate was 1.0 μL/min with Amplex Stop Reagent push flow rate of 0.167 μL/min, mixing sample with stop reagent at 5:1 ratio according to manufacturer instructions. The quenched sample was monitored every

minute with FIA at 570 nm, using 50 mM phosphate buffer at 5.0 μL/min as the carrier fluid.

To verify quenching and show that the reaction may be monitored online as well as offline the experiment was repeated with 1 mU/mL HRP. While sampling with the push-pull sampler, 200 μL aliquots were removed manually every one minute and quenched offline by adding to 40 μL Amplex Red Stop Reagent in a microtiter plate. Absorbance for the offline samples was measured at 570 nm on a plate reader and compared to the online absorbance.

Reaction monitoring with HPLC. Base-catalyzed hydrolysis of acetylsalicylic acid (aspirin) was monitored with HPLC monitoring. A 0.2 M solution of acetylsalicylic acid was prepared in methanol. A stirred vial containing 14.5 mL of 25 mM bicarbonate buffer (pH 11.2) was sampled at a pull flow rate of 1.0 μL/min. A constant push flow rate of 0.5 μL/min was applied with 10 mM monopotassium phosphate as the quenchant, which changed the pH of the mixed solution to approximately 7, quenching the hydrolysis. After 5 minutes of sampling, 0.5 mL of the acetylsalicylic acid solution in methanol was added to the sampling vial, starting the hydrolysis reaction. The reaction was monitored for 110 minutes using HPLC.

Results and Discussion

Sampler Design. The heart of the push-pull sampler is a pair of concentric fused-silica capillaries. Solution is pulled through the outer (pull) capillary directly to an HPLC valve (or on-line detector) using a syringe pump (Figure 2-1). At the same time, the diluent/quenchant solution is pushed through the center (push) capillary with a syringe

pump, mixing with the sample solution in the mixing zone as it moves toward the mixing tee. Solution added through the push capillary can be used to dilute the sample and may include quenchant to stop the reaction. By varying the flow rate through the push capillary, it is possible to change the degree of sample dilution. To ensure that the push solution does not contaminate the reaction vessel, the sampler capillaries were arranged so that the push capillary was recessed within the pull capillary.

While this system is similar to push-pull capillary systems used for in vivo monitoring,[41, 42] it differs in two ways. First, in vivo push-pull samplers use the same flow rate for the push and pull solutions to avoid changing the volume of extracellular fluid. By using different flow rates, we can adjust dilution or quenching of the sample. Secondly, for in vivo sampling, the inner and outer capillaries are flush at the end to provide a region of solution exchange with the extracellular space. In our case, recessing the push capillary prevents contamination of the sampled solution. In principle, adding solution at a tee downstream of sampling could fill the role of the push solution for quenching or dilution; however, the approach described here allows quenching to occur more rapidly.

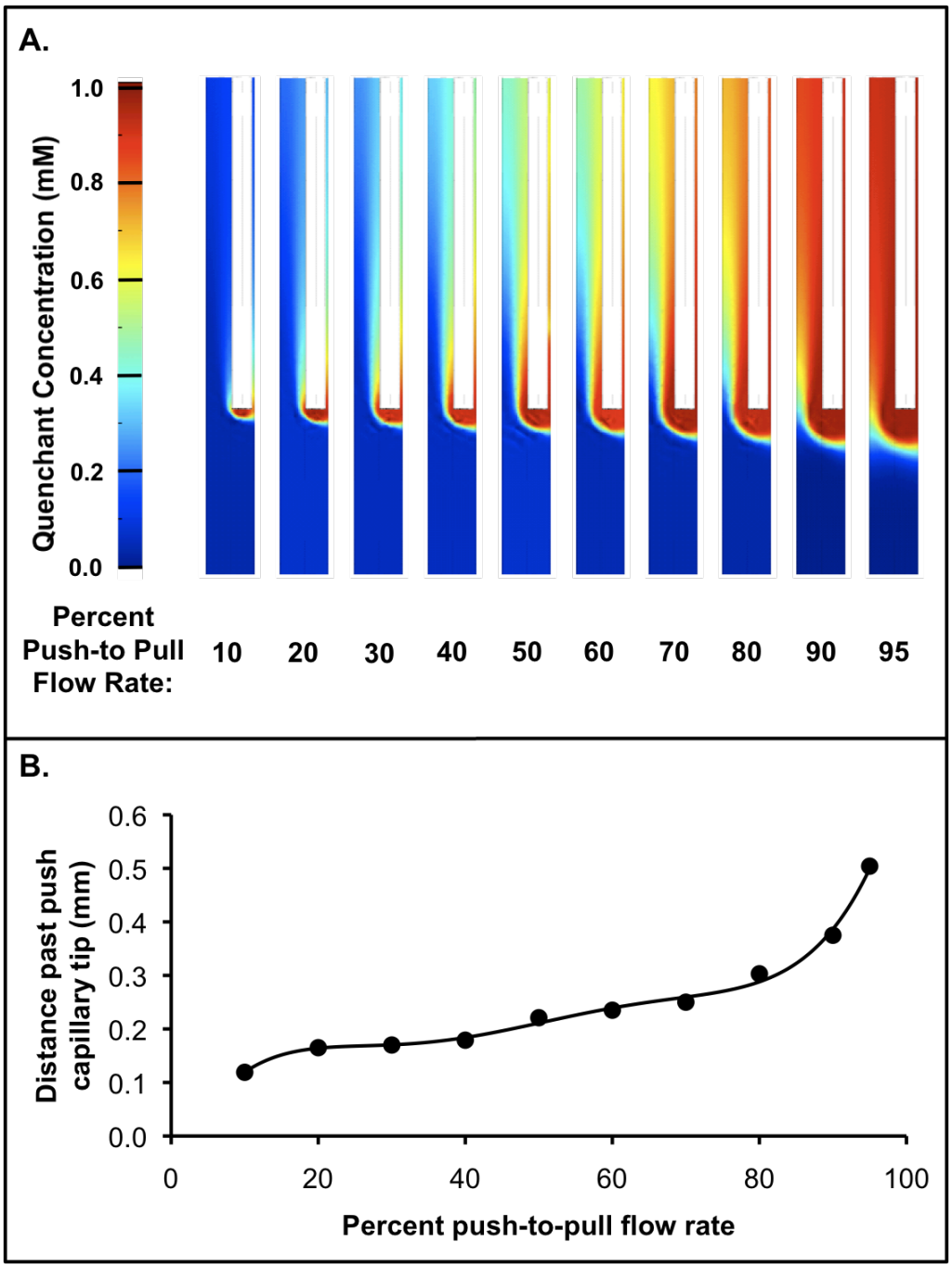

Figure 2-4. Effect of push flow rate on mixing with a constant pull flow rate. A. COMSOL models showing effect on mixed concentration and spatial distribution of quenchant. B. Distance from push capillary tip (mm) where concentration of quenchant/diluent decreases to <1% of the original concentration. The pull flow rate was kept constant at 1.0 µL/min while the push flow rate was increased. It was determined that up to a flow rate of 0.95 µL/min an offset of 1 mm was sufficient to prevent leakage.

Sampling tip modeling with COMSOL. We modeled the push-pull sampler system using COMSOL with the basic construction shown in Figure 2-3. As shown, the diluent/quenchant and sampled solution mix within the pull capillary and reach homogeneity downstream from the sampling tip as it flows toward the mixing tee. Furthermore, the diluent/quenchant solution does not reach the sampling tip and therefore does not contaminate the reaction solution (Figure 2-4 A). Using this basic model, we examined how the pull capillary ID, flow rates, and distance between the outer tip of the push and sample capillary (offset) affect performance parameters such as time required for mixing of quenchant with sample. We also evaluated what conditions would prevent leakage of diluent/quenchant into the reaction solution.

Table 2-1. Modeled effect of pull capillary ID on mixing time and travel time. Pull flow rate was modeled at 1.0 µL/min and a push flow rate was modeled at 0.5 µL/min.

Pull Capillary I.D.	Mixing Time	Travel Time	Total Time
150 µm	3.5 s	2.6 s	6.1 s
200 µm	3.5 s	2.8 s	6.3 s
250 µm	4.3 s	3.8 s	8.1 s
300 µm	8.6 s	5.0 s	13.6 s
400 µm	17.2 s	8.3 s	25.4 s
400 µm (centered)	9.4 s	12.4 s	21.8 s

Sample capillary inner diameter. The effect of sample capillary diameter was modeled (structure shown in Figure 2-3) to determine suitable dimensions for construction. Mixing time was defined as the time required to reach ≤ 5% variation in concentration across a plane perpendicular to the pull capillary, upstream of the pull capillary tip. Travel time was defined as the time required for sample to flow from the

outer tip of the pull capillary to the tip of the push capillary at the modeled flow rate. The effect of the pull capillary ID on time required to reach complete mixing is summarized in Table 2-1. Increasing the diameter dramatically increases the model-predicted mixing time because the solutions mix primarily by diffusion under the flow rates tested. Increasing the pull capillary ID also increases travel time due to a slower linear flow velocity. Although short mixing times are desirable, we found that fabricating the sampler with a pull capillary ID <250 μm was difficult because the push capillary was very flexible and tended to rest against the pull capillary. Therefore, the sampler design tested had a 250 μm ID pull capillary. The nested capillary system was modeled with the push capillary off-center in the pull capillary, based on observations of the push capillary resting against the pull capillary in initial sampler prototypes. Further decreases in mixing time can be achieved by centering the push capillary within the pull capillary (see Table 2-1); however, using the materials and methods described here, it was difficult to achieve centered capillaries.

Effect of modeled flow rate on mixing. We next evaluated the effect of flow rates on mixing time. The time required for complete mixing increases with decreased pull flow rate when the push flow rate is modeled at 50% of the pull flow rate (Table 2-2). Time required for mixing is increased by less than 1 s for a 10-fold decrease in pull flow rate. Because mixing is primarily diffusion-controlled and thus dependent on the width of the channel, the slower mixing time at lower flow rates is due to a higher percentage of time spent in the wider pull channel before being swept into the more narrow space between the push and pull capillary where mixing occurs more rapidly. The difference in travel time from 3.8 to 37.4 s for the same 10-fold decrease in pull flow

rate is much more dramatic. To minimize the effect of travel time, the offset between the pull capillary and the recessed push capillary may be decreased to <1 mm at lower flow rates.

Table 2-2. Modeled effect of flow rate on mixing time and travel time. When relative push-to-pull flow rate is held constant, an increase in pull flow rate results in a small decrease in mixing time.

Pull Flow Rate	Push Flow Rate	Mixing Time	Travel Time	Total Time
0.1 μL/min	0.05 μL/min	4.7 s	37.4 s	42.1 s
0.5 μL/min	0.25 μL/min	4.5 s	7.5 s	12.0 s
1.0 μL/min	0.5 μL/min	4.3 s	3.8 s	8.1 s
2.0 μL/min	1.0 μL/min	4.3 s	1.9 s	6.2 s

Relative push flow rates and capillary offset. Modeling was used to determine the appropriate offset between the pull capillary tip and the recessed push capillary (marked on Figure 2-3 B). The offset needs to be small to minimize time between when the sample is removed from the reaction vessel and when it is mixed with diluent/quenchant. If the offset distance is too short, however, the diluent/quenchant may be able to leak into the bulk solution, affecting the ongoing reaction that is being monitored. It was determined that for a push flow rate of 95% of the pull flow rate, the distance to which the diluent/quenchant spread (local concentration 1% of the original quenchant concentration) was 0.51 mm (Figure 2-4). Based on this result, a 1 mm offset should be sufficient to ensure that the diluent/quenchant does not leak into the bulk sample for a push flow rate up to 95% of the pull flow rate.

In practice, when blue food color, diluted in water, was flowing through the push capillary, leakage into the bulk solution was observed visually when the push rate was

only 90% of the pull rate. This discrepancy may be due to small fluctuations in the flow rate due to pulsing from the syringe pumps. We used a 1 mm offset distance in all subsequent investigations, but a shorter offset distance could be used to facilitate faster mixing if a lower push flow rate is used.

On-line Dilution. The total volumetric flow rate through the pull capillary is the sum of the volumetric flow rates through the push capillary and the volumetric flow rate from the sample. Therefore, adjusting the ratio of the push to pull volumetric flow rates controls the mixing ratio of the sample with either a quenchant or diluent. For a constant pull flow rate, increasing the push flow rate should result in predictable dilution of the sample. To confirm this performance, we varied the push flow rate with a constant pull flow rate while sampling dilute blue food color and monitoring the resulting using the direct monitoring system. We found that diluting resulted in the expected decrease in UV absorption (Figure 2-5) for diluted sample as measured downstream. These results also match modeling data (Figure 2-4B). These results further supported that the push solution does not leak out of the sampler and demonstrated predictable operation of the sampler for on-line dilution.

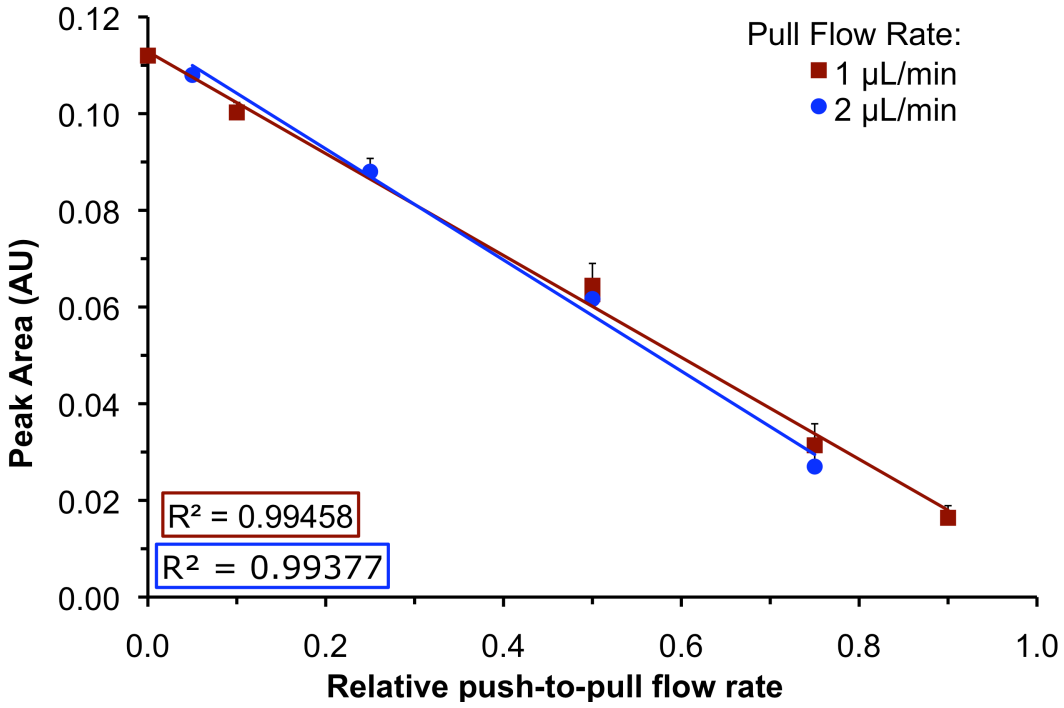

Figure 2-5. Peak areas versus push-to-pull flow rate. As the relative push-to-pull flow rate increases, the sample is more diluted. Peak area decreases linearly with increasing relative push-to-pull flow rates.

Delay and Response Time. An inherent delay time exists between the time sample is collected and the time that signal is detected downstream of the sampler. Delay time is defined as the difference between the time when a chemical that causes a change in absorbance (observed downstream) is added to the stirring sample vial and when 50% of the maximal value of the step change is observed at the detector. Response time is defined as the time required to observe a change from 10% to 90% of the maximal value following a step change in analyte concentration. Delay times ranged from 111.5 ± 3.4 s to 317.0 ± 8.8 s (Table 2-3), depending on the flow rate and agreed with expected delays based on tubing volume. Response times varied from 26.6 ± 1.0 s to 52.4 ± 5.8 s over the same flow rate range. Tests performed without the sampler and only the transfer tubing revealed that both parts of the system contributed significantly to the delay and response

time. These results suggest the limits of feedback control and rate of reaction that can be monitored by this approach.

Table 2-3. Delay and response time. Time (s) is ± standard deviation (n=3) for each value. Step changes in blue food color concentration were recorded with the sampler connected to the detection capillary as well as with the sampler removed (to show delay and response time due only to the detection capillary).

	Delay Time		Response Time	
Pull Flow Rate	Sampler	No sampler	Sampler	No sampler
1 (μL/min)	317.0 ± 8.8 s	203.9 ± 3.6 s	52.4 ± 5.8 s	19.6 ± 1.3 s
2 (μL/min)	160.0 ± 1.2 s	103.3 ± 3.9 s	34.9 ± 2.2 s	11.9 ± 0.8 s
3 (μL/min)	111.5 ± 3.4 s	69.1 ± 1.8 s	26.6 ± 1.0 s	10.4 ± 0.5 s

Stop-flow sampling. The sampler was designed for continuous sampling; however, with small samples or slow reactions, it may be advantageous to run the sampler in a non-continuous mode to minimize sample consumption. One approach is to remove the sampler from the solution, but this may not always be feasible depending on the reactor. Therefore, we examined using flow effects within the sampler to stop and start sampling. As discussed above, the total pull flow rate is equal to the sum of the sampling flow rate and the push flow rate. This allows the sampling flow rate to be decreased by increasing the push flow. If the push rate equals the pull flow rate, there would be no sampling; however, the push solution would likely diffuse into the reaction solution. Experimentally, we observed that the push flow rate could be increased to 90% of the pull flow rate without push solution leaking into the reaction vessel. At this fraction, the sampling flow rate was only 10% of the total pull flow rate and nearly

stopped, e.g. at 1.0 µL/min, only 100 nL/min of sample was withdrawn. By modulating the push flow rate between 10% and 90% of the pull flow rate, sampling could be effectively switched from "on" to off".

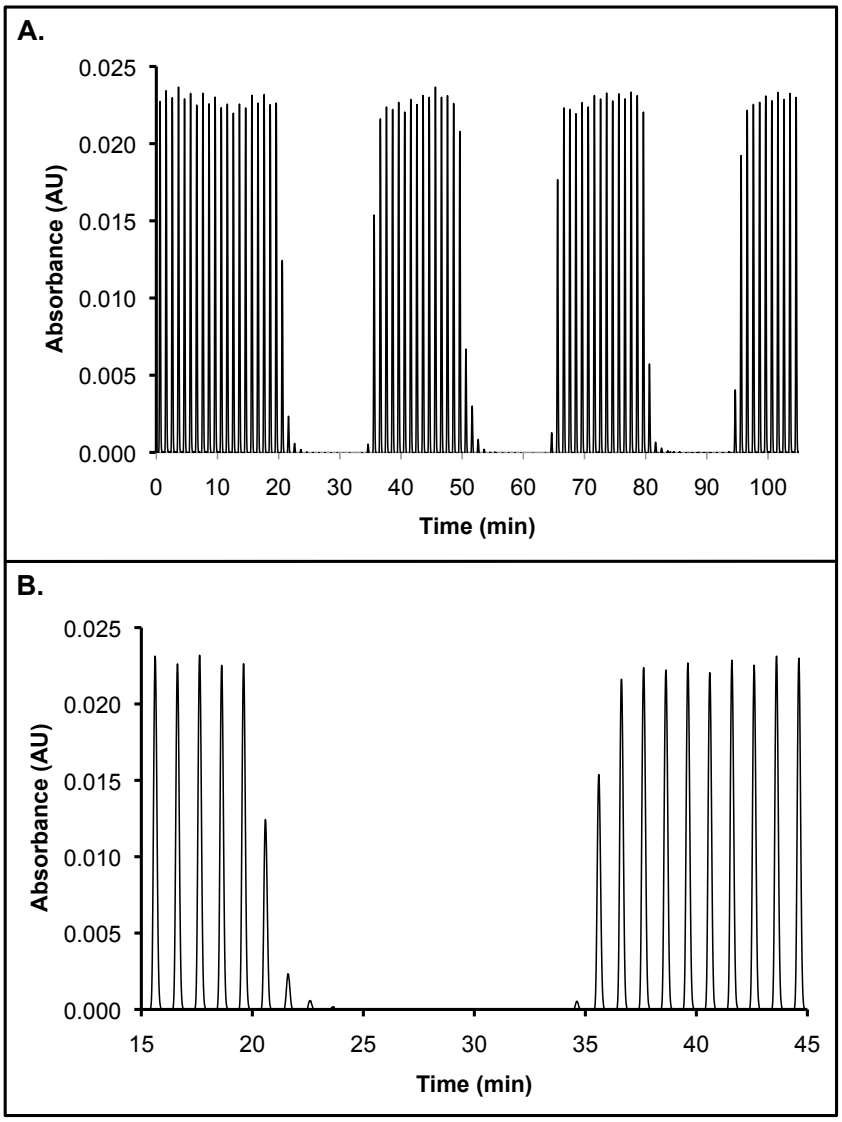

Figure 2-6. Stop-flow sampling. A. Plot showing FIA peaks when the push flow rate is switched from 10% of the total pull flow rate ("sampling on") to 90% ("sampling off") and back to 10% every 15 minutes. This feature may be used to control sample consumption when continuous sampling is not desired. B. Zoomed view of FIA peaks.

To demonstrate the possibility of stopping and starting sampling in this way, we sampled dilute blue food color, diluted in water, with water flowing through the push

capillary. Sampling was performed at 1.0 μL/min and the mixed solution was monitored by FIA. Switching the flow rates from 0.1 μL/min ("on") to 0.9 μL/min ("off") showed a change in the FIA peak heights in less than 5 minutes. Switching sample flow to "on" had a faster response of less than 3 minutes (Figure 2-6). Although the process of minimizing sample flow is not fast, it may be useful for conserving sample during slow reactions. While monitoring an enzymatic reaction, the reaction could be monitored continuously during the rapid early substrate turnover, and stop-flow sampling could be used for monitoring the reaction as turnover slowed.

Particles. While this sampler was designed for homogenous samples, pharmaceutical reactions may have solid particles present, either cells and cell debris for biological reactions, or solid catalysts and precipitated reagents for organic synthesis reactions. We investigated the effect of particulates on sampling using polystyrene beads. We first tested beads of several different sizes, suspended in solution, to determine any differences in sampling as compared to a solution with no beads present (Figure 2-7 A). It was determined that 10.0 μm beads generally passed through the sampling system and the peak heights were the same as a solution with no particles. At higher flow rates, the 100 μm beads did not enter the sampler and consistent sampling was observed. However, the 100 μm beads clogged the detection capillary at 1 μL/min pull flow rate and sampling could not be continued without disassembly of the sampler (no data point provided). The 100 μm beads appear to flow into the pull capillary, stopping the flow through the system. The 500 μm bead sample ran without clogging while sampling at 4 μL/min, but exhibited flow problems when the system was switched to 2 μL/min, which increased with time as the system was switched to a 1 μL/min flow

rate (thus the low peak height for 500 μm particles, 50% sample). The 500 μm beads appear to stick to the tip of the pull capillary, causing irregular flow and lower sample flow rates.

We also investigated the effect of bead concentration on sampling, using 10.0 μm beads. At higher flow rates, consistent sampling between bead concentrations (from 0 beads/mL to $1x10^6$ beads/mL) was observed. At a pull flow rate of 1 μL/min, clogging was observed for the solution with 1×10^5 beads/mL, resulting in lower sample flow (Figure 2-7 B). While this clog was able to be cleared by reversing the flow through the sampler, high concentrations of particles may cause clogging of the sampler and result in inaccurate sampling. To ensure regular sampling, free-floating solid materials should be avoided or minimized in samples.

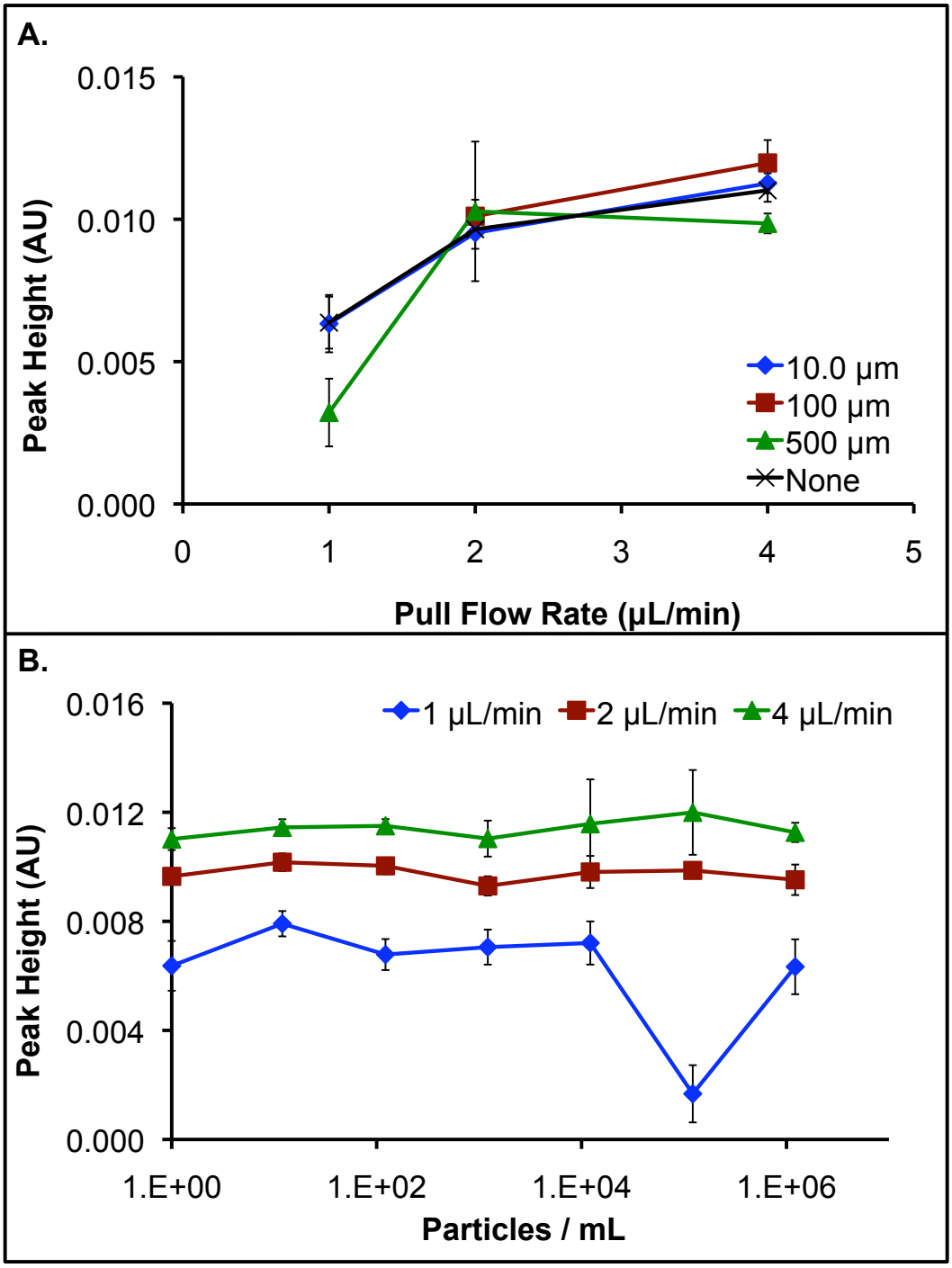

Figure 2-7. Effect of particles on push-pull sampler. A. Peak heights at increasing flow rates for three bead diameters, as compared to a solution with no beads present. B. Effect of 10.0 µm bead concentration of peak height at various flow rates.

Viscosity. As pharmaceutical reactions may take place in solutions over a range of viscosities (0.2 – 6 Pa•s is the range of interest, see Table 1-1) we examined the effect of viscosity on the ability to sample by sampling blue food color in solutions with different viscosities that were adjusted by addition of glycerol. Viscosity of the solution was found to affect the maximal pull flow rate that could be used. For any solution, a threshold pull flow rate exists above which cavitation is observed in the pull syringe, resulting in unreliable flow rates. Above a viscosity of 4.5 Pa•s, it was not possible to sample without cavitation down to the minimal flow rate tested of 1.0 μL/min (Figure 2-8 A). This effect imposes a restriction on the system that lower flow rates must be used for sampling high viscosity solutions. The reproducibility of sampling was evaluated at viscosities ranging from 1.5 to 4.8 Pa•s as a function of flow rate. At a pull flow rate of 2.0 μL/min, and a push flow rate of 1.0 μL/min, the absorbance readings for 1.5 Pa•s, 2.6 Pa•s and 4.8 Pa•s viscosity solutions were $3.1 \pm 0.2 \times 10^{-3}$, $3.3 \pm 0.2 \times 10^{-3}$ and $3.2 \pm 0.1 \times 10^{-3}$, respectively, averaged over 20 injections (Figure 2-8 B). The constant absorbance with increasing viscosity shows that the viscosity does not affect quantitative sampling in this range.

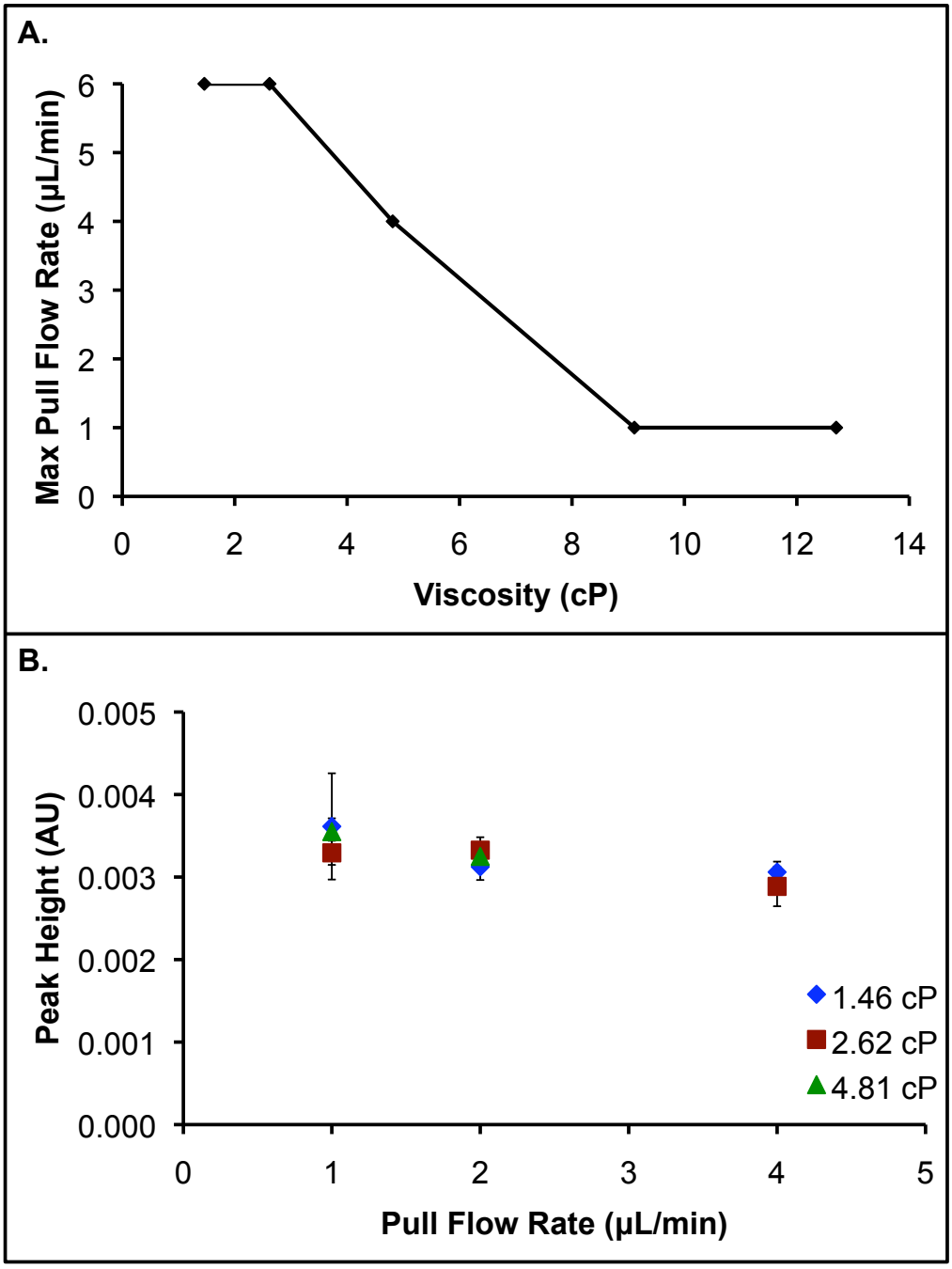

Figure 2-8. Effect of sample viscosity on push-pull sampler. A. Maximum pull flow rate achieved before cavitation observed for solutions of a range of viscosities. B. Peak height is not affected by the solution viscosity at pull flow rates less than maximum at each viscosity.

Monitoring an enzymatic reaction with FIA. The utility of the sampler for monitoring reactions that change on a minute time-scale was demonstrated by monitoring the turnover of colorless substrate Amplex Red to a highly colored product, resorufin, in the presence of horseradish peroxidase and hydrogen peroxide with FIA (Figure 2-9 A). The reaction was quenched using Amplex Red Stop Reagent, a proprietary reagent that halts the turnover of Amplex Red for 3 hours, according to the manufacturer. As expected, the reaction rate increased with greater concentrations of horseradish peroxidase present in the solution. The push-pull sampler is able to monitor this change, with injections of quenched sample to the capillary detector every minute (Figure 2-9 B), demonstrating the utility of the sampler for monitoring an enzymatic reaction.

This system was also used to verify quenching of the sample solution. Without quenching with Amplex Red Stop Reagent, the Amplex Red substrate continues to turn over quickly in the presence of HRP and hydrogen peroxide. To verify the sample is quenched in online push-pull sampling, aliquots of the reaction were removed manually while the reaction was running and were quenched manually offline. The absorbance for each offline sample was recorded using an absorbance plate reader. A plot of offline sampling versus online sampling shows that although the absolute value of the absorbance is different (different path lengths, different detectors), the two plots may be overlaid (Figure 2-9 C). If quenching did not occur, the plots should not overlap.

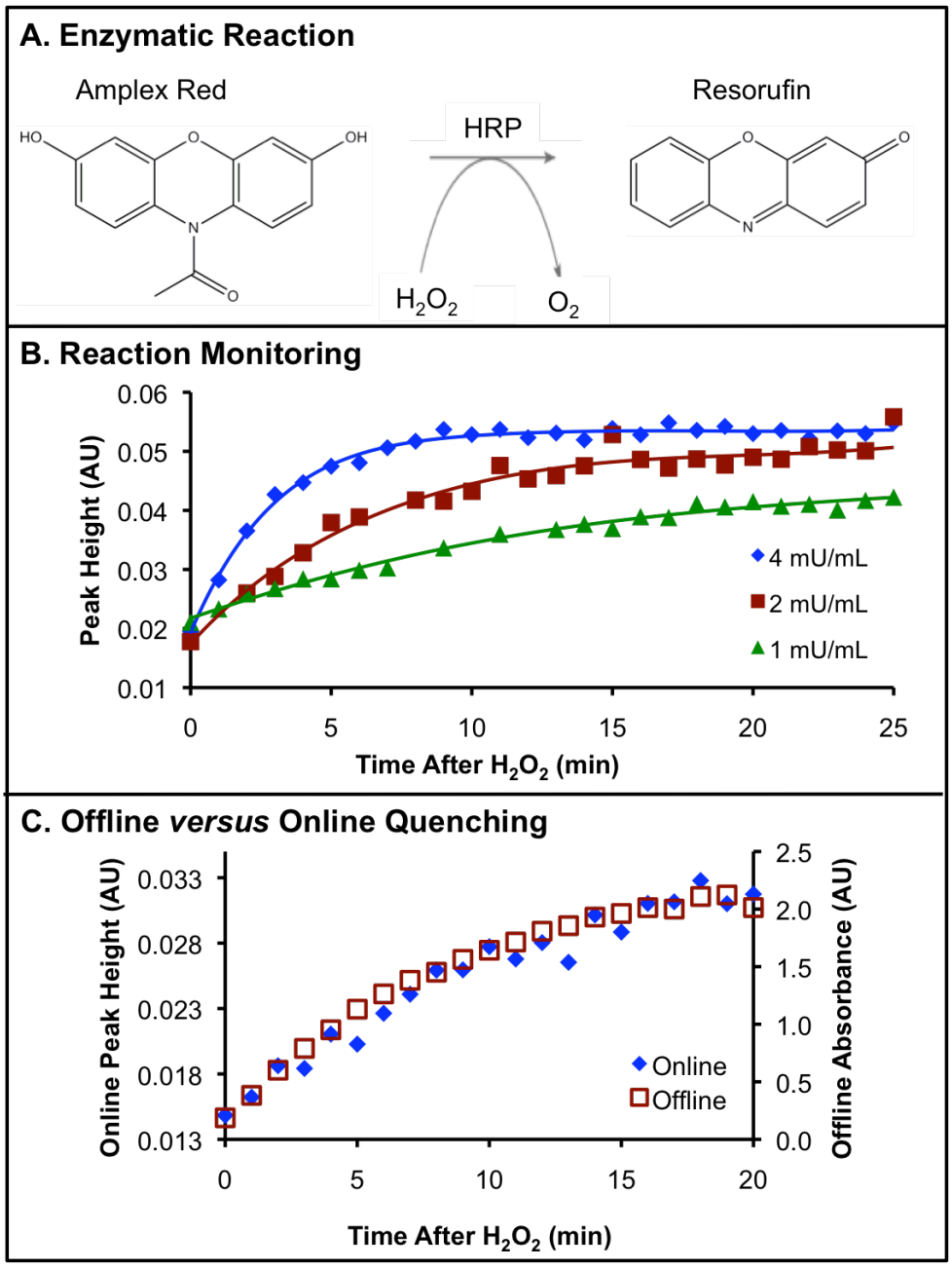

Figure 2-9. Monitoring an enzymatic reaction with push-pull sampler. A. Amplex Red substrate turn-over in the presence of horseradish peroxidase (HRP) and hydrogen peroxide to form the colored resorufin product. B. Resorufin product formation monitored after the addition of hydrogen peroxide to a solution of Amplex Red and 1, 2 or 4 mU/mL HRP, demonstrate the ability to monitor an enzymatic reaction with the push-pull sampler. C. Overlay plot of reaction quenched online (push-pull) versus offline (well plate) indicating online quenching is equally effective.

Organic reaction monitored by HPLC. The system was coupled to an HPLC system to show on-line monitoring of a reaction with automated separation and detection. Base-catalyzed hydrolysis of acetylsalicylic acid (aspirin) results in the production of salicylic acid and acetic acid (Figure 2-10 A). Monopotassium phosphate buffer (10 mM, pH 2.3) was used as the quenchant as it changed the pH of the mixed sample to approximately 7, stopping the reaction long enough for it to be analyzed with the HPLC. The efficacy of the phosphate buffer to halt the turnover of acetylsalicylic acid is demonstrated in Figure 2-10 B. After adding acetylsalicylic acid to the bicarbonate buffer, an aliquot was immediately removed, mixed with quenchant offline, and run on the HPLC using the autosampler (Figure 2-10 B, 0 min). This was repeated for the same sample after it was allowed to hydrolyze for 15 minutes (Figure 2-10 B, 15 min). The increase in the salicylic acid peak (open circle) can be seen over just 15 minutes. After standing at room temperature for 2 hours, the quenched sample from 0 minutes was run again (Figure 2-10 B, 0 min (2 hr)). Although there is a small increase in the salicylic acid peak compared to the initial run, it is considerably less than the product formation due to just 15 minutes of hydrolysis. The phosphate buffer was deemed an acceptable quenchant for this reaction.

As acetylsalicylic acid was hydrolyzed, sample was collected, quenched, and automatically injected onto the HPLC every 5 minutes for 1.5 hours. For each injection, acetylsalicylic acid and salicylic acid were separated within 3.5 minutes, with a decrease in acetylsalicylic acid peak area and an increase in salicylic acid peak area over time (Figure 2-10 C). Peak areas, normalized to the initial acetylsalicylic peak are shown for three replicate experiments (Figure 2-10 D). It is believed that the increased standard

deviation at the end of the experiment was due to air becoming trapped in one of the sample loops for one of the replicates.

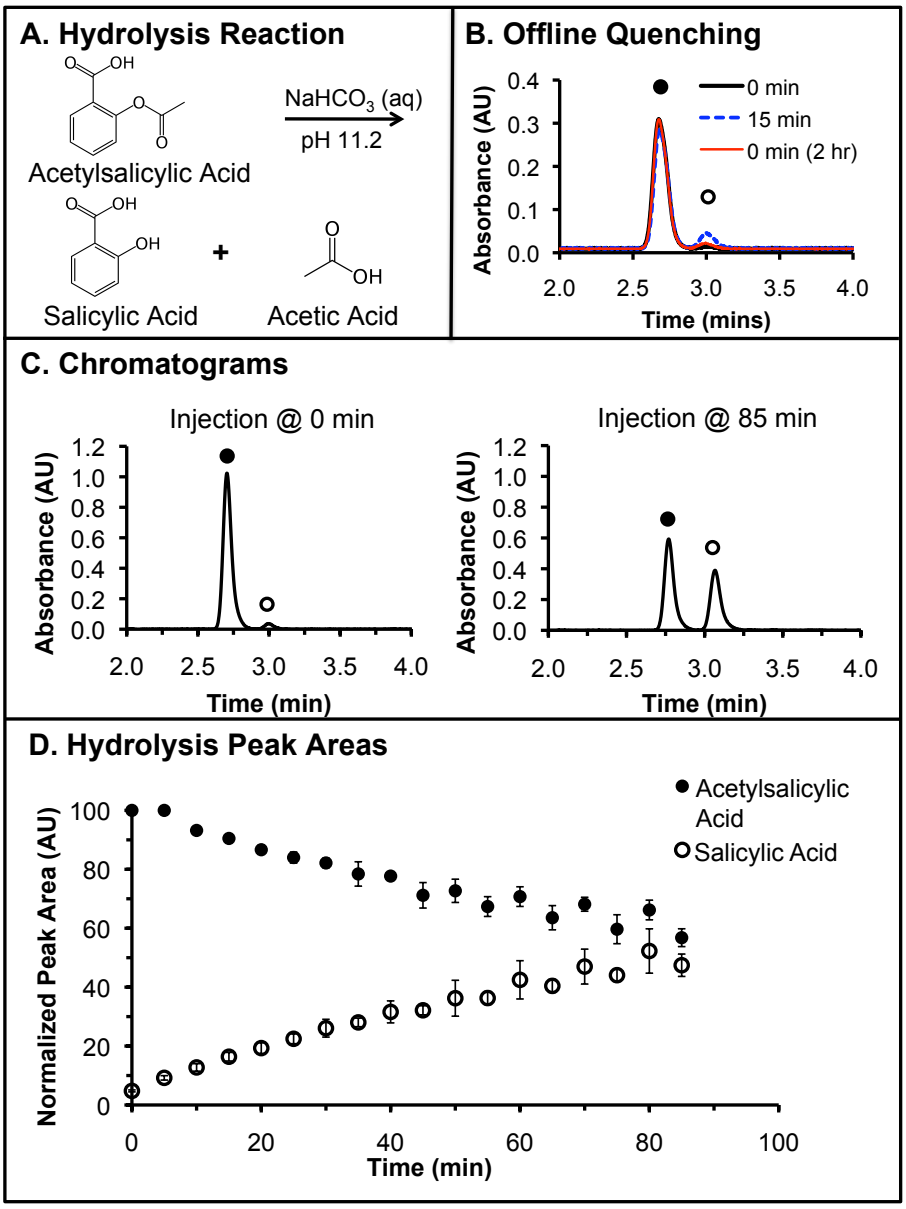

Figure 2-10. Monitoring an organic reaction with push-pull sampler. A. Base-catalyzed hydrolysis of acetylsalicylic acid to salicylic acid and acetic acid. B. Acetylsalicylic acid sample quenched at 0 minutes hydrolysis and allowed to stand for 2 hours has less turnover to salicylic acid than a sample that is allowed to hydrolyze for 15 minutes and is immediately quenched and run. C. Chromatogram of aspirin and salicylic acid injected at 0 minutes and 85 minutes following the start of the hydrolysis reaction. D. Plot of aspirin and salicylic acid peak areas monitored with HPLC. Peak areas were calculated from chromatograms using in-house software.

This experiment demonstrated the utility of the sampler for near real-time monitoring of an ongoing reaction. For each sample, the reaction was halted upon removal by a shift in pH caused by the addition of phosphate buffer (pH 2.3) through the push capillary, and was automatically analyzed with HPLC. The reaction progress from acetylsalicylic acid to salicylic acid was observed and individual chromatograms could be obtained for any given time point, showing a snapshot of the reaction in progress. Beyond initial loading of reagents, the entire monitoring process was automated, removing the time and potential errors from manual interventions.

Conclusions

A push-pull sampling device was demonstrated for monitoring API synthesis. The system allowed sampling from solutions with a range of viscosities and automated the mixing of quenchant or diluent with sample as part of pre-analysis processing. The system was readily coupled to an on-line detector, flow injection analysis, or HPLC. The device is capable of quenching in 5 s at the sampling site. Flow properties prevented quenchant or diluents from leaking into the reaction vessel and allowed the possibility of stopping sampling periodically. The ability to monitor an ongoing reaction has been demonstrated under completely automated conditions. Computer control of pumps, valve and detector through LabVIEW software allow for sampling to be automated.

This sampler design fills a need in pharmaceutical PAT for sampling from very small-scale reactions (several milliliters). At the flow rates tested in this work, only 30 μL of sample is removed for every hour of continuous monitoring. The system may be run at lower flow rates if needed, and the stop-flow feature could be utilized if it was

necessary to sample for several days, necessitating the minimization of sample volume removal.

While this sampler design is promising, it is not suitable for all types of reactions. As the sampler is directly in contact with the reaction for long periods of time, the fused silica sampling tip would not be suitable for high pH samples. The fused silica capillary is also relatively fragile, which may require the use of coatings or other material to improve the robustness of the sampler for daily use in a pharmaceutical setting. Future work will be focused on testing the sampler system with a broad range of reactions, particularly with homogenous reactions to further evaluate its utility for pharmaceutical PAT and to determine if other materials would be more suitable for the sampler design.

CHAPTER 3

SEGMENTED FLOW SAMPLING DEVICE WITH FAST REACTION QUENCHING COUPLED TO HPLC FOR PHARMACEUTICAL PAT

Introduction

One of the primary challenges in near real-time pharmaceutical sampling is the ability to sample from very small-scale research reactions (several milliliters total volume). In this work we present a sampler design that is capable of drawing up a small volume of sample (0.1 – 2 μL), mixing each sample with quenchant, and injecting the mixed sample into an HPLC. This system allows for sampling on demand, rather than continuously, using less of the reaction volume over a long period of monitoring.

Segmented flow uses two or more immiscible fluids in a microfluidic system to create small, isolated fluid segments. In order for the fluid of interest to form a plug, the surface tension between the fluid of interest and the other, immiscible fluid must be lower than the surface tension between the fluid of interest and the channel wall.[79] These sample plugs have limited axial dispersion (not able to undergo dispersion beyond the length of the plug) and do not interact with previous or subsequent plugs.[80] The additional of a third immiscible fluid aids in keeping each sample plug separate when adding reagents or transporting plugs through tubing.[81] When sampling, this allows for each plug to be representative of a particular time point, even after multiple manipulations (reagent addition, mixing, splitting) downstream. This was demonstrated

with microdialysis sampling from a rat brain for offline analysis with a temporal resolution of as little as two seconds.[82] Additional information about segmented flow may be found in reviews of the topic.[79, 83, 84]

One of the problems with using segmented flow is interfacing the droplets with separations methods downstream. One of the phases may be detrimental to the separation process, and it must be removed before analysis may occur. The effect of fluorinated oil continuous phases on and RP-HPLC column has been presented in Appendix A. While it is possible to use a continuous phase that is not detrimental to the separation (such as small volumes of air with RP-HPLC), it is often preferable to simply remove the continuous phase before the separation step. One method for separating multiphase flow is to press a membrane between two channels, applying pressure to the segmented flow in one channel. The surface properties of the membrane will allow one phase to preferentially wet the membrane, passing through to the second channel, while the other phase remains in the first channel. This has been demonstrated to separate hexane and perfluorohexane from water, although the separation of hexane and perfluorohexane was not achieved with the membranes tested.[85] Similar principles were used to separate chloroform and water, even in the presence of particulates, using a micro-machined polytetrafluoroethylene (PTFE) comb-like structure to preferentially push chloroform through the hydrophobic channels, leaving the aqueous phase behind.[86] Aqueous samples have been separated from a fluorinated oil using derivatized channels on a microfluidic chip coupled directly to capillary electrophoresis (CE) separation and on-chip laser-induced fluorescence detection.[87]

Segments were produced by aspirating up small volumes of sample or quenchant, followed by the continuous phase (a fluorinated oil) using a syringe pump in withdrawing mode. This method is particularly useful when multiple samples are being prepared for later analysis downstream. We were inspired by a paper that used this method,[88] along with the coalescence properties of segmented flow, to achieve rapid mixing of sample and enzymes for reverse transcription polymerase chain reaction (RT-PCR). We developed a sampling method that utilizes the unique properties of segmented flow for sampling over time from a set of 5 mL glass vials, with rapid mixing of quenchant to stop the reaction for downstream analysis.

Experimental Section

Materials. Perfluorodecalin (mixture of cis and trans, 95%) and dibutyl phthalate (99%) were purchased from Acros Organics (Morristown, NJ, US). Fluorinert FC-40 and 1H,1H,2H,2H-perfluoro-1-octanol were purchased from Sigma Aldrich (St. Louis, MO, US). Fluorinert FC-770 was obtained from 3M (St. Paul, MN, US). Red, yellow, green and blue food color was sourced from McCormick (Sparks, MD, US). All water used was deionized to 18 MΩ resistivity with an E-pure 1090 series system from Barnstead Thermolyne Cooperation (Dubuque, IA, US). Unless otherwise noted, all other chemicals were purchased from Fisher Scientific (Chicago, IL, US).

Sampler probe. The sampler probe consists of a length of narrow-bore (150 μm I.D., 360 μm O.D.) perfluroalkoxy (PFA) aspirating capillary (Upchurch Scientific, Oak Harbor, WA) inserted into a length of wide-bore (508 μm I.D., 1588 μm O.D.) PFA mixing capillary, secured externally with sticky wax (KerrLab, Orange, CA). A length of narrow-bore PFA transfer capillary was used to connect the other end of the mixing

capillary to a syringe on a withdrawing syringe pump (Harvard Instruments, Holliston, MA). The pump may be started and stopped to aspirate a volume of fluid through the tip of the aspirating capillary.

Sample stage. The sampler consists of the sampler probe and a sample stage. The sample stage tray typically holds a 7 x 4 array of 1 dram glass vials (Fisher), but may be used with a 96-well plate or other reactor vessels as well. The sample tray is mounted on an XY-stage in order to select an individual vial/well. A Z-axis linear actuator is used to move the sampler probe up and down to gain access to the vials. The vials are labeled rows A-D and columns 1-7. For a typical run, a quenchant/diluent is placed in vial A1, sample in A2, fluorinated oil in A3, a waste vial in A4 and fluorinated oil in A5. The sampler probe, previously filled with oil, is lowered into the quenchant/diluent, and the pump is turned on for a specified amount of time to aspirate a small volume of quenchant/diluent (A1) into the aspirating capillary (Figure 3-1 A). The pump is stopped, and the droplet mixer is lifted out of the sample vial. The sample tray is moved and sample (A2) is pulled into the aspirating tip adjacent to the plug of quenchant/diluent (Figure 3-1 B). The droplet mixer is then moved to fluorinated oil (A3). The quenchant/diluent and the sample plugs are pulled sequentially into the wide mixing capillary (Figure 3-1 C).

The transfer capillary passes through either a variable wavelength detector (for direct detection) or an 8-port injection valve for transfer to HPLC. If using direct injection, the droplet is pulled past the detection point for analysis. When used with HPLC, the mixed sample is pulled through an injection loop on a switching valve, overfilling the loop. The valve is actuated and the sample is injected without oil. Once

detection is complete, or sample is injected, the stage is moved to a waste vial (A4) and the pump is reversed, clearing the sample from the system. The stage is finally moved to a secondary vial of fluorinated oil (A5) where a small volume is aspirated to ensure the sampler is primed for the next sample. The droplet mixer is mounted on a Z-axis linear positioner, allowing the mixer tip to be lowered into the desired sample vial. A program to control the XY-stage, the Z-axis positioner, and starting and stopping the syringe pump was created in-house with LabVIEW by Mr. Stephen Parus.

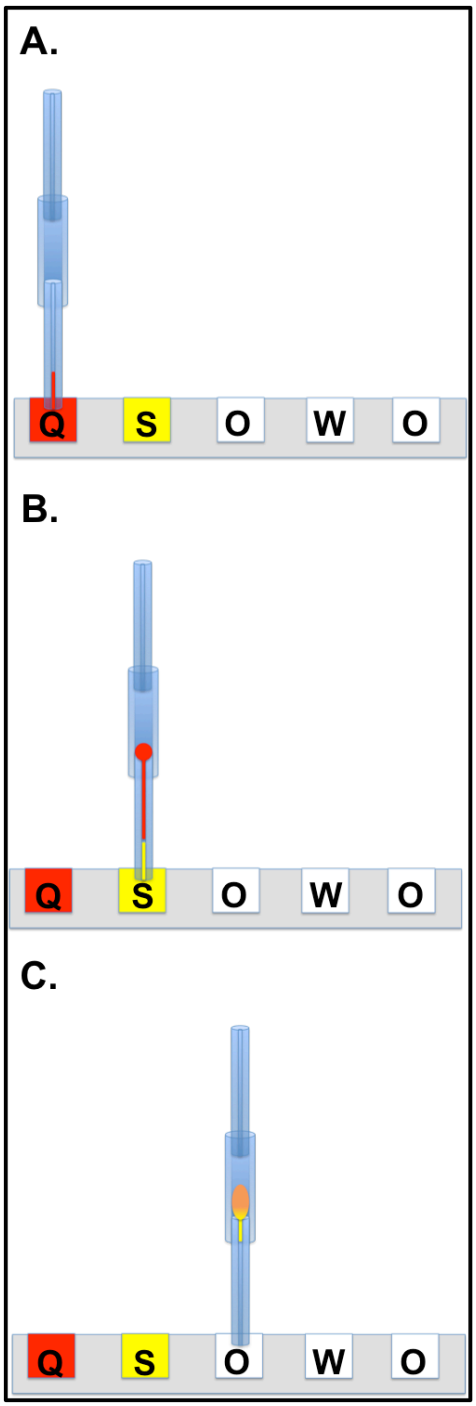

Figure 3-1. Overview of droplet sampling. Quenchant (Q), sample (S), fluorinated oil (O) and waste (W) vials are placed on a movable stage. A. Small volume of quenchant is aspirated into the probe using a withdrawal syringe pump. B. Small volume of sample is aspirated into the probe. C. Oil is pulled into the probe and the quenchant and sample plugs coalesce, mixing as they travel up the mixing capillary.

Oil/solvent capability. Glass vials containing 1 mL of each solvent (toluene, methanol, water, ethanol, or isopropanol) were placed in sample positions 1 and 2. A fluorinated oil, selected from FC-770, FC-40, or PFD, was placed in a glass vial in sample position 3. The same oil was used to fill the PFA sampler tubing. To aid visibility, one vial of toluene was colored with Disperse Blue 14 while the other was colored with Disperse Orange 25. Water, methanol, ethanol and isopropanol were colored in a similar manner with blue food color (BFC) and yellow food color (YFC). Aliquots of each solvent (1 μL yellow, 1 μL blue) were drawn up into the PFA capillary in turn, followed by 2 μL oil. All droplets were ejected from the Teflon tubing between solvents. The PFA tubing was rinsed with air and the new oil three times before tests were started with new oil.

Droplet Coalescence. Solutions of 0.2 M iron (III) nitrate and 0.6 M potassium thiocynate were prepared as sample and quenchant. The two solutions are pale yellow and clear, respectively, but turn deep red upon mixing. Equal volumes of each reagent were pulled into the sampler probe for the time and at the flow rate indicated. Each point was identified as coalescing, not coalescing (droplets remained separate), borderline (3/5 droplets coalesced) or poor mixing (droplets coalesced, but they did not mix across the new droplet).

On-line Dilution. The XYZ stage was set up with water in a glass sample vial in sample slot 1. BFC diluted in water was placed in sample vial 2. FC-770 was used in sample vial 3. Water and BFC were drawn up in turn (total droplet volume 0.5 μL). Each droplet was sampled 6 times and the absorbance data was measured with a variable

wavelength detector at 280 nm. The relative volume of BFC was varied to create a calibration curve.

Using HPLC to Monitor the Hydrolysis of Dibutyl Phthalate. To better mimic a reaction of interest to the pharmaceutical industry, we monitored the base-catalyzed hydrolysis of dibutyl phthalate (DBP) using HPLC. To determine appropriate separation conditions, a mixed solution of hydrolyzed DBP and un-hydrolyzed DBP were mixed as a test solution (after quenching with acetic acid). Separation was performed on a guard column (Waters XBridge C18 column, 4.6 x 20 mm, 3.5 μm particles). Mobile phase A was 0.1% TFA in water and mobile phase B was MeOH. The best separation conditions were at 2 μL/min flow rate, with 1 minute @ 25% B and 1.5 min @ 75% B. With column re-equilibration, samples could be injected every 5 minutes. Samples were segmented with FC-770.

These conditions were used to analyze the base-catalyzed hydrolysis of dibutyl phthalate over a period of 3 hours. The sample was 2 mL 0.1 g/mL DBP in methanol mixed with 1 mL potassium hydroxide solution in methanol. The quenchant was 0.01 g/mL acetic acid in methanol (mixed with blue food color to visualize droplets in sampler). 2 μL acetic acid quenchant was drawn into the sampler, followed by 0.2 μL dibutyl phthalate sample. FC-770 was drawn in after the sample, causing it to mix with the quenchant. The quenched plug was pulled through a 0.5 μL fused silica injection loop by syringe pump (Figure 3-2). When the loop was overfilled with sample, the valve was triggered, injecting a portion of the quenched sample onto the column (Waters XBridge C18 column, 4.6 x 20 mm, 3.5 μm particles). While the sample was undergoing separation and detection, the syringe pump was reversed, ejecting excess sample to waste

and preparing the sampler for the next run. The sampler is able to perform runs "on demand", although the cycle time for this set of conditions was set to 15 minutes.

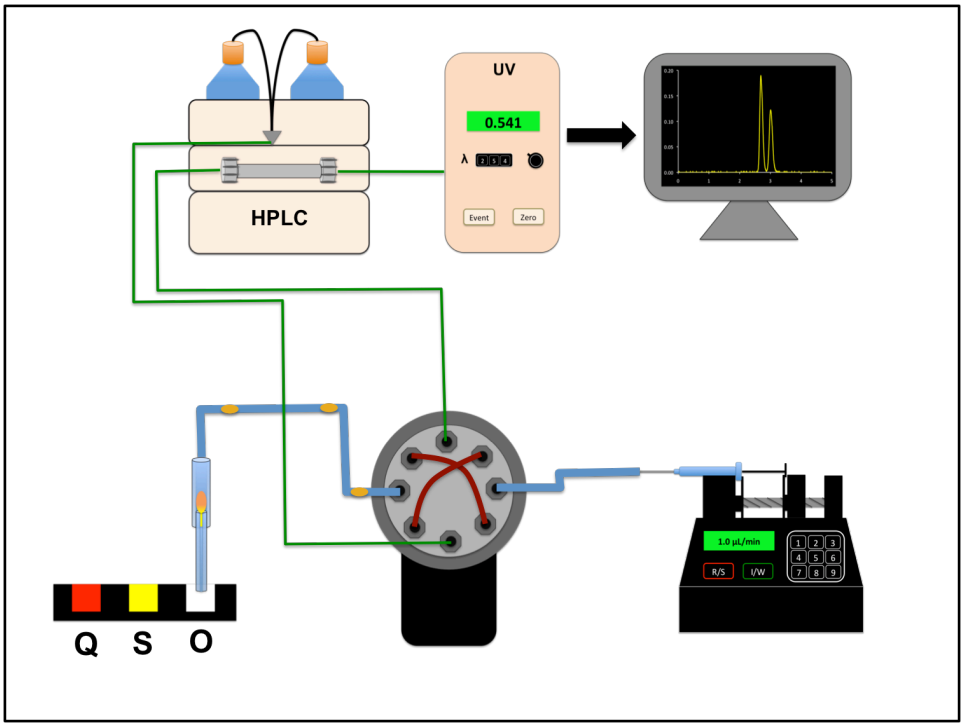

Figure 3-2. Overview of droplet sampler connected to HPLC. Mixed sample and quenchant is pulled through an injection loop on the 8-port valve and is injected onto the HPLC when the valve is triggered.

Improving automation. The bi-directional syringe pump was replaced with a flow selector valve (Valco) connected to syringes at a slow (1 µL/min) pull flow rate (for drawing up samples), a fast (4 µL/min) pull flow rate (for quickly moving samples to the HPLC), a stopped flow syringe (for moving the sampling probe between vials) and a fast (50 µL/min) push flow rate (for clearing samples and oil from the sampler probe). The computer program controlling the system was re-written to control this valve to select the appropriate flow rate. The new system was used to run a calibration curve with 0.067 g/mL dibutyl phthalate in methanol as the sample and 0.01 g/mL acetic acid in methanol as the quenchant. A volume of dibutyl phthalate was drawn into the sampler probe and

mixed with acetic acid for a total droplet volume of 2.2 μL. These droplets were injected onto the HPLC as described previously.

Results and Discussion

Sampler probe design. The original version of the probe used a short (1 cm) narrow-bore Teflon PFA capillary inserted within wide-bore Teflon PFA capillary. The capillaries were held in position using super glue. We determined that the super glue was too rigid and bending of the capillaries would release them to be free to move relative to each other. We also determined that if the full probe was dipped into a reaction, the solvent could wick between the outside of the narrow capillary and the inside of the wide capillary. This would not typically be a concern with biological solutions, as the super glue has been shown in other applications to fill spaces between capillaries and prevent wicking of solvents. When testing the probe with toluene as a solvent, the toluene was able to dissolve the super glue and wick between the capillaries. This necessitated the construction of a new probe, which would require several hours to insure the glue is sufficiently dry for further use. Two adjustments were made to the probe to solve this problem. First, the narrow capillary was made at least as long as the deepest part of the vessel that it was created to dip into, making sure the interface between capillaries never came in contact with the reaction fluid. Only Teflon PFA (relatively chemically inert) could come in contact with the reaction. The fluorinated oil preferentially coating the inside surface of the PFA tubing insured that the reaction did not make contact with the interface between capillaries internally. Second, super glue was no longer used to connect the two capillaries. Capillary wax or sticky wax was used to secure the

connection as they could be melted, applied in a small area, cooled, and ready to use in a matter of minutes. The waxes, however, have not been tested for compatibility with any of the reactions, so it is recommended that they not come in contact with the reaction solvent as it may dissolve the wax, destroying the probe or contaminating the reaction.

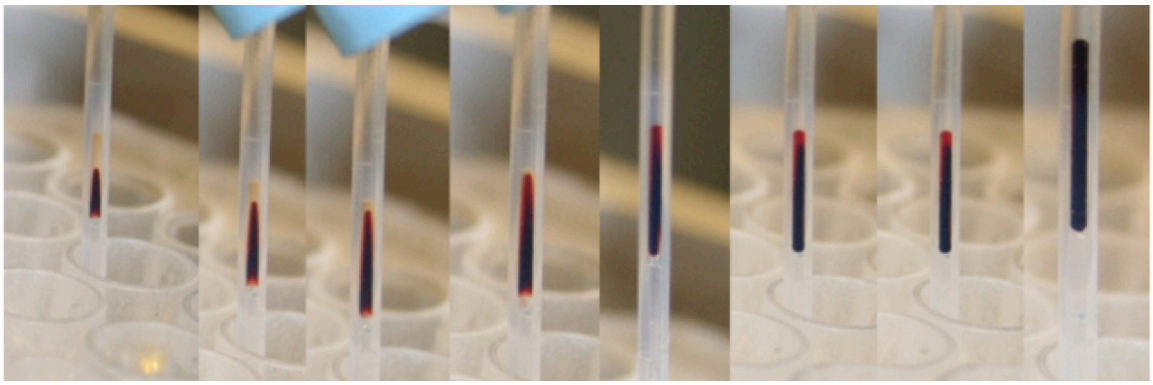

Figure 3-3. Visualization of droplet coalescence: Solutions of 0.2 M iron (III) nitrate and 0.6 M potassium thiocynate were used to provide a visual indication of droplet coalescence. The iron (III) nitrate solution is pale yellow and the potassium thiocynate solution is clear but upon mixing they rapidly turn a deep red-brown color.

XYZ motion. A stainless steel stage was originally built to appropriate dimensions to hold a standard 96-well plate securely. Polystyrene plates are commonly used for many biological assays, but they are not chemically compatible with many organic solvents, such as acetone or toluene. The stage was adapted to hold 1 dram glass vials. A simple system of cardboard inserts held the vials in a grid pattern, increasing the variety of volumes and types of reactions that could be carried out. The stage could easily be adapted to other vessel sizes and shapes if an appropriate adapter was created to hold the vessel securely in place on the stage.

The stage was mounted on linear actuators that allowed programmed movement in the x and y directions. This provided random access to any well or vessel by moving to the correct x and y coordinates. The stage design creates the possibility that multiple reactions could be sampled from using the same apparatus. The sampler probe was mounted on a third linear actuator, fixed in the x and y directions, but allowed to move up and down in the z direction. To access a particular reaction vessel, the stage was moved to the appropriate position so the sampler probe was directly over the vessel opening. The sampler probe was lowered in the z direction until it was at the selected height in the reaction volume. This design allows for sampling from any height in the reaction vessel, which would be very useful if the reaction contains immiscible liquids and the researcher wishes to select from one layer or the other.

Reaction Vessels. Initial testing was performed with 96-well polystyrene plates. Our first experiments repeated the work performed by Chabert et al.[88] The plates were modified by filling each well with 100 μL water and spraying the entire plate with a Teflon aerosol spray to change the surface properties of the plate. Once the coated plate was dry, the water would be removed and the plate would be rinsed and dried, leaving the bottom section of each well hydrophilic and the top section very hydrophobic. The reaction mixture would be placed into the bottom of the previously prepared well, and fluorinated oil would be layered on top. The entire plate would be covered in an aqueous wash layer. The surface tension of the fluorinated oil against the Teflon-modified portion of the plate was sufficient to overcome the density difference between the more dense oil and the less dense water. While this was demonstrated to work very well for PCR reactions, this method was not suitable for reactions not carried out in an aqueous

environment. Testing the system with alcohols caused the oil and alcohol reaction layer to invert. When the sampling probe was placed at the bottom of the well, oil was sampled rather than the alcohol that was floating at the top of the well after inversion. We performed tests and demonstrated that the wash layer was not necessary. This still left us with the problem that non-aqueous samples would invert. After further testing, we determined that the oil layer was not necessary. The small amount of air pulled into the sampler did not cause problems with the segments coalescing into each other upon entering the wide-bore capillary. As a result, we abandoned the plate concept and began using open glass vials, which were amenable to organic solvents. These would not be suitable for high pH, however.

Oil/solvent capability. We tested whether 1 μL droplets of solvent would coalesce within each fluorinated carrier fluid when mixed with the same solvent. We determined that each solvent coalesced with another droplet of the same solvent for all three oils (PFD, FC-40, FC-770). These droplet segments are on the upper end of volumes that would be used with this sampler. It was noted that both toluene and water did not mix thoroughly across the full droplet length. It is likely that for these systems it would be better to use smaller total droplet volumes to ensure full mixing across the newly-formed droplet.

It was observed over the course of all experiments, that selection of an appropriate fluorinated oil continuous phase was necessary for good performance. While methanol samples coalesced well using all oils, we found that when we had dibutyl phthalate dissolved in methanol as the sample, it would not coalesce well with another droplet containing methanol. Through trial and error, it was determined that FC-770 was the best

oil to use for these samples, resulting in coalescence for all droplets. The use of a fluorinated surfactant, such as perfluorooctanol (PFO) may aid in coalescence for other samples. When testing aqueous samples, it was determined that FC-40 with 1% PFO gave optimal droplet coalescence. Using a lower surfactant concentration resulted in sample and quenchant droplets that would not coalesce, while using a higher surfactant concentration resulted in breakup of mixed droplets as they were pulled along the mixing capillary. Droplet coalescence and breakup are primarily controlled by adjusting surface tension between the continuous fluorinated phase and the sample and quenchant droplets. As surface tension for all samples may not be known, it may be necessary to test multiple oils before finding the best option to monitor a particular reaction.

Droplet coalescence. Iron (III) nitrate and potassium thiocynate were used to test a range of flow rates and sample times that could be used for droplet coalescence. These two reagents start as pale yellow and clear solutions, respectively, but result in a deep red color upon mixing, resulting in a definitive visual test for determining if a droplet had or had not mixed. After determining the ideal continuous phase composition for the aqueous samples (FC-40 with 1% PFO), each reagent was pulled into the sampler for the specified time at the specified flow rate. Each combination of oil and solvent was tested five times. If all five droplets for a particular solvent/oil pair coalesced and mixed, that combination of time and flow rate was defined as coalesced. If the droplets did not coalesce at all, that flow rate and time combination was defined as having no coalescence. If at least three of the five droplets coalesced, that combination was defined as borderline. For some higher flow rates and longer sample times, the droplet volume was sufficient that while the droplets coalesced, mixing across the droplet was not

complete. Those flow rates and times were defined as incomplete mixing. The combinations of flow rates and times are plotted in Figure 3-4. Interestingly, there is not a minimum volume needed for coalescence. Small droplet volumes (0.25 µL or less total droplet volume), created at low flow rates and low sample times, tended to not coalesce. However, the same size droplets, when created at higher flow rates, are able to coalesce. It appears the droplet velocity is high enough that it forces contact between the two droplets, injecting one reagent droplet into the other and causing very rapid mixing. The upper limit on droplet volume (around 2.7 µL total droplet volume) is important to consider, ensuring good mixing across the droplet. One of the advantages to using droplets is the rapid mixing caused by coalescence, but if the droplet is too large, that advantage is removed and more active forms of mixing would have to be incorporated into the system, adding additional layers of complexity to the sampler probe.

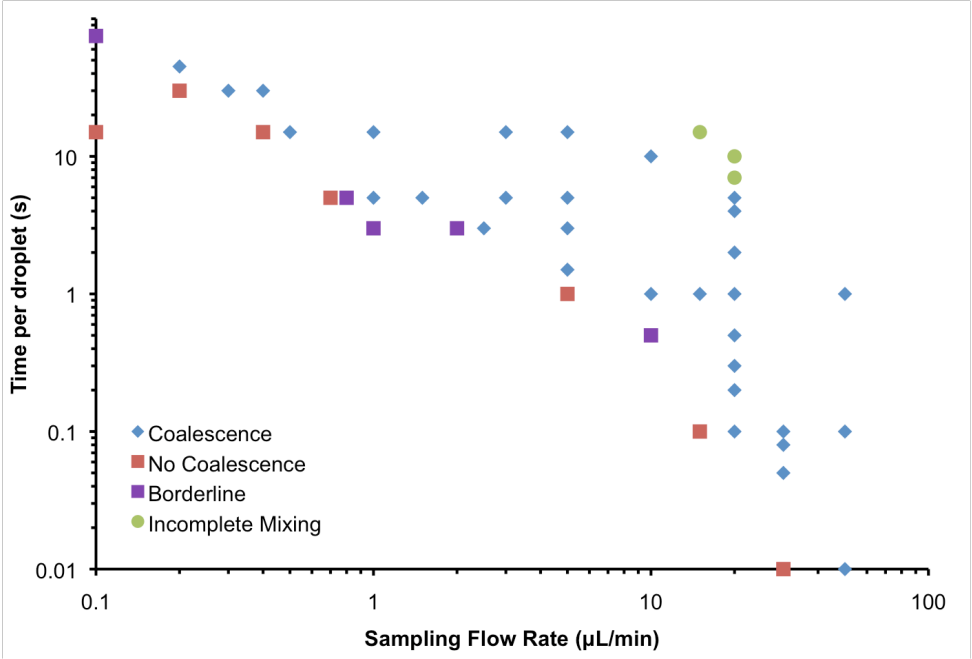

Figure 3-4. Plot of flow rate and sampling time necessary for coalescence of aqueous samples. Iron (III) nitrate and potassium thiocynate were used as reagents, with 1% PFO in FC-40 as the fluorinated continuous phase.

Droplet dilution. For the sampler to be effective, it must be able to withdraw a set volume of sample and mix it thoroughly with quenchant before downstream analysis. Dilute blue food color and water were used to demonstrate the linearity of sampling and mixing. Absorbance at 280 nm is shown for each mixed droplet in Figure 3-5. Each data point is n=6 droplets. The R^2 value for a line fit to the points is 0.99614 indicating that the sampler probe withdraws and mixes sample in a defined manner.

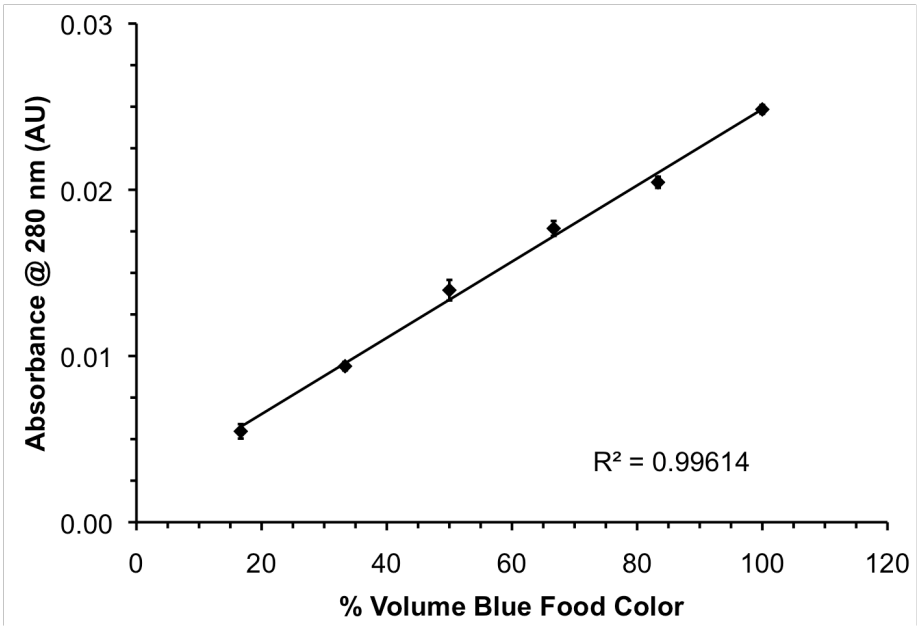

Figure 3-5. Linearity of droplet sampling. Water colored with blue food color (BFC) was mixed with plain water for total droplet volume of 0.5 µL. Mixed droplet absorbance was monitored using a variable wavelength detector. The plot shows absorbance for each set of droplets at a particular percentage of BFC in water.

Using HPLC to Monitor the Hydrolysis of Dibutyl Phthalate. The hydrolysis of dibutyl phthalate to phthalic acid was monitored over a period of 3 hours. The sampler is able to perform runs "on demand", although the cycle time for this set of conditions was set to 15 minutes. Selected chromatograms are presented in Figure 3-6. For the run marked "BFC", the sample was replaced with MeOH to determine which peaks (D and a small peak at C) are due to the blue food color in the acetic acid quenchant solution. The

run marked “DBP” is 0.667 g/mL dibutyl phthalate in methanol (no potassium hydroxide) in order to identify the pure dibutyl phthalate peak before hydrolysis began (F). The next three chromatograms are from immediately after addition of potassium hydroxide (0 min), and 75 and 165 minutes after the addition of potassium hydroxide. After the addition of potassium hydroxide, the dibutyl phthalate peak (F) decreased over time, while the hydrolysis peak (B) increased over time, with intermediate half-hydrolysis peaks (C, E) evident. The sample was also analyzed with the system after reacting overnight (24 hr) to show changes in the chromatogram overnight. Peak areas for over time are plotted in Figure 3-7.

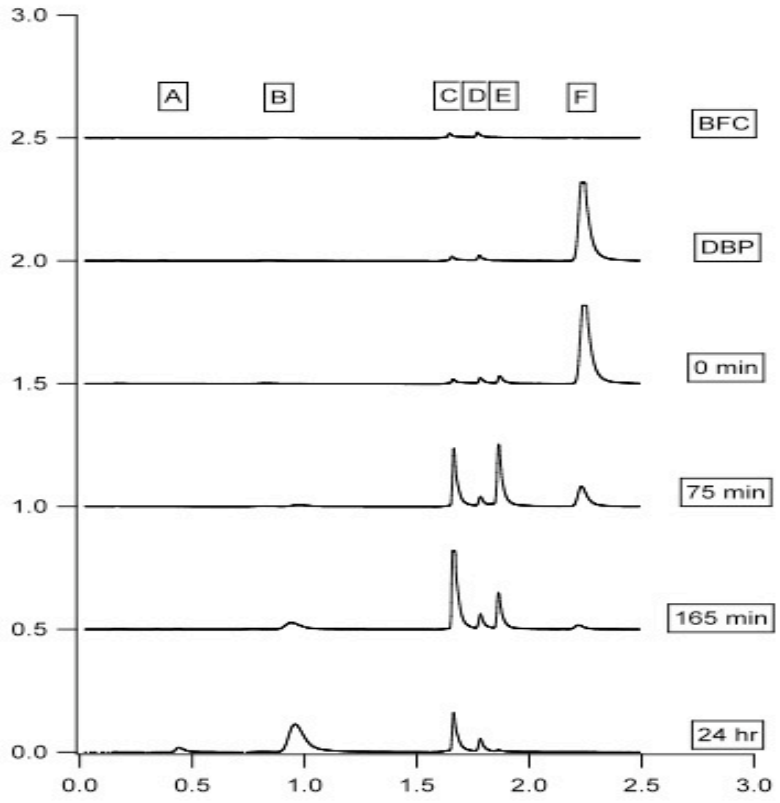

Figure 3-6. Selected dibutyl phthalate hydrolysis chromatograms as monitored with the droplet sampler. BFC run has blue food color only, showing the contribution to peaks C, D. DBP run has blue food color and dibutyl phthalate, identifying peak F as dibutyl phthalate. The other runs show intermediate peaks. The product, pthalic acid, is peak A, visible after 24 hours.

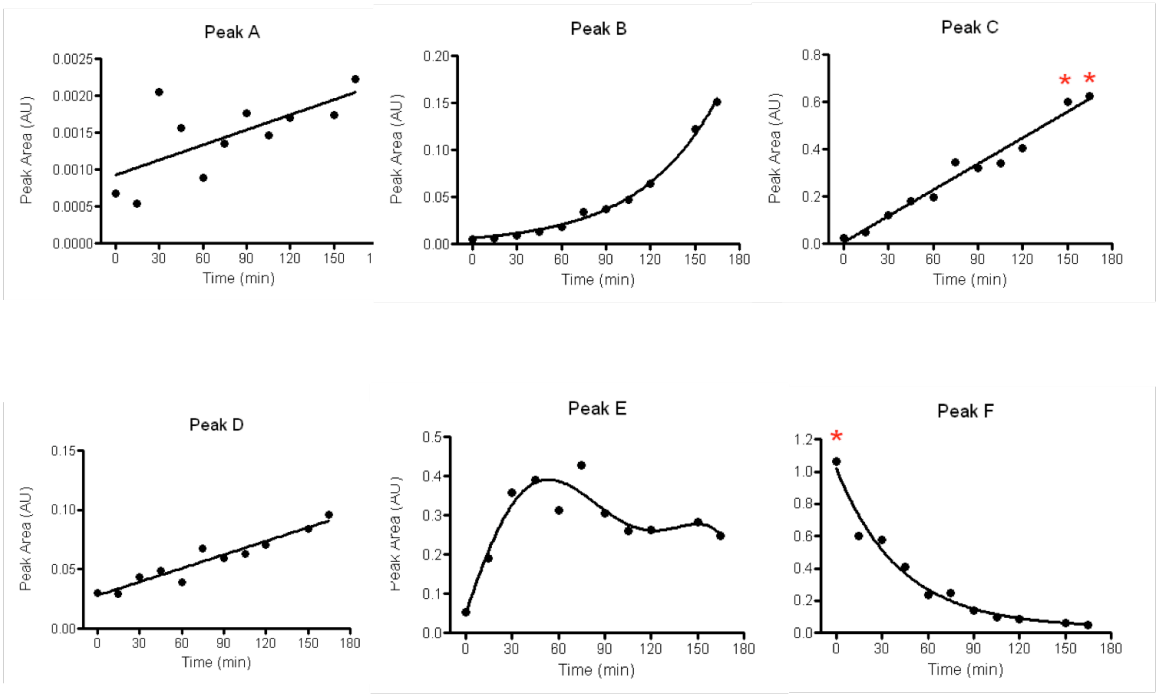

Figure 3-7. Dibutyl phthalate hydrolysis peak areas as monitored by droplet sampler. Peak A is the product, phthalic acid. Peak F is the reactant, dibutyl phthalate. The other four peaks are intermediates, marked on Figure 3-6.

Improving automation. The bi-directional syringe pump was replaced with a flow-selection valve to improve automation of the system. Previously, the syringe pump could be stopped and started automatically, but changes in flow rates and pumping direction were performed manually. As there is a finite time required for the pump to reverse flow, rather than program the flow using the pump itself, we opted to use a flow-selecting valve. The valve was connected to four syringes, each at a different flow rate (slow pull, fast pull, fast push, stop). The flow path for the valve allowed continuous flow through the syringes to an oil reservoir to avoid any delay in starting or stopping flow. The desired syringe could be selected automatically, applying that flow rate to the

sampler probe. The droplet sampler software was modified to accommodate these automation improvements.

The change in the system did improve the automation of the system by eliminating the need to manually adjust flow rates during the sampling process. Efforts to fully automate the system were not successful, as the droplets did not move at the same flow rate for each injection. As a result, when overfilling the injection loop, the droplets were not properly centered prior to injection, and the portion of the droplet that was injected was not reproducible. Without adjustments by the user, oil, rather than sample, could be injected on to the column, necessitating column rinsing before additional samples could be run (see Appendix A for more information on fluorinated oils injected onto an RP-HPLC column). Based on observations of gas bubbles forming in the oil fluid lines while the droplet is being transferred to the injection loop, it appears that compressible gas bubbles are causing the instability in flow rate that leads to irreproducible injections of the droplets. All connections have been checked to eliminate air leakage as much as possible. It is likely that the source of these bubbles is dissolved gasses within the fluorinated oil itself. Using lower pull flow rates can improve the reproducibility of droplet flow, but it significantly increases the time needed to transfer the droplet to the injection loop. This is a limitation on the system that will need to be solved if the system is to be fully automated. One possible solution would be to place a small sensor on the fluid lines leading into the injection loop to determine when the droplet is fully centered within the loop, automatically triggering the injection valve.

The automated system was used to run a calibration curve (Figure 3-8 A) to compare with a calibration curve run with the bi-directional pump (Figure 3-8 B) and a

calibration curve run with smaller droplets without the HPLC (Figure 3-5). A volume of quenchant (0.01 g/mL acetic acid in methanol with added blue food color) was drawn up followed by a volume of sample (0.67 g/mL dibutyl phthalate in methanol) for a total volume of 2.2 μL. The droplet was centered on the injection loop and the injection was triggered manually. The quenched dibutyl phthalate sample was separated using a gradient as described previously. Peak area for the DBP peak was calculated with in-house software.[89] The calibration was linear, but RSDs for each point ranged from 1.4-23.9%, with the highest RSD for the smallest sample volume (Figure 3-8 A). As a comparison, the same experiment was run with the previous iteration of the system (bi-directional pump) using the same flow rates. Peak area RSDs ranged from 6.2-14.9% for this system. These RSDs are higher than our goal of 5%, and include variation due to sampling, injection, and the HPLC itself. We had postulated that the a primary source of variation was due to the stopping and starting of the bi-directional pump, leading to variation in the volume of fluid drawn up by the sampler probe; however, if that were the case, we would expect to see significant improvement in RSDs when the pump was replaced by the flow-selection valve, which is not the case. Smaller droplets that are not injected onto the HPLC (Figure 3-5) have much better reproducibility, indicating that variability in drawing up samples may not be the major problem. It appears that part of the reproducibility problem may be due to incomplete mixing within the droplet. Using smaller droplets to improve mixing may solve this problem, but smaller droplets are more difficult to reproducibly inject using the current injection valve system. Improvements to the injection valve would allow for the system to be fully automated and for smaller

droplets to be tested with the HPLC, determining if reproducibility may be improved for the system.

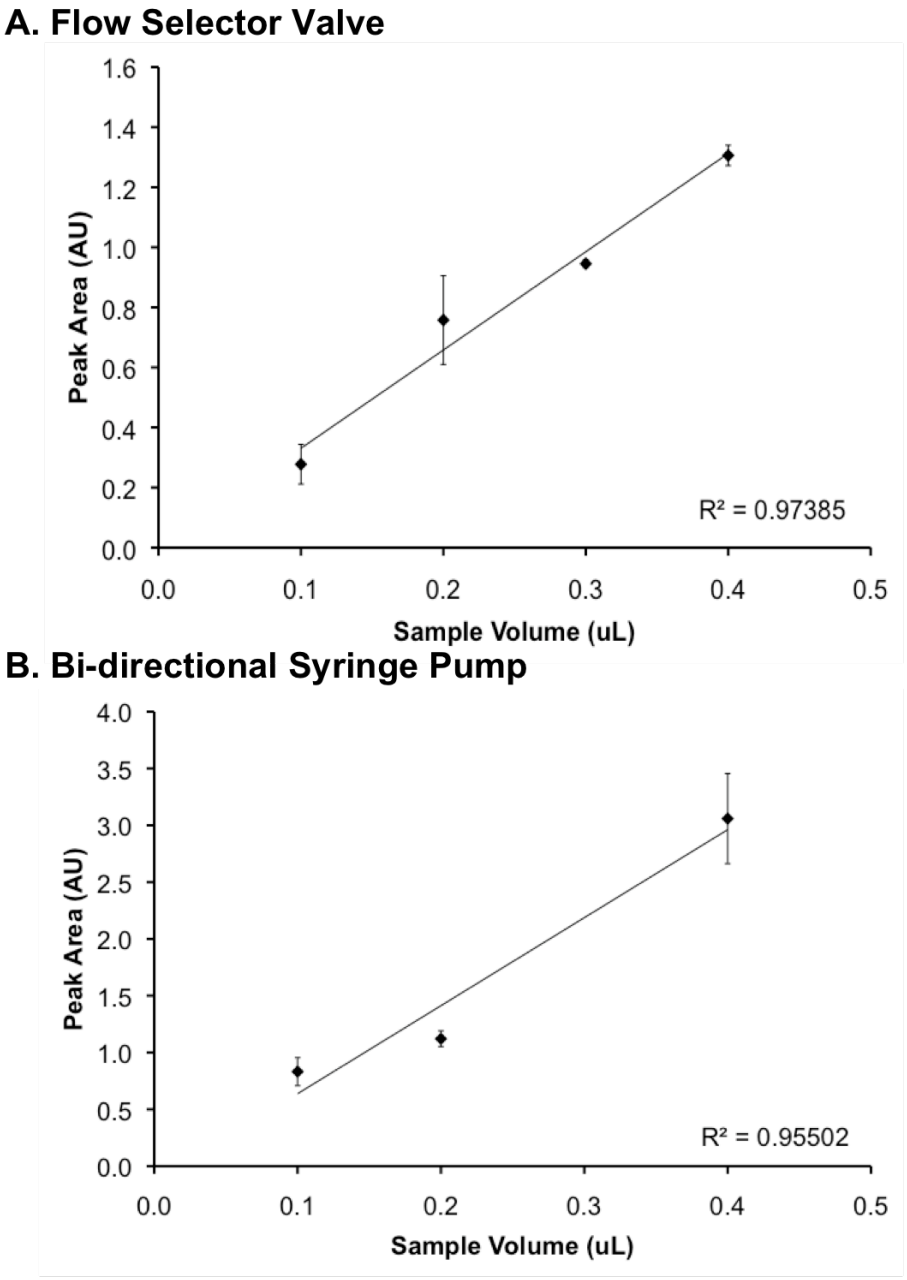

Figure 3-8. Comparison of calibration curves with improved automation. A. Calibration curve run with a flow-selector valve in place to automate flow rates in the sampler probe. B. Calibration curve run with a bi-directional syringe pump and manual switching of flow rates.

Conclusions

A sampling system was designed to monitor very small (several milliliters) reaction volumes. The sampling probe was constructed from Teflon PFA tubing for high chemical resistivity and used the principles of droplet microfluidics to mix sample and quenchant before injection onto an HPLC. A stage for manipulating the sampling probe was constructed with automated software, allowing sampling to occur from a variety of small reaction vessels. The sampler has the potential to monitor multiple reactions simultaneously, although that capability has not yet been tested. Base-catalyzed hydrolysis of dibutyl phthalate was monitored for three hours using the droplet sampling system, demonstrating its capabilities for reaction monitoring coupled to HPLC. While the system holds promise, there are concerns with automating the system and improving reproducibility. Future work for this sampler design will be focused on improving reproducibility, automation and testing the sampler with multiple reaction monitoring.

CHAPTER 4

DEVELOPMENT AND CHARACTERIZATION OF SAMPLING DEVICE FOR PHARMACEUTIAL REACTIONS CONTAINING SOLID PARTICLES

Introduction

The ability to sample from a reaction containing solid particulates is a challenge for the pharmaceutical industry. Particulates may be present in biological samples due to cell debris. They may also be present in organic reactions either due to reactants that have precipitated out of the solution, or the presence of solid catalysts. Representative sampling of these reactions is important for understanding the reaction process. Many sampler designs simply avoid the problem by installing filters on sample intake. Some commercial automated samplers are designed to handle particulates and larger sampler volumes. However, these samplers are restrictive in what size and shape of reactor for which they may be used. We envision a sampling system that will work with solid particulates and can be mounted on a range of reactors, from a 50 mL round-bottom flask up to a multi-liter manufacturing-scale reactor.

We have developed a prototype sampler that meets these requirements, constructed from glass, Teflon, PEEK and stainless steel for compatibility with a wide variety of potential reactions. After evaluating several versions, we have developed a prototype that is capable of monitoring a reaction for at least three hours as well as handling particulate matter. We envision further development of this prototype to

improve automation and portability with the ultimate goal of a standardized sampling system suitable for commercial use.

Experimental Section

Materials. Dibutyl phthalate was sourced from Acros Organics Morristown, NJ, US). Blue food color (water, propylene glycol, FD&C Blue 1, 0.1% propylparaben) was obtained from McCormick (Sparks, MD, US). Polystyrene beads were purchased from Polysciences, Inc. (Warrington, PA, US). All water used was deionized to 18 MΩ resistivity with an E-pure 1090 series system from Barnstead Thermolyne Corporation (Dubuque, IA, US). Unless otherwise noted, all other chemicals were purchased from Fisher Scientific (Chicago, IL, US).

Sampler Body Construction. The sampler body was constructed in-house from glass tubing and a Teflon stopcock (Figure 4-1 A). The main sampler body is 10 mm OD, 1.5 mm wall Kimax borosilicate tubing (Chemglass Life Sciences, Vineland, NJ, US) that has been modified to incorporate inlets and outlets. The top of the sampler is 8 mm glass thread removed from a Wheaton 2 mL specimen vial (Fisher Scientific). The thread is topped with a twist cap equipped with a Teflon-backed rubber septum (Fisher) for syringe access. Two pieces of 1" long 3 mm OD, 0.2 mm wall Kimax borosilicate tubing (Chemglass) were welded on to the sampler body to allow liquid (90° to main body) and gas (45° to sampler body) access through the two side arms. The sampler body was welded on to a straight bore stopcock with 1 mm bore Teflon plug (Chemglass) to allow sample access. The stopcock had been altered to allow full drainage of the sampler body to the outlet using the transfer position (Figure 4-1 B). A 1 mm angled

hole was drilled to intersect with a 1/8” hole drilled into the side of the stopcock. Teflon PFA tubing (1/8” OD) was pressed inside the side hole to create an outlet for mixed sample.

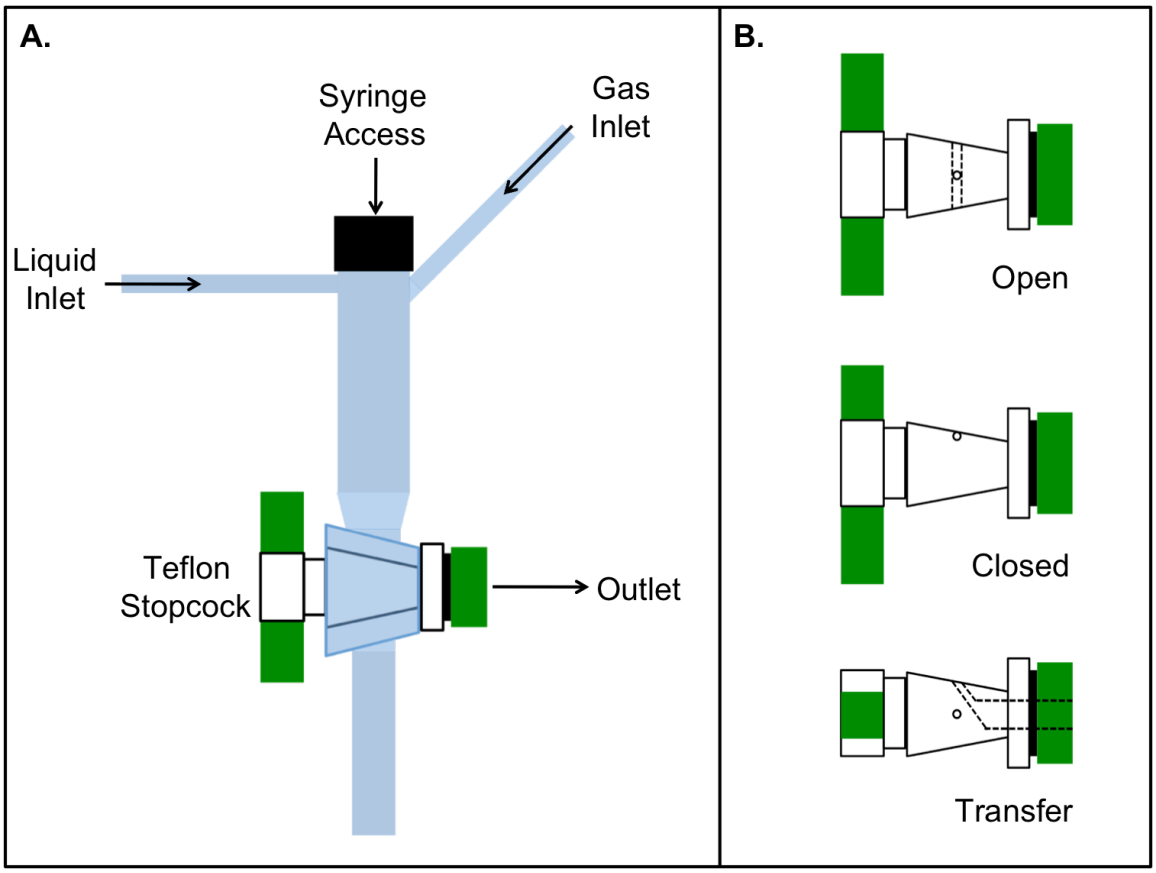

Figure 4-1. Overview of soup pot sampler construction. A. The sampler was welded together from Kimax borosilicate glass tubing (main body, liquid inlet, gas inlet) and a 1 mm bore Teflon stopcock. Glass threading from a specimen vial was welded to the top and a cap with a Teflon-backed rubber septum was added to provide sealed syringe access. B. The stopcock has three positions: open, closed and transfer. When open (handle is 0° to sampler body), the stopcock allows the syringe needle to pass completely through the 1 mm hole to reach into the reactor placed below the sampler. When closed, (handle is 45° to the sampler body) the sampler is completely sealed to fluids and the syringe. When in transfer position (handle is 90° to sampler body) fluid is able to flow out of the sampler body and is transferred out the side of the stopcock to the outlet.

Sampler System. The sampler was connected to 1/16" OD x 0.02" ID Teflon PFA tubing (Upchurch Scientific, Oak Harbor, WA, US) with 1/8" OD x 0.063" ID silicone tubing (New Age Industries, Southampton, PA, US). The inlet was connected to a syringe pump (Harvard Instruments, Holliston, MA, US) with Teflon PFA tubing for fluid flow. Peek unions (Valco) were used to connect syringes to the tubing. The gas inlet was connected to Teflon PFA tubing in the same manner. An air-filled syringe was connected to this tubing to provide pressure for clearing solution from the sampler body. A 250 μL syringe connected to a removable 6" long 22 gauge non-coring needle (Fisher Scientific) was inserted through the septum in the cap and remained in place during all experiments. The outlet through side of the stopcock was connected to Teflon PFA tubing press-fit into the outlet hole. The outlet tubing was connected to a 250 μm ID tee (Valco) with the majority of flow going through another piece of Teflon PFA tubing to a waste container. For any experiments with HPLC, the side arm of the tee had a piece of fused silica capillary (250 um ID, 360 um OD) connected through an injection valve to vacuum to pull a portion of the outlet fluid for injection. The 8-port micro-actuated injection valve (Valco) was fit with 5 μL fused silica injection loops connected to an Agilent 1100 series HPLC (Figure 4-2).

Sampler operation. To start sampling, the stopcock was manually turned to the open position, and the syringe was lowered through the stopcock opening into the sample. A 40 μL volume of sample was manually pulled up into the syringe needle, and the syringe was withdrawn so the tip of the needle was inside the glass sampler body. The stopcock was switched to the closed position, and the syringe plunger was pressed to release sample into the sampler body. At the same time, 400 μL of quenchant was

pushed into the sampler body using the syringe pump. To aid mixing, the syringe tip was lowered to just above the stopcock, and the sample was mixed with the quenchant five times by withdrawing and releasing the syringe plunger to pull 100 μL of fluid into the syringe. Once the sample was mixed, the syringe needle was lifted to above the liquid level, and the stopcock was turned to the transfer position. The sample, mixed with quenchant, was allowed to flow out the side of the stopcock and through the outlet tubing. Pressure was applied to aid flow by depressing the syringe plunger on the gas syringe. Once the sampler was empty, the stopcock was returned to the closed position to reseal the sampler body. Wash fluid (800 μL) was added to the sample body. The syringe plunger was raised and depressed five times to mix the sample. This process was repeated during each wash, rinsing the syringe as well as the sampler body. The stopcock was then turned to the transfer position and the fluid was flushed out in the same manner as described previously. This process was completed for the required number of washes. Once washing was complete, the stopcock was returned to the open position to begin sampling again.

When the sample was analyzed using HPLC, a vacuum pump was used to pull mixed sample through the sample capillary and through the injection loops on the injection valve. When the loops were full, the injection valve was triggered to begin the HPLC run. An XBridge C18 column, 4.6 x 20 mm, with 3.5 μm particles (Waters Corporation, Millford, MA, US) was installed on the Agilent 1100 system (Agilent Technologies, Inc., Santa Clara, CA, US). Mobile phase A was 0.1% trifluoroacetic acid in water and mobile phase B was methanol. Separation was performed at 2 mL/min using a gradient of 1 minute at 25% mobile phase B, 0.5 minute ramp to 75% mobile

phase B and 1 minute hold at 75% B. Effluent absorbance was monitored at 254 nm with a Spectra 100 variable wavelength detector (Spectra Physics, Mountain View, CA, US). The detector output was recorded with USB-6008 DAQ card combined with in-house LabVIEW software (National Instruments, Austin, TX, US).

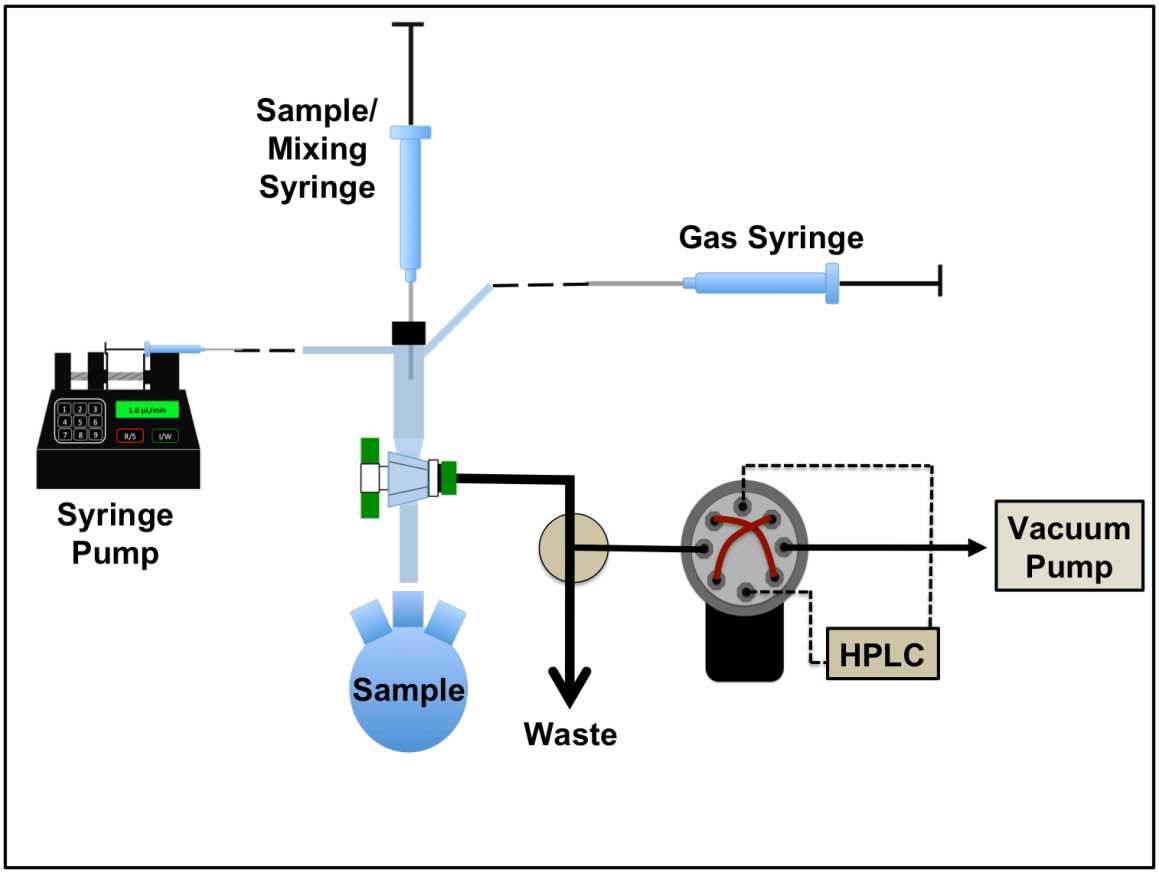

Figure 4-2. Overview of soup pot sampling system. A syringe pierced the septum at the top of the sampler body and is moved down and up with the stopcock in the open position to obtain sample from the reactor. The liquid inlet is attached to a syringe pump, which flows quenchant/wash solution into the sampler body. The gas inlet is attached to an air-filled syringe, which applies pressure when the plunger is depressed to aid in evacuating liquids from the sampler body. The sampler outlet is connected to a tee that splits flow between an injection valve and a waste vial. A vacuum pump is used to pull mixed sample through an injection loop. When the loop is full, the valve is actuated to start HPLC analysis.

Sampler washing. Dibutyl phthalate (0.067 g/mL in methanol) was the sample and acetic acid (0.01 g/mL in methanol) was used as both the quenchant and wash solution. Sampling was performed as described previously, and the quenched sample was analyzed with HPLC.

On-line Dilution. Dibutyl phthalate (0.067 g/mL in methanol) was the sample and acetic acid (0.01 g/mL in methanol) was used as both the quenchant and wash solution. Sampling was performed as described previously except sample and quenchant volumes were changed. An aliquot of sample was drawn into the sampler body and mixed with the appropriate volume of quenchant for a total fluid volume of 440 μL. The sampler was washed three times between each sample with the acetic acid solution. The quenched sample was analyzed with HPLC.

Reaction monitoring with HPLC. The sampler was used to monitor the hydrolysis of dibutyl phthalate every 15 minutes. The sample was 10 mL dibutyl phthalate (0.1 g/mL in methanol) mixed with 5 mL 10 equivalent potassium hydroxide solution diluted to 1.5 g/mL in methanol. The quenchant and wash solution was glacial acetic acid diluted to 0.01 g/mL in methanol. Samples were processed and the sampler was rinsed as described previously. The sampler was washed three times between each sample. The quenched samples were analyzed using HPLC.

Bead slurry. A slurry of 105-125 μm diameter polystyrene beads in dilute aqueous blue food color was prepared as the sample. Water was used as both the model quenchant and wash fluid. Sampling was performed as described previously.

Results and Discussion

Sampler Design. The primary consideration of this sampler design was the ability to sample from solutions that contain suspended particles. In order to do this, all parts of the sampler had to be wide enough to allow particles up to 500 μm (see Table 1-1) to fit through all portions of the sampler. The sampler was designed to be compatible with larger sample volumes (10 μL up to 1 mL) that might be obtained from a round-bottom flask or from a larger reactor in a manufacturing setting. The sampler was designed to remove an aliquot from a slurry, quench and mix the sample, including any particles present, and then analyze the sample, excluding particles from entering the HPLC.

Additionally, we wanted to ensure that the materials used for the sampler were generally chemically inert and physically robust. We used glass, Teflon, PEEK and stainless steel for these reasons. The sampler body was crafted out of a glass body fit with a Teflon stopcock on the bottom to allow access to a reactor. The top of the reactor is reversibly sealed with a cap equipped with a rubber septum coated with Teflon (to be chemically inert). A syringe with a long needle is used to access samples and deposit them in the sampler body. Two glass access tubes are welded to the top of the sampler to allow for the addition of liquids (quenchant, wash fluids) or gases (to provide pressure and for drying the sampler).

Sampler washing. The system was tested to determine how many washes were required to fully rinse the sampler body between each sample. An aliquot of dibutyl phthalate was quenched and the mixed sample was analyzed with HPLC (Figure 4-3) along with the fluid from each subsequent wash. The dibutyl phthalate peak area from

the third wash was determined to be 0.4% of the original sample peak area. We determined that three washes were sufficient to minimize cross contamination between samples.

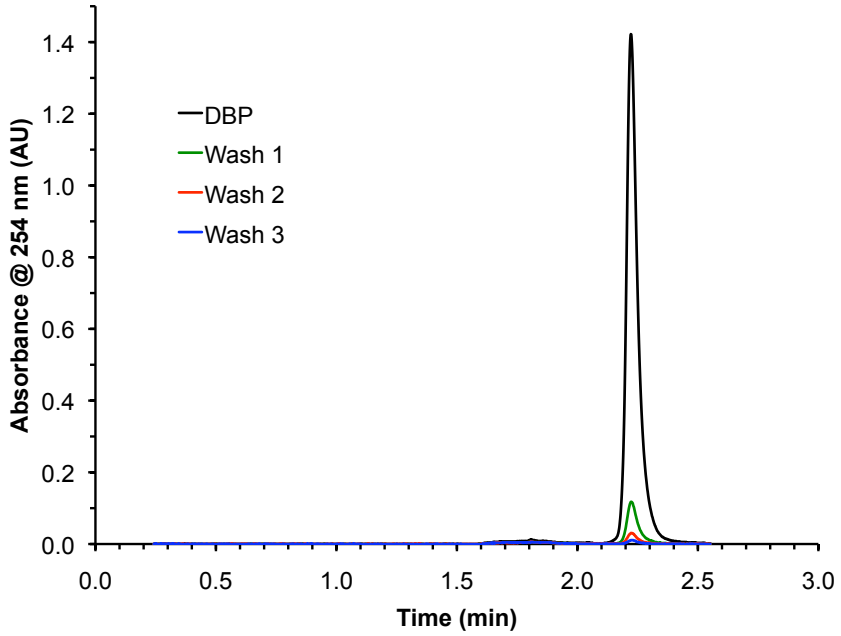

Figure 4-3. Washing soup pot sampler. Plot of dibutyl phthalate (DBP) analyzed using HPLC after initial quenching and after each wash. After three washes, the DBP peak area is 0.4% of the initial peak area. Three washes were determined sufficient to clean the sampler body between runs.

Dilution curve. Varying volumes of dibutyl phthalate were mixed with acetic acid to verify linear sampling could be accomplished. The sampler body was washed three times with 800 µL of wash fluid each between samples. The dibutyl phthalate peak areas were linear with respect to sample volume with an R^2 value of 0.9969 for the five sample volumes (Figure 4-4). Sampling reproducibility was good, with peak area relative standard deviation (RSD, n = 3) of 2.4%, 2.2%, 4.4% and 0.56%, for 20, 40, 60 and 80 µL samples, respectively. The RSD is for the entire system, including variation from the

sampler itself as well as the HPLC. The RSD for the 0 µL sample was 67%. As no sample was pulled up at this volume, the variation is primarily due to any residual dibutyl phthalate that sticks to the syringe needle as it is lowered into the reactor.

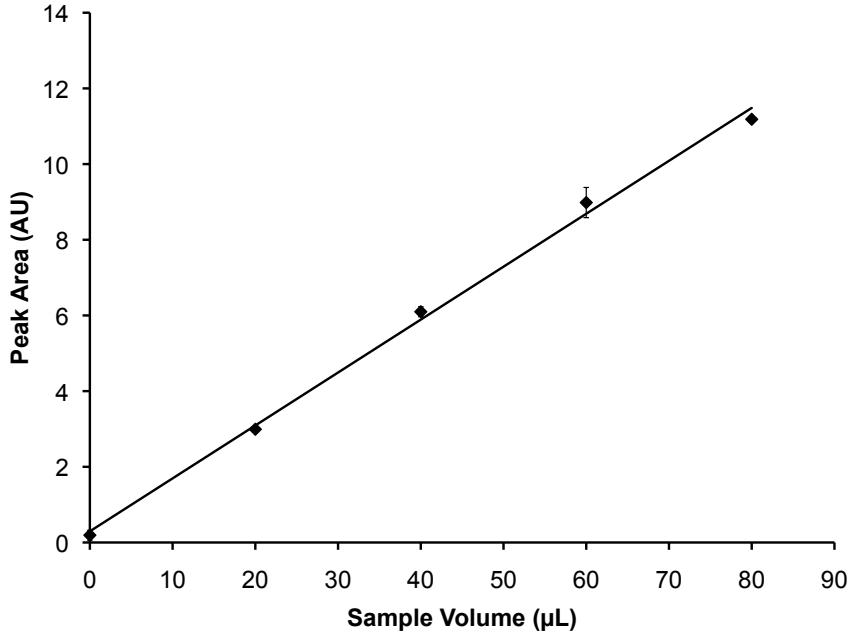

Figure 4-4. Plot illustrating linearity of dibutyl phthalate sampling. Increasing volumes of dibutyl phthalate were mixed with acetic acid quenchant, adjusted for a total volume of 440 µL. R^2 for the line was 0.9969. Relative standard deviation (RSD) for 0, 20, 40, 60 and 80 µL samples were 67%, 2.4%, 2.2%, 4.4% and 0.56%, respectively, for n = 3 samples at each volume.

Reaction monitoring with HPLC. We tested the ability of the sampler to monitor the hydrolysis of dibutyl phthalate every 15 minutes for a total of 3 hours. As this sampler was designed to handle larger volumes than previous samplers (see chapter 2 and 3) we sampled aliquots of 40 µL, mixed with 400 µL quenchant. The peak areas for the dibutyl phthalate reactant, the phthalic acid product and the intermediate peaks were calculated and plotted for each time point (Figure 4-5). The plots are comparable to the plots obtained for the same reaction using the droplet sampler (Figure 3-7).

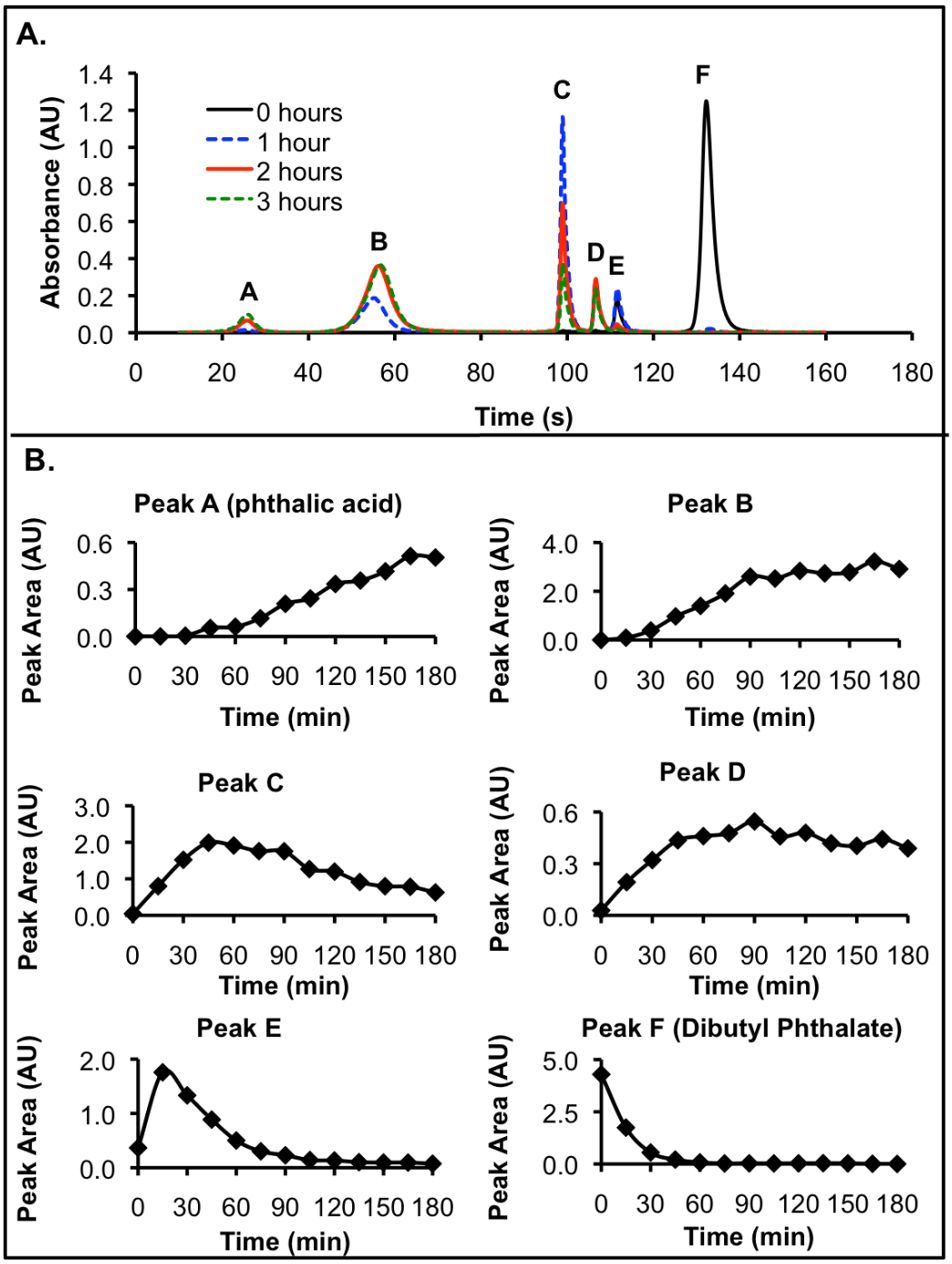

Figure 4-5. Dibutyl phthalate base-catalyzed hydrolysis monitored with soup pot sampler. Samples were mixed with quenchant every 15 minutes in the sampler body and analyzed using HPLC. Peak A is the product, phthalic acid. Peak F is the reactant, dibutyl phthalate. Peaks B-E are unidentified intermediates. A. Chromatograms every hour following start of hydrolysis reaction. B. Peak areas over time for each identified peak in part A.

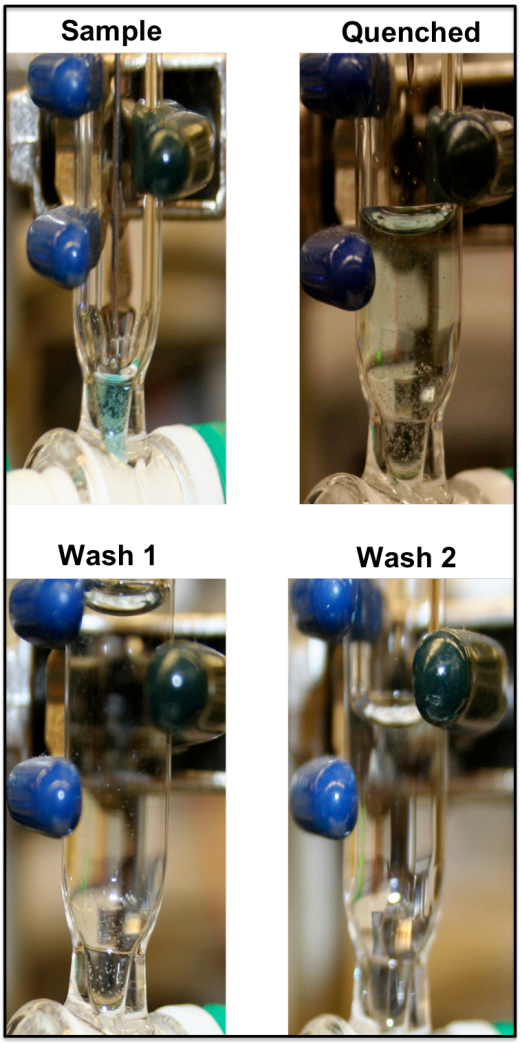

Figure 4-6. Sampling beads with soup pot sampler. Slurry of 105-125 µm polystyrene beads in dilute blue food color was sampled to illustrate the ability of sampler to handle solid particles. A 40 µL aliquot was deposited in the sampler body (SAMPLE). The sample was mixed with 400 µL quenchant and mixed using the syringe (QUENCHED). The effervescent look to the image is due to beads suspended in solution. After the sampler body had been drained, 800 µL of quenchant was added and the solution was mixed (WASH 1). Beads were still clearly visible in the solution. At the second wash, only a few beads were visible in the solution and do not show up on the image (WASH 2). Wash 3 showed no beads visible in the solution (image not shown) indicating the sampler is capable of clearing particulate matter in the same number of washes necessary to clean homogenous samples from the sampler body.

Bead slurry. Of primary concern was the ability to sample solutions solid particulates. We tested a solution of suspended beads to determine if the beads could pass through the sampler and how many washes would be required to remove the solids from the sampler. When working with beads, we operated the system without the HPLC. We determined that the sampler is compatible with a bead slurry. The beads were observed in the aliquot of sample pulled into the sampler body as well as in the quenched sample (Figure 4-6). The beads appear to be fully rinsed from the sampler after the third wash, indicating that particles in a sample would be removed under the normal course of washing.

A previous prototype of the sampler had glass tubing welded directly above the Teflon stopcock (similar to the inlets). This design caused about 40 μL of fluid to remain in the sampler after fluid was removed through the outlet. While this fluid could be drawn up by the syringe and then ejected from the sampler, it was difficult to fully remove all liquid from the sampler. This design made it particularly difficult to sample beads, as it took five washes to remove beads from the sampler body. The current design allows for more complete flushing of the sampler body and more rapid removal of particles.

While this sampler design is promising, only 105-125 μm polystyrene beads have been tested with this sampler design. It would be informative to test a wider range of bead sizes to determine if it will have problems with clogging of the sampler. Testing particles of other shapes and surface chemistry would also need to be included to gain a comprehensive understanding of how the sampler handles particulate matter.

Conclusions

A sampler was constructed out of relatively rugged and chemically inert materials for periodic sampling of reactions containing particles. The sampler prototype was quick to produce and could be easily reproduced with the assistance of a scientific glassblower. The sampler utility was demonstrated by monitoring the hydrolysis of dibutyl phthalate with the sampler coupled to HPLC. It was determined that only three washes were needed between each sample to avoid carryover. We demonstrated that the peak area of dibutyl phthalate is linearly related to the volume of sample drawn into the sampler body, indicating that sampling is representative of the bulk solution. We demonstrated the monitoring of a dibutyl phthalate hydrolysis reaction every 15 minutes for 3 hours and showed that the peak areas follow the same trend for analysis of this reaction using other sampling systems. We also determined that the sampler is tolerant of 105-125 μm polystyrene beads and that they are able to be removed from the system in the same number of washes as was necessary to remove the dibutyl phthalate from the sampler body.

This sampler prototype is promising for larger samples that contain solid particles. Further testing needs to be done with other reactions and particles of other sizes, shapes and surface functionalities. Another key improvement for this sampler would be to increase the level of automation. Currently the sample syringe, quenchant/wash syringe pump and stopcock are all moved manually. The HPLC gradient program and the computer program to trigger the injection valve and record absorbance must also be triggered manually. We have proposed a design to automate the system and make it more amenable to commercial use in chapter 5.

CHAPTER 5

SUMMARY AND FUTURE DIRECTIONS

Summary

In this dissertation, we have presented three designs for microscale samplers coupled to HPLC for use in near real-time monitoring of pharmaceutical reactions. Two sampler designs, the push-pull and droplet samplers, fill a niche for sampling from very small (milliliters) reactors. The push-pull sampler is a continuous sampling system, removing low volumes of sample (30 μL per hour of sample under normal conditions) from a reactor. The system has been shown to be tolerant of particulate matter in the reactor, although it was not designed to sample the particulates. This system has been fully automated for sampling, mixing with quenchant, injection to the HPLC and data collection and has been demonstrated with near real-time monitoring of an organic reaction. Improvements to this sampler are focused on making the system more robust by using less fragile materials, to make it more suitable for daily use in a pharmaceutical laboratory setting. The second sampler design, the droplet sampler, has also been used for near real-time monitoring of an organic reaction. This sampler uses a batch design, sampling only when necessary to reduce overall reagent consumption. This sampler has the possibility of being used to monitor multiple reactions, but there are currently concerns with automating the system and improving reproducibility.

The third sampler design, the soup pot sampler, fills a niche for sampling from reactions containing solid particulates, as modeled by a slurry of polystyrene beads. This sampler removes larger volumes of a reaction than the previous two designs, but could be scaled down for smaller samples if necessary. This system has also been used to monitor an organic reaction and has been demonstrated with a polystyrene bead slurry. Future work with this sampler will be focused on building a prototype of fully a automated system for use in a pharmaceutical testing laboratory.

Push-Pull on a Microfluidic Chip

One of the concerns with the push-pull sampler is that the fused silica capillaries used for the body of the sampler may be too fragile for regular use in a pharmaceutical environment. Additionally, while all off-the-shelf parts are used for the push-pull system, building the sampler requires careful placement of each component, making mass-production difficult using its current design. Creating a push-pull sampler on a microfluidic chip would allow for easy mass-production, and the thicker glass used for a chip would make the sampler more robust for regular use. Additionally, smaller channels may be produced on-chip, improving mixing for the sampler.

A basic chip design for 1:1 quenching, followed by 10:1 dilution of quenched sample has been proposed (Figure 5-1). The entire chip would be 1 cm wide x 4.5 cm high x 2.2 mm thick (if made from Borofloat glass). The etched area is 4 mm x 40 mm and the chip is designed to slide into a round-bottom flask neck. As mixing is due to diffusion across the channels, 40 μm channel widths were used in this design for all channels other than the main dilution channel which is 100 μm wide. For modeling

purposes, the channel depth is assumed to be 20 µm and the channels are assumed to have a rectangular profile, although if this chip were etched in glass, that would not be the case. The serpentine channel design provides sufficient length for mixing in a compact footprint.

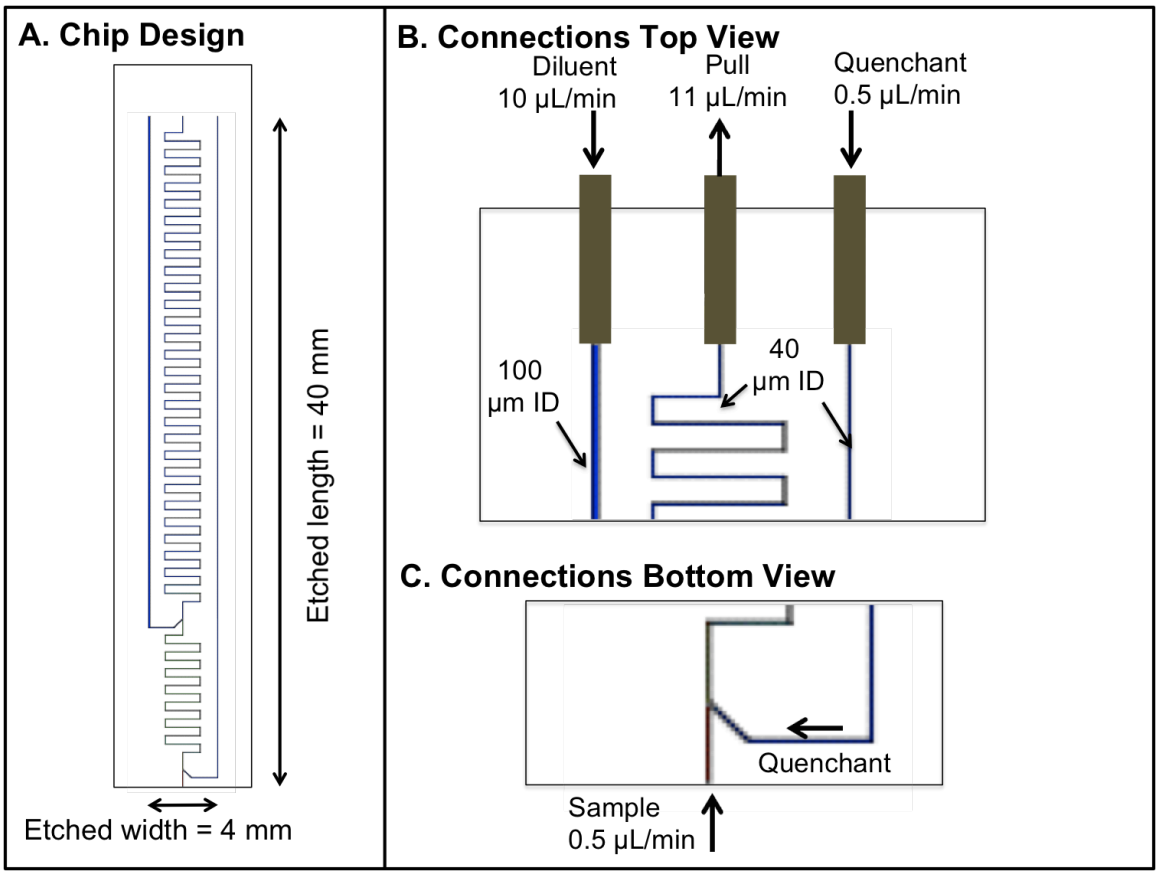

Figure 5-1. Illustration of push-pull sampler on a microfluidic chip. A. Overall chip design. B. Connections would be made through capillaries at the top of the chip. C. Sampling would be performed at the bottom edge of the chip.

Connections between the chip and syringe pumps will be made with fused silica capillaries. The chip may be etched deeper or drilled to allow capillary access, and the capillaries may be sealed to the chip with epoxy. In the design shown, fluid is pulled out of central mixing channel at 11 µL/min while diluent (10 µL/min) and quenchant (0.5 µL/min) are pumped in continuously. Sample that has been quenched and diluted may be

pulled through injection loops to interface the chip to HPLC in a manner similar to that used for the current push-pull sampler design.

Sample is pulled into the chip at 0.5 μL/min in this design, but flow rate may be adjusted by altering the flow rates at the top of the chip. Sampling may be performed by dipping the chip directly into sample, or a capillary may be attached if longer distance is needed, which will increase the time needed to quench reaction. In this design, a sample is mixed with quenchant 1 mm inside the chip edge to be consistent with the non-chip push-pull design, using a Y-shape interface for slightly faster mixing than a T-shape. Modeling this design shows that the sample mixes with the quenchant in 0.45 s under these conditions (assuming square channels).

The chip was designed for production out of borosilicate glass, as it is chemically resistant, physically strong, and reusable. However, borosilicate glass is not suitable for long-term use in high pH solutions, and requires a clean room and dangerous chemicals such as hydrofluoric acid for the etching process. A likely alternative to borosilicate glass in these cases would be poly(methyl methacrylate) (PMMA). PMMA can be laser-etched and injection molded for commercial production. PMMA is not as versatile as glass, however, as it is subject to chemical attack by a wide variety of solvents as well as concentrated acids and bases.

Automation of the Soup Pot Sampler

Future work for the soup pot sampler should be focused on automation. Currently, all steps for sampling, mixing and injection are performed manually. The proposed system is shown in Figure 5-2. The entire system could be contained on a

rolling cart, with the HPLC and computer controls on the bottom level. The cart could be placed next to a variety of reactor types. A detachable unit containing the sampler body and syringe for sampling/mixing (**5**) would be placed on top of the reactor (Figure 5-3). Several solvent bottles (orange caps) will be attached to a flow-selector valve. The solvent bottles may contain quenchant (**Q**), diluent (**D**), or rinse (**R1, R2**) solutions as needed. A computer-controlled flow selector valve (**2**) would be used to select between solvent bottles for quenching, dilution, and washing, as needed. A small-footprint pump (**3**) would be used to drive fluid from the solvent bottles to the detachable sampling unit. A solenoid valve (**4**) may be incorporated to flush excess fluid to waste (**W**) when switching between solutions. A detachable unit (**5**) will contain the sampler body and syringe housing for placement on top of a reactor. A small nitrogen gas tank (**6**) provides pressure to drive fluid out of the sample body. A tee (**7**) will split the flow from the sampler body. One portion will be pulled through an injection valve (**8**) using a small-footprint vacuum pump (**9**), while the majority of fluid flows to waste (red cap). The injection valve will be actuated, and the quenched sample filling the injection loop will be flushed to the HPLC using the HPLC pump.

The detachable unit (Figure 5-3) would consist of an outer body with fluid lines (liquid inlet, gas inlet, and fluid outlet) entering the sides of the unit (as marked). The sampler body would be mounted into the unit for stability and portability. Arms for moving the syringe up and down (**1**) into the reactor as well as drawing up precise volumes of fluid would be incorporated into the unit. Linear actuators would be mounted to the side of the unit. The main linear actuator (**LA1**) would move the entire syringe and the second linear actuator (**LA2**) down and up to access the reactor. LA2 will operate

independently to move the syringe plunger up and down to draw up precise sample volumes and for mixing. These arms would be computer-controlled. As an alternative, the injection syringe unit from a GC instrument could be repurposed. A computer-controlled arm for turning the stopcock (**2**) would be attached to the body of the detachable sampler. Telescoping tripod legs on the bottom of the sampler (**3**) would allow the sampler to access a wide variety of reactor vessels. The legs can rest on a bench to access a small (5 mL) vial, or rest on the top of a round bottom flask (as shown), or be mounted above the opening to a larger reactor. For stability, a bar on the back of the unit should be attached to a sturdy bar to ensure the unit does not get overturned during use.

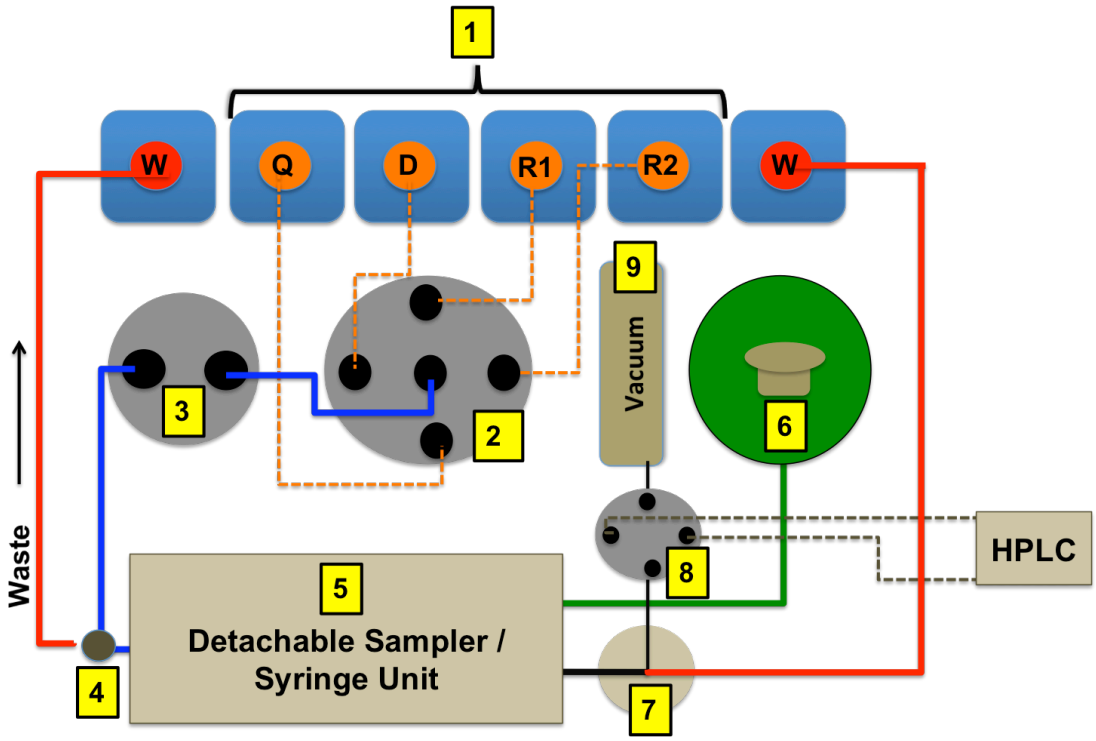

Figure 5-2. Top view of proposed automated soup-pot sampler system (not to scale). 1. Solvent bottles to hold quenchant (Q), diluent (D), rinse solutions (R1,R2), and waste (W). 2. Flow selector valve for switching between solvent bottles. 3. Small-footprint fluidic pump. 4. Solenoid valve for priming fluid lines. 5. Detachable sampling unit. 6. Small gas cylinder for pressurizing the sampler. 7. Tee for splitting flow to injection valve. 8. Injection valve for HPLC. 9. Vacuum pump for pulling samples through the injection valve.

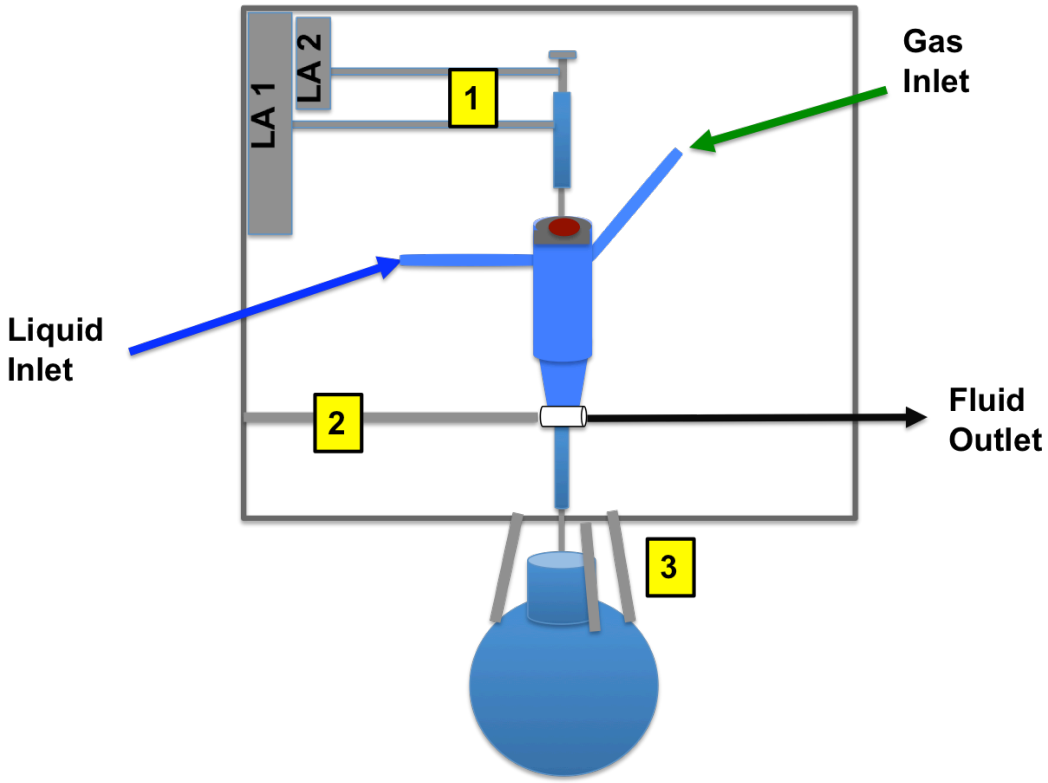

Figure 5-3. Detachable unit for automated soup pot sampler (not to scale). 1. Linear actuators (LA1, LA2) for moving syringe down and up for sampling and moving syringe plunger for mixing. 2. Arm for rotating the Teflon stopcock. 3. Telescoping tripod legs for placing the detachable sampling unit on a variety of surfaces.

APPENDIX A

EFFECT OF INJECTED PERFLUORINATED OILS ON THE HPLC SEPARATION OF ACETYLSALICYLIC ACID AND SALICYLIC ACID

Introduction

Segmented flow microfluidics is a useful tool for processing small sample volumes (nL – μL). The sample is sequestered into a droplet or plug within a non-miscible carrier fluid, typically fluorinated oil. Reagent may be added directly to the sample plug, ensuring that all reagents are mixed only where needed, reducing overall reagent consumption. The technique is even more powerful when coupled to a separation method for analysis. The fluorinated oil is typically stripped out of the system before the mixed sample is subjected to separation. While removing oil before injecting samples onto a high performance liquid chromatography (HPLC) reversed-phase column is possible, maintaining the plugs would allow for very small sample plugs to be injected. The injection loop could be filled with the entire sample segment, as well as oil, allowing sample segments smaller than the injection loop to be analyzed consistently. However, the effect of fluorinated oils on the separation capabilities of a reverse-phase high performance liquid chromatography (RP-HPLC) column has not been previously studied. In this work, we tested the effect of four directly injected fluorinated oils to determine their effect on the separation of acetylsalicylic acid and salicylic acid on a C18 reversed-phase column.

Experimental Section

Materials. Acetylsalicylic acid and salicylic acid were obtained from Acros Organics (Morristown, NJ, US). All water used was deionized to 18 MΩ resistivity with an E-pure 1090 series system from Barnstead Thermolyne Cooperation (Dubuque, IA, US). Unless otherwise noted, all other chemicals were purchased from Fisher Scientific (Chicago, IL, US).

Separation Conditions. A fixed concentration of acetylsalicylic acid (aspirin) and salicylic acid was prepared in methanol and diluted into 10 mM monopotassium phosphate buffer (pH 2.3). A C18 column, 4.6 x 100 mm, 3 um particle size (Varian, Inc., Palo Alto, CA, US), was installed on an Agilent 1100 HPLC (Agilent Technologies, Santa Clara, CA, US) equipped with an autosampler. Separation occurred under isocratic conditions at a flow rate of 1 mL/min, with 70% methanol mixed with 0.1% trifluoroacetic acid aqueous solution as the mobile phase.

Testing oils on the HPLC column. A mixture of acetylsalicylic acid and salicylic acid (SA solution) was prepared in methanol and diluted in water. The autosampler was used to inject 10 μL volume of either the SA solution or fluorinated oil. Absorbance at 254 nm was monitored using a variable wavelength detector for every injection of SA solution and the retention time and separation efficiency for each peak was calculated using in-house software.[89] For experiments with methanol rinsing, the column was rinsed for ten minutes with 100% methanol then re-equilibrated at 70% methanol after each injection of oil.

Results and Discussion

Selection of fluorinated oils. The oils selected for these experiments are commonly used in segmented flow microfluidic experiments. Each is fluorinated, but has slightly different chemical structures and physical properties (Table 6-1). Perfluorodecalin (PFD) is a perfluorinated cyclic alkane with the highest density and viscosity of the oils tested. Fluorinert FC-40 is a mixture of two fluorinated alkanes, while Fluorinert FC-77 is a mixture of a fluorinated straight-chain alkane and fluorinated cyclic ether. Perfluorooctanol (PFO) is typically used as a surfactant in the fluorinated continuous phase. As it would also be injected onto the HPLC column along with the rest of the fluorinated oils, we were interested in what role it might play in the separation. There are numerous other fluorinated oils available, each with their own set of chemical and physical properties that may be selected for optimal performance in the desired application. We sought to select a commonly-used representative from the most-used chemical classes to gain the most understanding of the interaction of fluorinated oils with an RP-HPLC column.

Table A-1. Perfluorinated oils and selected physical properties.

Oil Name	Chemical Name	Density	Viscosity
PFD	perfluorodecalin	1.917 g/mL	5.1 Pa•s
FC-40	perfluoro-tri-n-butylamine & perfluoro-di-n-butylmethylamine	1.855 g/mL	4.1 Pa•s
FC-77	C_8F_{18} and cyclic $C_8F_{16}O$	1.789 g/mL	1.3 Pa•s
PFO	1H,1H,2H,2H-perfluorooctanol	1.651 g/mL	---

Perfluorodecalin. PFD is one of the most commonly used oils in segmented flow applications. Injecting PFD on an RP-HPLC column has a dramatic effect on the peak shape and retention time of alternating injections of SA solution (Figure 6-1 A). Plotting the separation efficiency indicates that a single injection of PFD does not have a dramatic change on the separation efficiency, but with subsequent injections it decreases rapidly (Figure 6-1 B). Rinsing the column for 10 minutes with 100% methanol after each injection of PFD yields reproducible peak shape (Figure 6-1 C), retention time, and separation efficiency (Figure 6-1 D).

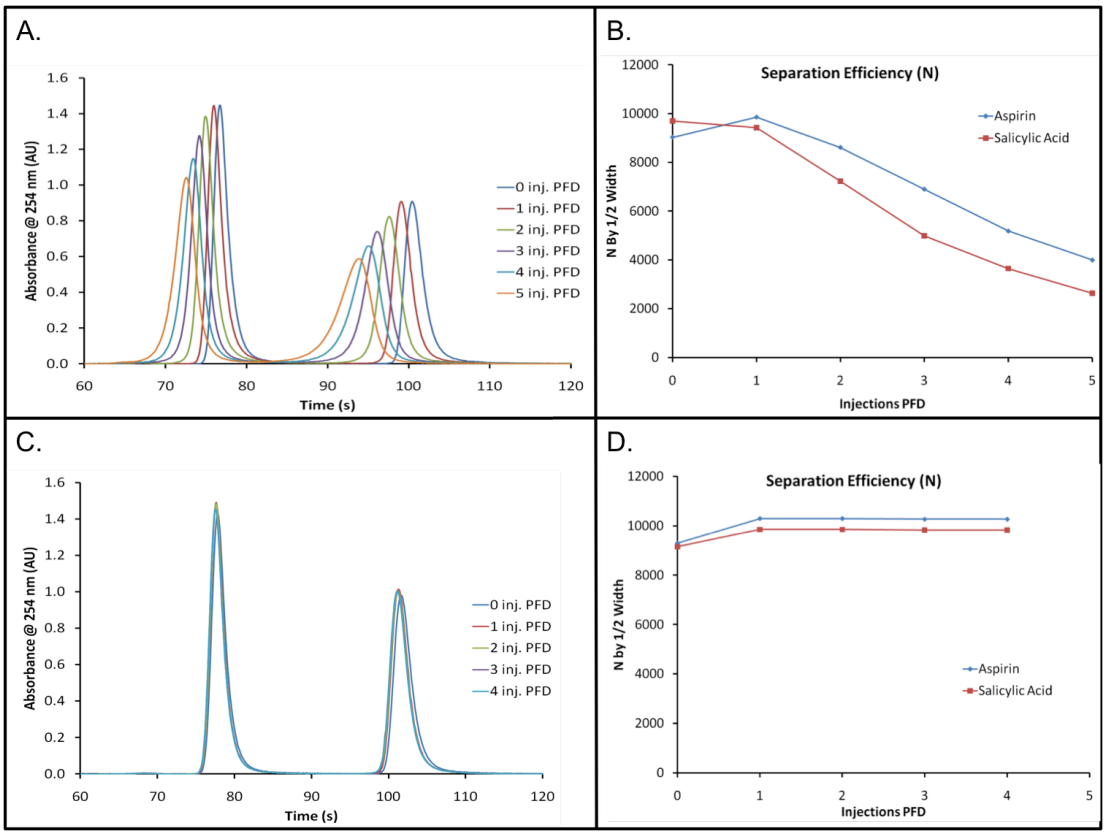

Figure A-1. Perfluorodecalin. A. Separation of acetylsalicylic acid (aspirin) and salicylic acid on an RP-HPLC column after each injection of PFD. B. Separation efficiency decreasing after each injection of PFD. C. Separation of acetylsalicylic acid and salicylic acid when the column is rinsed with 100% methanol for 10 minutes after each injection of PFD. D. Separation efficiency remains constant after multiple injections of PFD.

Fluorinert FC-40. FC-40 is a mixture of two amines, and was shown to have a more persistent effect on the RP-HPLC column. Each injection of FC-40 caused a rapid degradation of peak shape (Figure 6-2 A), separation efficiency (Figure 6-2 B) and a decrease in retention time (Figure 6-2 D). While a 10 minute rinse with 100% methanol improved retention time and peak shape, a rinse sequence with 20 minutes each of methanol, isopropanol, hexane, isopropanol and methanol again was required to regenerate the peak shape (Figure 6-2 C). Even with this extensive rinse (100 minutes, plus column equilibration time) the peak shape and retention time did not match the

initial separation. FC-40 does not appear to be suitable oil for use with an RP-HPLC column, although it is possible that other solvents may remove it from the column.

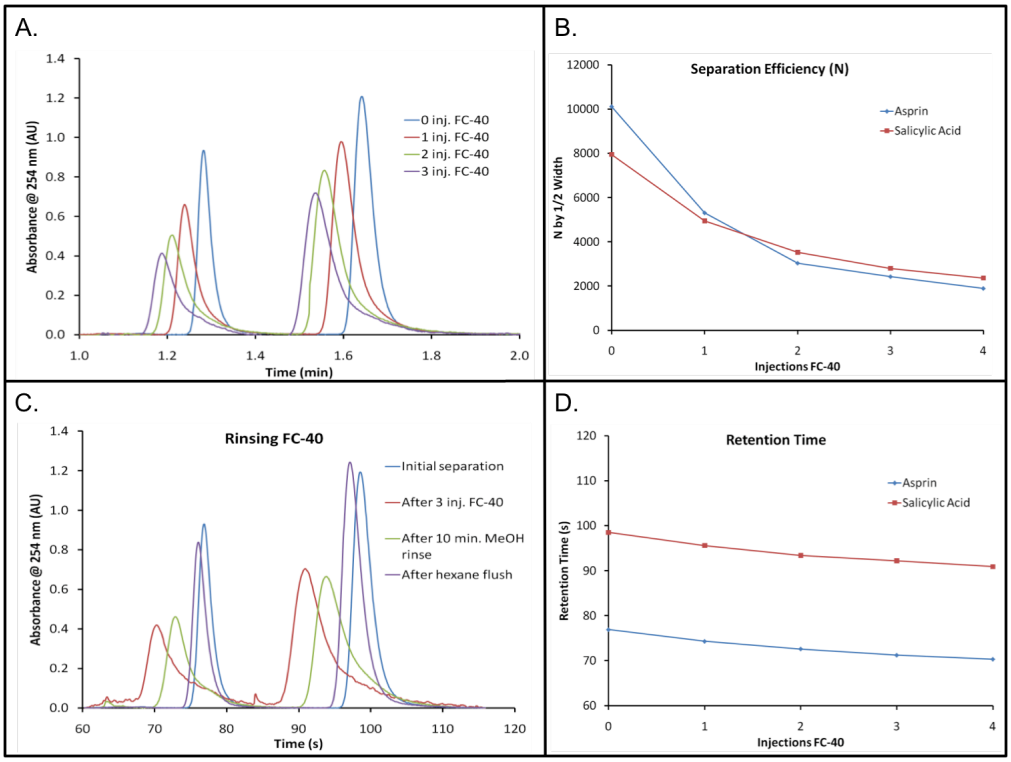

Figure A-2. Fluorinert FC-40. A. Separation of acetylsalicylic acid (aspirin) and salicylic acid on an RP-HPLC column after each injection of FC-40. B. Separation efficiency decreasing after each injection of FC-40. C. Hexane is required to rinse FC-40 from the column. D. Retention time decreases after each injection of FC-40.

Fluorinert FC-77. FC-77 had a similar effect on the RP-HPLC column as PFD. Degradation in peak shape with decreased retention time (Figure 6-3 A) and decreased separation efficiency (Figure 6-3 B) were evident after just one injection of FC-77. Methanol was effective in rinsing the column, yielding reproducible peak shape and retention time (Figure 6-3 C) and steady separation efficiency (Figure 6-3 D). FC-77, along with PFD, may be suitable for use with an RP-HPLC column with methanol rinsing.

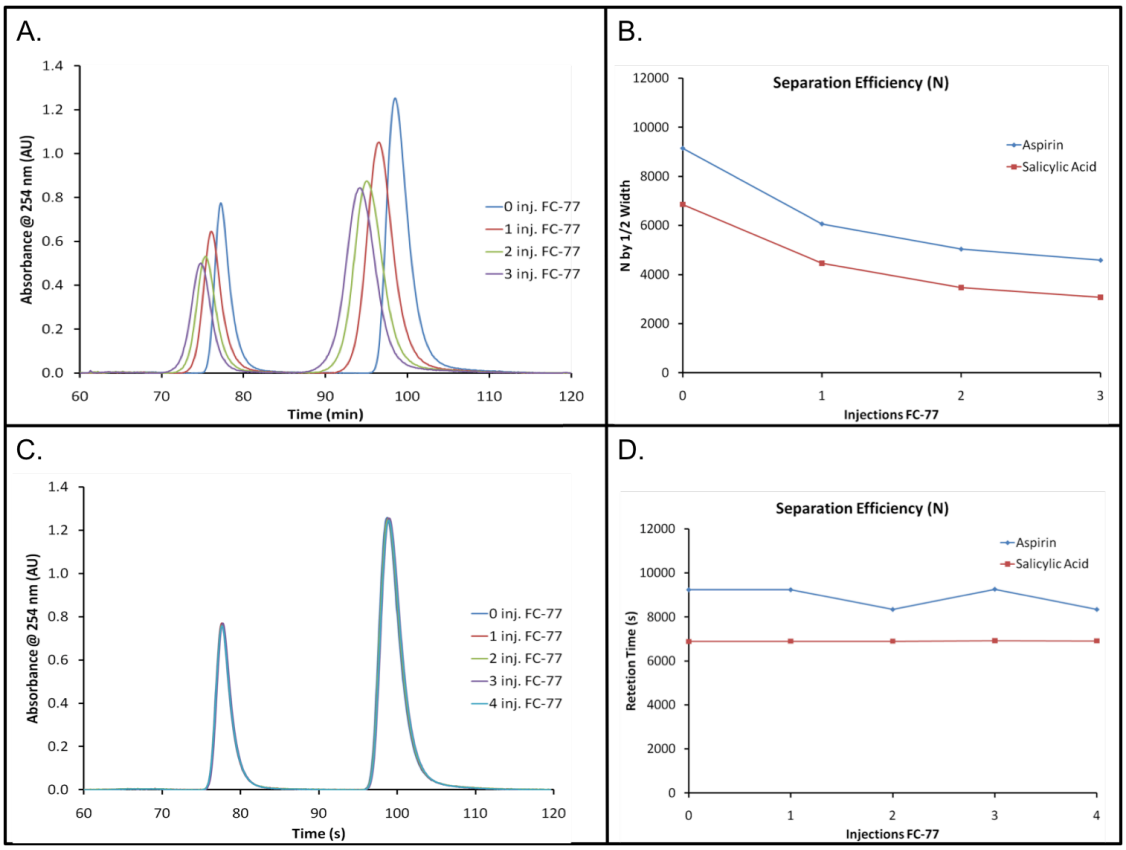

Figure A-3. Fluorinert FC-77. A. Separation of acetylsalicylic acid (aspirin) and salicylic acid on an RP-HPLC column after each injection of FC-77. B. Separation efficiency decreasing after each injection of FC-77. C. Separation of acetylsalicylic acid and salicylic acid when the column is rinsed with 100% methanol for 10 minutes after each injection of FC-77. D. Separation efficiency remains constant after multiple injections of FC-77.

Perfluorooctanol. PFO, while not a commonly used as a continuous phase, is often incorporated as a surfactant. Interestingly, PFO did not have any effect on the separation. Even after multiple injections of PFO, the peak shape (Figure 6-4), retention time and separation efficiency (data not shown) were not affected. The effect of PFO on the column using a mobile phase with a lower organic concentration was outside the scope of this work. PFO may be a good continuous phase or surfactant for use in this particular application, but further testing would need to be performed to determine if it would have the same properties under other conditions.

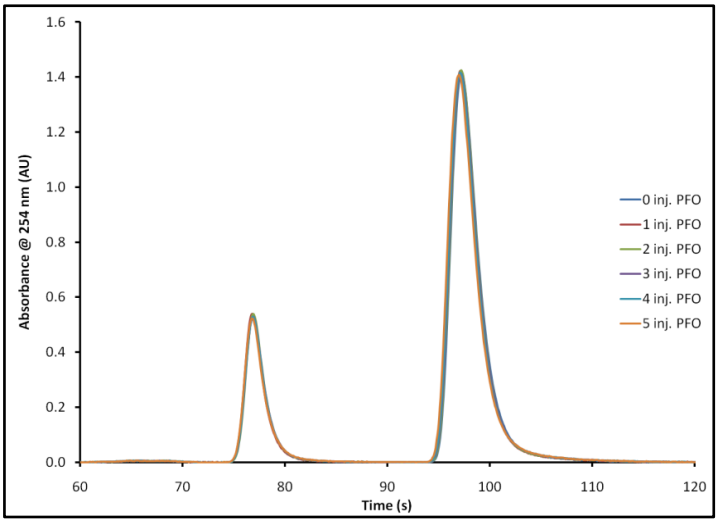

Figure A-4. Perfluorooctanol. Separations of acetylsalicylic acid and salicylic acid were reproducible after multiple injections of PFO.

Conclusions

The ability to inject fluorinated continuous phase directly onto an RP-HPLC column would enable sample segments smaller than the injection loop to be reproducibly analyzed. This would enable the direct coupling of segmented flow to HPLC without requiring removal of the fluorinated phase, incorporating the sample processing possibilities of segmented flow with the reliability of HPLC. We have determined that three of the fluorinated oils tested (PFD, FC-40, FC-77) were detrimental to column performance under the tested conditions, while PFO did not have an observed effect on column performance. It was also observed that flushing the column with 100% methanol was able to reverse the column degradation for PFD and FC-77, while FC-40 required hexane to restore column performance. We believe that the fluorinated oils are coating the column surface, reducing the interaction of sample with the stationary phase. This would result in reduced retention times and decreased separation efficiency, both of

which are observed. We have shown that reproducible separations may be achieved with fluorinated oil injected onto an RP-HPLC column and the technique holds promise. Further testing with other fluorinated oils and common HPLC solvent systems, such as acetonitrile/aqueous mixtures, would be needed to determine if this technique would be practical for common use.

APPENDIX B

FINITE ELEMENT MODELING OF MICROFLUIDIC CHAMBER FOR MONITORING SECRETIONS FROM ADIPOCYTES

Introduction

Finite element modeling was used validate experimental measurements characterizing a three-layer, resealable microfluidic chip for monitoring fatty acid release from adipocytes. The chip was constructed from two bonded layers, and one detachable layer. The top, detachable layer could be removed to allow a glass coverslip with a layer of cultured adipocytes to be placed in the cell chamber (Figure B-2). The chip was used to monitor non-esterified fatty acid (NEFA) secretions from the cultured cells by mixing effluent from the cell chamber with NEFA enzyme assay reagents and Amplex Red (10-acetyl-3,7-dihydroxyphenoxazine), which was turned over to produce a fluorescent product, resorufin. Fluorescence signal from the enzyme assay was detected on-chip.[90]

The chip was characterized experimentally by flowing resorufin, the fluorescent product, through the chip inlet and calculating the time needed to observe a 10% to 90% change in the concentration at a points downstream from the cell chamber. Due to the space constraints of the chip design, measurements were unable to be obtained directly at the outlet of the cell chamber, making it impossible to directly characterize just the cell chamber. Resorufin flow into the cell chamber was modeled to provide a deeper understanding of the fluid flow dynamics and validate experimental results. A similar chip with a larger cell chamber for monitoring glycerol release from adipocytes has been

modeled previously in a similar manner.[91] Two additional cell chamber designs with equal volume were modeled to determine if changing the cell chamber geometry would have an effect on the assay temporal resolution. Finally, the release of oleic acid from adipocytes within the cell chamber was modeled to gain an understanding of how fatty acids were rinsed out of the cell chamber as well as whether fatty acids released upstream might be affecting cells located downstream within the cell chamber.

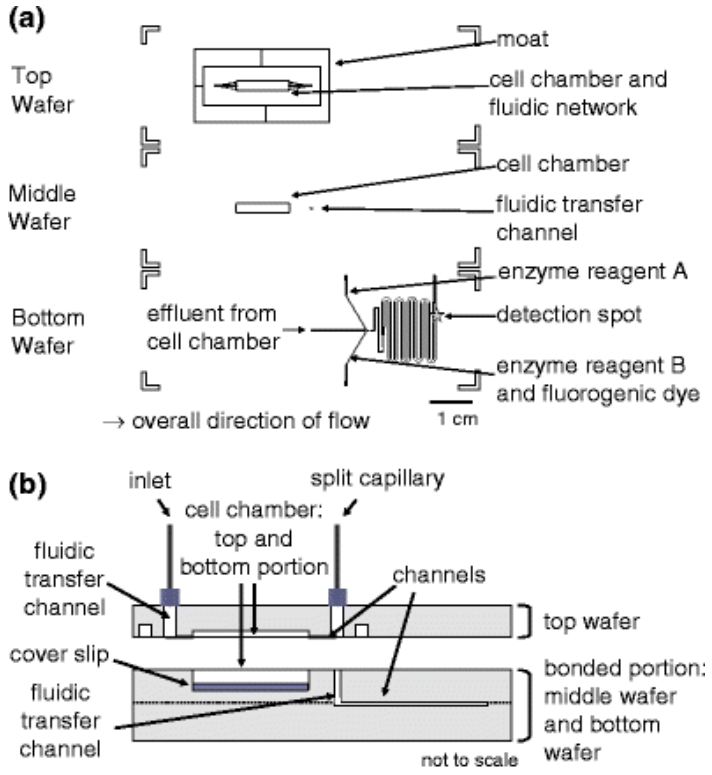

Figure B-1. Microfluidic chip design for monitoring adipocyte fatty acid release. A. Top view of each layer of the chip. Only the cell chamber was modeled for this work. B. Side view of the chip with the cover slip shown inside the cell chamber. Figure created by Anna M. Clark. Adapted with permission from source.[90]

Experimental Section

COMSOL Multiphysics 3.5a (Comsol, Inc., Burlington, MA) was used to model the flow and concentration of resorufin or oleic acid within the cell chamber. For the standard design, the cell chamber was modeled as a box 12.5 mm long x 2.0 mm wide x 0.4 mm deep. On each end of the chamber (2.0 cm x 0.4 mm), rectangular 5 μm tall inlet and outlet slits were placed 0.3 mm from the bottom of the cell chamber and spanned the full 2.0 mm width of the channel. The actual chip design (Figure B-1 A) uses a three channel weir for the inlets and outlets, but slits were used instead for ease of modeling. For the "sideways" cell chamber configuration, the cell chamber was modeled as 2.0 mm long x 12.5 mm wide x 0.4 mm deep. Inlet and outlet slits (5 μm tall) were placed 0.3 mm from the bottom of the cell chamber and spanned the full 12.5 mm width of the side of the chamber. The "square" cell chamber configuration was modeled as 5.0 mm long x 5.0 mm wide x 0.4 mm deep. Inlet and outlet slits (5 μm tall) were placed 0.3 mm from the bottom of the cell chamber and spanned the full 5.0 mm width of the chamber. Both alternate configurations had the same total chamber volume and volumetric flow rate as the standard cell chamber configuration.

Fluid flow was defined as laminar, with a volumetric flow rate of 8 μL/min through the cell chamber. The model used a temperature of 37 °C and diffusion constants were adjusted for temperature. The density of water used was 993 kg/m^3 and the viscosity of water was 6.90×10^{-4} Pa•s. Resorufin flowing into the cell chamber was modeled at a concentration of 30 μM, with a diffusion coefficient of 9.01×10^{-10} m^2/s. The diffusion coefficient for oleic acid was modeled as 5.26×10^{-10} m^2/s.[92]

Oleic acid release from adipocytes was modeled using the standard cell chamber. Release from the cells was modeled to occur 31.25 μm above the cover slip to represent the radius of a differentiated adipocyte and an average point of release from the cells. An inward flux was selected that resulted in an oleic acid concentration at the outlet that matched experimental results.

Results and Discussion

Resorufin flow into the standard cell chamber was modeled first. The concentration of resorufin at the center of the outlet slit was monitored over time. Based on the model, the response time (time to change from 10% to 90% of the resorufin concentration) was calculated to be 43 s as modeled (date not shown). The response time for the experimental system was calculated to be 41 s based on observing the response time before the inlet and after the outlet. Anna M. Clark calculated the experimental values. The close match between calculated response times for the cell chamber in the modeled and experimental systems indicate that the model may be used to gain a valid understanding of the flow within the cell chamber.

The cell chamber geometry was based on a previous microfluidic chip design[91] which was miniaturized to decrease reagent use and enable a smaller number of cells to be studied. Two other cell geometries were tested to determine if they had better response times as modeled and determine if the chip should be altered to use a different cell chamber geometry.

Side views of each cell chamber design (Figure B-2) shows resorufin flowing into the chamber over time. In all three designs, the lower outlet corner of the cell chamber

does not reach the maximum resorufin concentration over time as the fluid is rapidly swept up and out of the cell chamber through the outlet. Although this is a small volume, this may have implications for how many cells are actually stimulated to release fatty acids when a drug is flowed into the cell chamber and may need to be considered when performing cell studies.

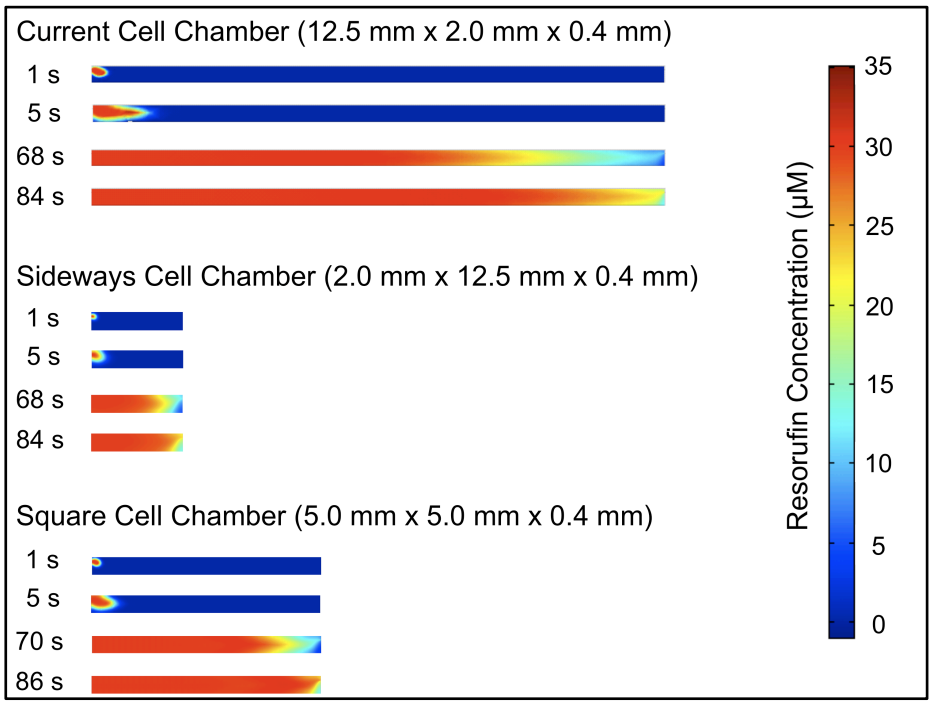

Figure B-2. Flow of resorufin into three cell chamber geometries. A side view of each cell geometry (current, sideways, square) is shown with 30 µM resorufin flowing into the chamber inlet (left side) at 8 µL/min at four time points for each geometry. Resorufin concentration across the cell chamber is indicated by colormap, with red indicating high resorufin concentration, and dark blue indicating a zero resorufin concentration. In all three geometries, resorufin can be seen flowing up and out of the outlet slit (right side), leaving a corner of the cell chamber at a lower resorufin concentration.

The time necessary to reach 90% resorufin concentration for percentage of cells reached was modeled to determine how quickly a drug could stimulate groups of cells as it flowed into the system. The modeled results show that the three cell chamber geometries are nearly identical in the time required to flow resorufin over a percentage of

cells (Figure B-3). The square cell chamber has slightly lower times overall, but the difference was not considered sufficient to change the cell chamber geometry for future experiments.

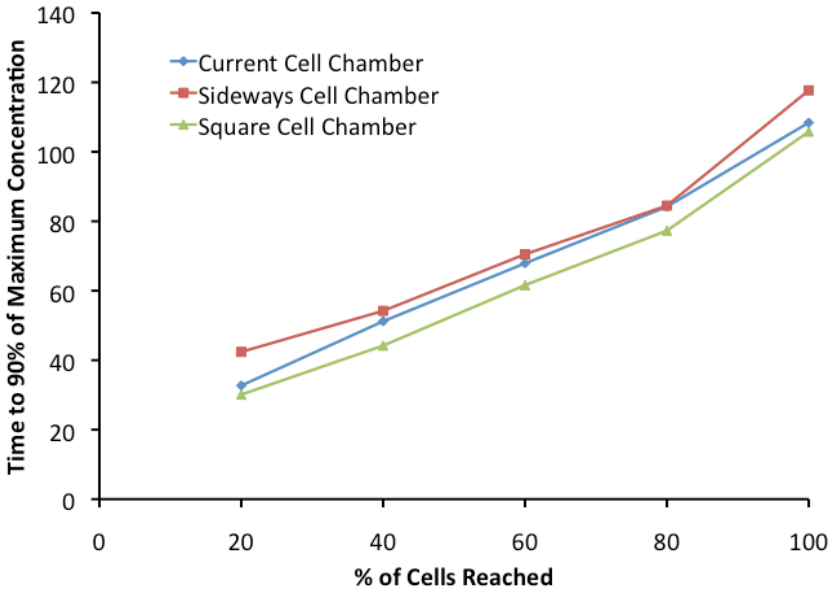

Figure B-3. Time required to flow resorufin over cells for three chamber geometries. Times for each chamber geometry were very close, with a slight improvement using the square cell chamber model. The difference in time was not considered sufficient to modify the cell chamber geometry for future experiments.

Efflux of oleic acid from cells was modeled to determine how rapidly a step change in NEFA efflux should be observed at the cell chamber outlet. A side view of the cell chamber (Figure B-3 A) shows that the oleic acid is rapidly flushed out of the system, remaining concentrated directly above the cells and not filling the chamber. The image shows a compressed cell chamber length so that the oleic acid concentration could be observed. A plot of the outlet concentration over time (Figure B-4 B) shows a 10% to 90% response time of 56 s, representing the fastest change in cell efflux that could be measured using this system.

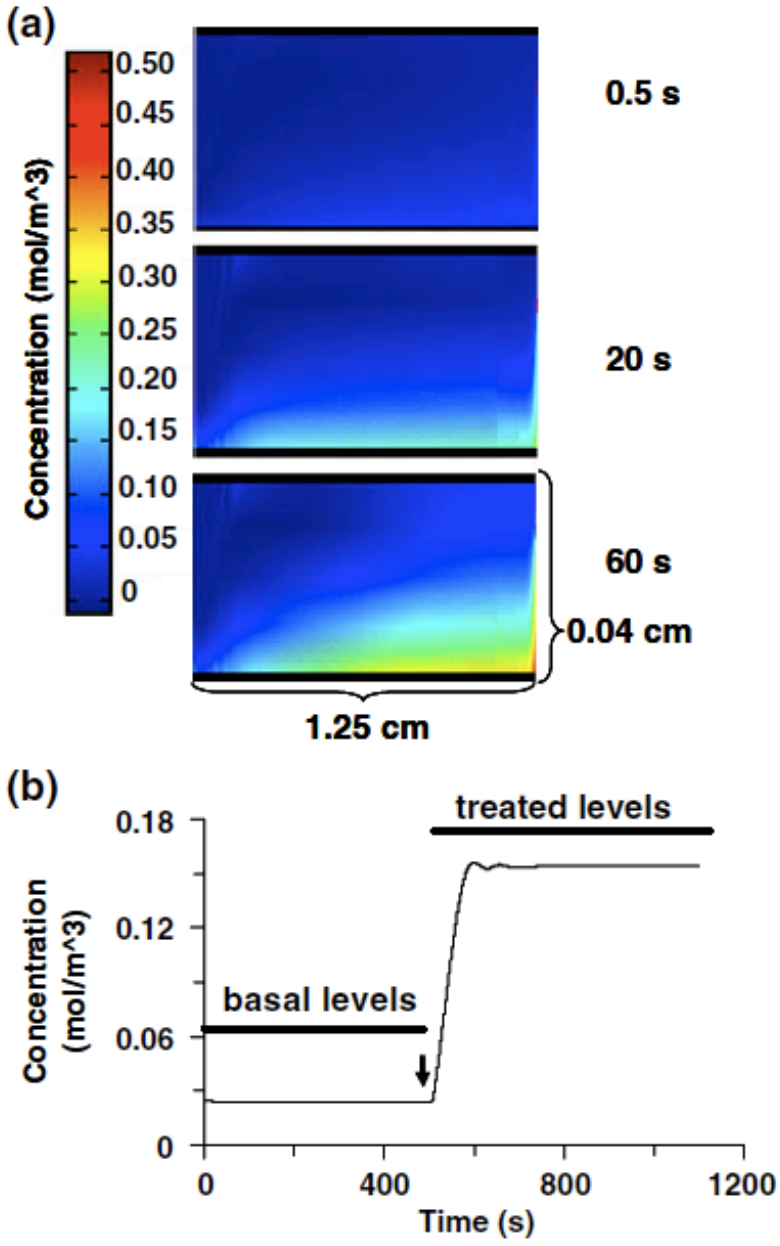

Figure B-4. Model of oleic acid release from adipocytes. A. Side view of standard cell chamber showing NEFA concentration distribution following a six-fold step increase in NEFA efflux. B. Plot showing the simulated NEFA concentration at the outlet after a six-fold increase in NEFA efflux. Arrow indicates start of step change (500 s). Figure created by Anna M. Clark. Used with permission from source.[90]

Conclusions

The cell chamber of a microfluidic chip was modeled using COMSOL to provide deeper insight into flow within the chamber, as it could not be directly observed due to fluidic ports crowding the chip surface. The cell chamber was first modeled with resorufin flowing into the inlet. The response time at the outlet was calculated to be 41 s experimentally, and 43 s using the model, indicating that the model can be used for understanding flow within the cell chamber. Three cell chamber geometries (standard, sideways, and square) were modeled and the time required for resorufin to flow over the bottom surface of the cell chamber was calculated. It was determined that the square geometry had slightly faster times than the other two geometries, but it was not a sufficient improvement to justify changes to the cell chamber design for this set of experiments. Finally, oleic acid release from cells lining the bottom of the cell chamber was modeled. Response time of 56 s at the outlet was calculated for a six-fold increase in fatty acid efflux, indicating this is the fastest change in fatty acid efflux that can be observed using this chip design.

APPENDIX C

PUSH-PULL SAMPLER CONSTRUCTION

The following work gives a detailed description of how the push-pull sampler probe was constructed. The push-pull sampler probe consists of a sampling tee, PEEK ferrules, a push capillary and a pull capillary (Figure C-1). Wrenches (1/4") and superglue are required for assembling the sampler. The push capillary (40 μm ID, 100 μm OD) was 25 cm long, with a short (~3 cm) piece of capillary (250 μm ID, 360 μm OD) attached with super glue at one end to facilitate connection to the push syringe using a union. The wider capillary was placed on the end of the push capillary, and a drop of superglue was placed on the end of the wider capillary, away from the end of the push capillary. The super glue was allowed to wick between the two capillaries, and was allowed to dry overnight. The pull capillary (250 μm ID, 350 μm OD) was 5 cm long. The sampling end (shown on left) had the polyimide coating burned off to facilitate alignment of the push and pull capillaries. The stainless sampling tee (Valco MT1XCS6) was 150 μm bore, and breaks apart into an insert, outer stainless ring and three nuts, as shown. A Valco FS1.2PK ferrule was used to connect the push capillary and two Valco FS1.4PK (2) used to connect the pull and transfer (not shown) capillaries.

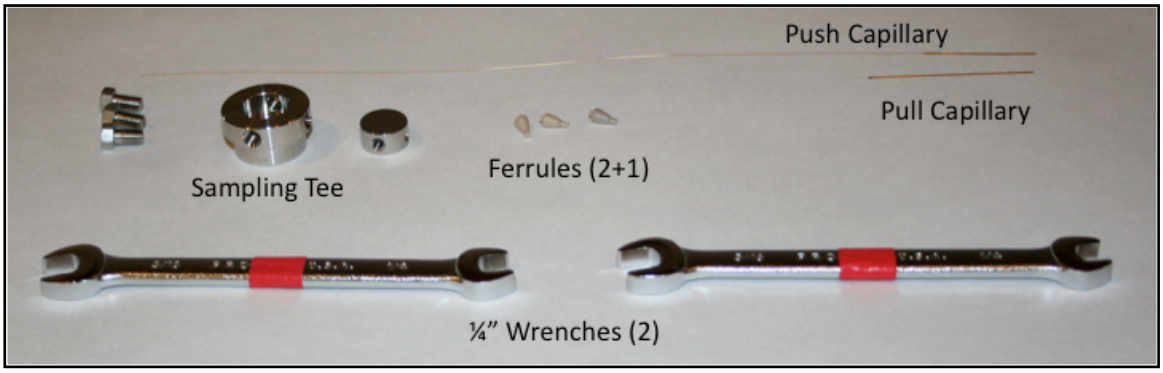

Figure C-1. Materials needed to construct the push-pull sampler probe.

To assemble the sampler, the sample tee and insert (Figure C-2, 1) holes were aligned and the insert was placed inside the tee (Figure C-2, 2). The push capillary (narrow end) was threaded through a nut, the FS1.2PK ferrule and completely through the main portion of the tee (Figure C-2, 3). Once the capillary was through the tee, the nut and ferrule were placed into the tee, but not tightened so the push capillary was free to slide through the tee (Figure C-2, 4). The pull capillary was threaded through a nut and one of the FS1.4PK ferrules. Note that the clear tip with polyimide removed was facing away from the tee (Figure C-2, 5).

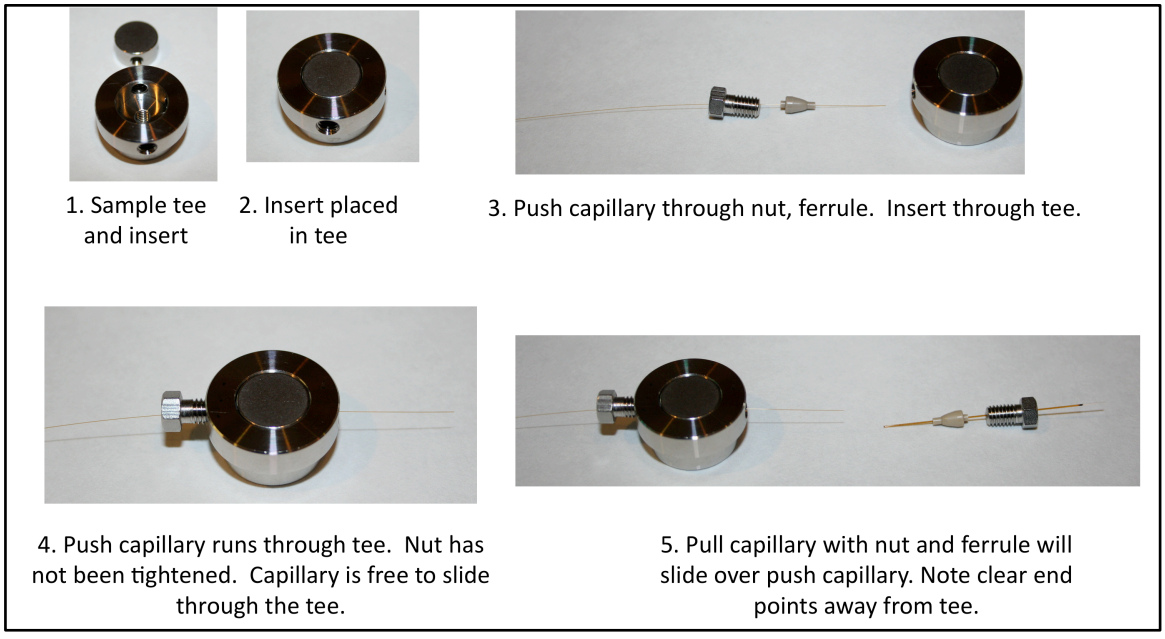

Figure C-2. Steps to assemble the push-pull sampler probe, part 1.

While holding the tee and push capillary in one hand and the pull capillary assembly in the other hand, the push capillary was threaded into the pull capillary (Figure C-3, 6) and completely through, until the push capillary was visible on the other side of the pull capillary. The pull capillary was secured inside the tee by tightening the nut down on the ferrule (Figure C-3, 7). The push capillary was securely attached to the tee, with the clear tip facing away from the tee, while the push capillary remained free to move. The push capillary was aligned so the tip of the capillary was recessed 1 mm inside the tip of the pull capillary (this was performed under a microscope). The push capillary was secured by tightening the nut to clamp down on the ferrule holding the push capillary in place (Figure C-3, 7).

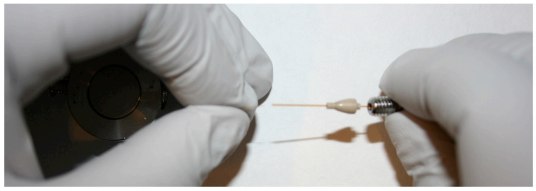

6. Insert push capillary into pull capillary.

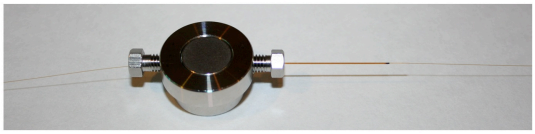

7. Tighten nut to secure pull capillary in place. Push capillary is free to slide.

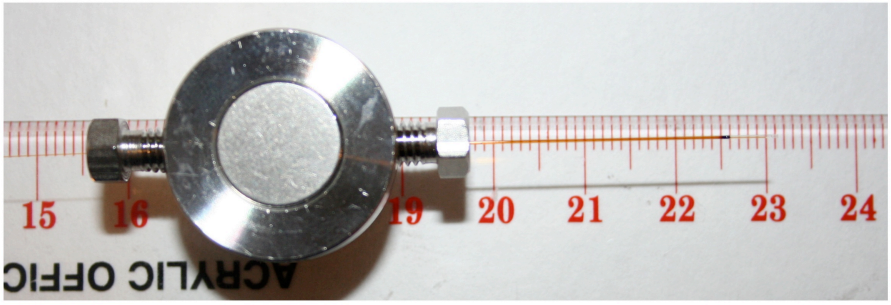

8. Slide push capillary so that it is one mm inside the tip of the sample capillary (alignment under microscope is ideal). Tighten nut securely to hold push capillary in place.

Figure C-3. Steps to assemble the push-pull sampler probe, part 2.

The probe was connected to the rest of the push-pull sampler system through a transfer capillary. The transfer capillary (150 µm ID, 360 µm OD) was connected to the side arm of the tee using a nut and a FS1.4PK ferrule (Figure C-4, 9). The nut was

tightened down to ensure air did not leak into the system. The push capillary was connected to a syringe using a stainless steel union (Valco) and FS1.4PK ferrules (Figure C-4, 10). The push capillary was flushed with the quenchant fluid (Figure C-4, 11). If the sampler probe was constructed properly, fluid should be observed at the tip of the pull capillary. The sampler probe was placed in a vial of liquid while all capillaries were primed to ensure no air was in the system (Figure C-4, 12). The push capillary was connected to a syringe pump, while the transfer capillary was connected to an injection valve (for FIA or HPLC monitoring) which was in turn connected to a withdrawing syringe pump (Figure C-4, 13). The rest of the system was constructed as described in Chapter 2.

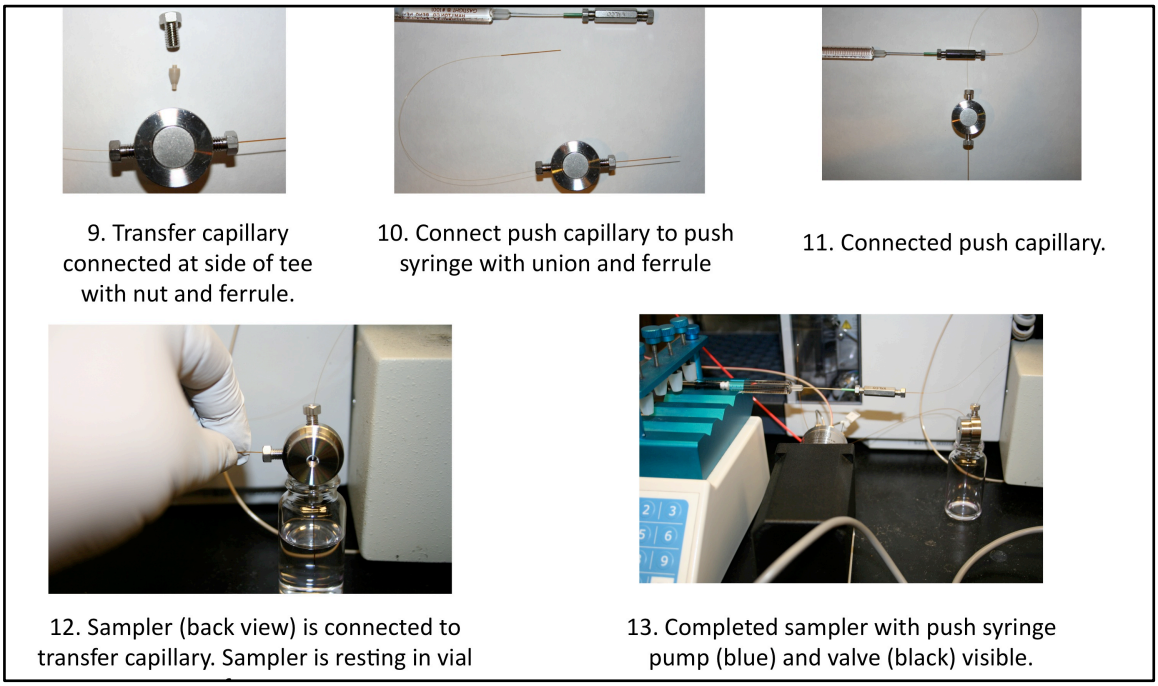

Figure C-4. Steps to assemble the push-pull sampler probe, part 3.

REFERENCES

1. Clark, J., Impacts of PAT. *J. Process Anal. Technol.* **2005,** *2* (6), 12-15.

2. United States Food & Drug Administration FDA guidance for industry, PAT - a framework for innovative pharmaceutical development, manufacturing and quality assurance. http://www.fda.gov/downloads/Drugs/GuidanceComplianceRegulatoryInformation/Guidances/ucm070305.pdf.

3. Workman, J.; Koch, M.; Lavine, B.; Chrisman, R., Process analytical chemistry. *Anal. Chem.* **2009,** *81* (12), 4623-4643.

4. Watts, D. C.; Clark, J. E., PAT: driving the future of pharmaceutical quality. *J. Process Anal. Technol.* **2006,** *3* (6), 6-9.

5. Aaltonen, J.; Gordon, K. C.; Strachan, C. J.; Rades, T., Perspectives in the use of spectroscopy to characterise pharmaceutical solids. *Int. J. Pharm.* **2008,** *364* (2), 159-169.

6. Schafer, W. A.; Hobbs, S.; Rehm, J.; Rakestraw, D. A.; Orella, C.; McLaughlin, M.; Ge, Z.; Welch, C. J., Mobile tool for HPLC reaction monitoring. *Org. Process Res. Dev.* **2007,** *11*, 870-876.

7. Rao, R. N.; Nagaraju, V., An overview of the recent trends in development of HPLC methods for determination of impurities in drugs. *J. Pharm. Biomed. Anal.* **2003,** *33* (3), 335-377.

8. Wu, N. J.; Thompson, R., Fast and efficient separations using reversed phase liquid chromatography. *J. Liq. Chromatogr. Relat. Technol.* **2006,** *29* (7-8), 949-988.

9. Kennedy, R. T.; German, I.; Thompson, J. E.; Witowski, S. R., Fast analytical-scale separations by capillary electrophoresis and liquid chromatography. *Chem. Rev.* **1999,** *99* (10), 3081-+.

10. Wu, N. J.; Clausen, A. M., Fundamental and practical aspects of ultrahigh pressure liquid chromatography for fast separations. *J. Sep. Sci.* **2007,** *30* (8), 1167-1182.

11. Heinisch, S.; Rocca, J. L., Sense and nonsense of high-temperature liquid chromatography. *J. Chromatogr. A* **2009,** *1216* (4), 642-658.

12. Wu, R.; Hu, L. G.; Wang, F. J.; Ye, M. L.; Zou, H., Recent development of monolithic stationary phases with emphasis on microscale chromatographic separation. *J. Chromatogr. A* **2008,** *1184* (1-2), 369-392.

13. Paliwal, S. K.; Nadler, T. K.; Wang, D. I. C.; Regnier, F. E., Automated process monitoring of monoclonal-antibody production. *Anal. Chem.* **1993,** *65* (23), 3363-3367.

14. Liu, Y. C.; Wang, F. S.; Lee, W. C., On-line monitoring and controlling system for fermentation processes. *Biochem. Eng. J.* **2001,** *7* (1), 17-25.

15. Hamlin, G. A., The Zymark BenchMate (TM). A compact, fully-automated solution-phase reaction work-up facility for multiple parallel synthesis. *J. Autom. Methods Manag. Chem.* **2000,** *22* (6), 181-186.

16. McLaughlin, K. J.; Faibushevich, A. A.; Lunte, C. E., Microdialysis sampling with on-line microbore HPLC for the determination of tirapazamine and its reduced metabolites in rats. *Analyst* **2000,** *125* (1), 105-110.

17. Nakao, R.; Okada, M.; Inoue, O.; Fukumura, T.; Suzuki, K., Combining high-performance liquid chromatography-positron detection and on-line microdialysis for animal metabolism study of positron emission tomography probes. *J. Chromatogr. A* **2008,** *1203* (2), 193-197.

18. Borjigin, J.; Liu, T., Application of long-term microdialysis in circadian rhythm research. *Pharmacol. Biochem. Behav.* **2008,** *90* (2), 148-155.

19. Cheng, G.-W.; Wu, H.-L.; Huang, Y.-L., Automated on-line microdialysis sampling coupled with high-performance liquid chromatography for simultaneous determination of malondialdehyde and ofloxacin in whole blood. *Talanta* **2009,** *79* (4), 1071-5.

20. Cheng, G. W.; Lee, C. F.; Hsu, K. C.; Wu, H. L.; Huang, Y. L., On-line microdialysis-nano-Au/TiO2-high-performance liquid chromatography system for the simultaneous determination of cobalt and nickel in water. *J. Chromatogr. A* **2008,** *1201* (2), 202-207.

21. Idris, A. M., An Overview of the Generations and Recent Versions of Flow Injection Techniques. *Crit. Rev. Anal. Chem.* **2010,** *40* (3), 150-158.

22. Evgen'ev, M. I.; Garmonov, S. Y.; Shakirova, L. S., Flow-injection analysis of pharmaceuticals. *J. Anal. Chem.* **2001,** *56* (4), 313-323.

23. Ruzicka, J.; Hansen, E. H., Flow injection analyses. 1. New concept of fast continuous-flow analysis. *Anal. Chim. Acta* **1975,** *78* (1), 145-157.

24. Rios, A.; Decastro, M. D. L.; Valcarcel, M., FLOW-INJECTION ANALYSIS - A NEW APPROACH TO PHARMACEUTICAL DETERMINATIONS. *J. Pharm. Biomed. Anal.* **1985,** *3* (2), 105-121.

25. Ruzicka, J.; Marshall, G. D., Sequential injection: a new concept for chemical sensors, process analysis and laboratory assays. *Anal. Chim. Acta* **1990,** *237*, 329-343.

26. Lee, S. H.; Sohn, O. J.; Yim, Y. S.; Han, Y. A.; Hyung, G. W.; Chough, S. H.; Rhee, J. I., Sequential injection analysis system for on-line monitoring of L-cysteine concentration in biological processes. *Talanta* **2005,** *68* (2), 187-192.

27. Dominguez, K.; Toth, I. V.; Souto, M. R. S.; Mendes, F.; De Maria, C. G.; Vasconcelos, I.; Rangel, A., Sequential Injection Kinetic Flow Assay for Monitoring Glycerol in a Sugar Fermentation Process by Saccharomyces cerevisiae. *Appl. Biochem. Biotechnol.* **2010,** *160* (6), 1664-1673.

28. Vidigal, S.; Toth, I. V.; Rangel, A., Sequential injection lab-on-valve system for the on-line monitoring of hydrogen peroxide in lens care solutions. *Microchem J.* **2009,** *91* (2), 197-201.

29. Horstkotte, B.; Werner, E.; Wiedemeier, S.; Elsholz, O.; Cerda, V.; Luttmann, R., At-line determination of formaldehyde in bioprocesses by sequential injection analysis. *Anal. Chim. Acta* **2006,** *559* (2), 248-256.

30. Ruzicka, J., Lab-on-valve: universal microflow analyzer based on sequential and bead injection. *Analyst* **2000,** *125* (6), 1053-1060.

31. Wu, C.-H. R.; Liu, J. L., Micro sequential injection lab-on-valve for process monitoring and bioanalytical assays. *Process Anal. Technol.* **2006,** *3* (3), 25-30.

32. Wu, C. H.; Scampavia, L.; Ruzicka, J.; Zamost, B., Micro sequential injection: fermentation monitoring of ammonia, glycerol, glucose, and free iron using the novel lab-on-valve system. *Analyst* **2001,** *126* (3), 291-297.

33. Wu, C. H.; Scampavia, L.; Ruzicka, J., Microsequential injection: anion separations using 'Lab-on-Valve' coupled with capillary electrophoresis. *Analyst* **2002,** *127* (7), 898-905.

34. Wu, C. H.; Scampavia, L.; Ruzicka, J., Micro sequential injection: automated insulin derivatization and separation using a lab-on-valve capillary electrophoresis system. *Analyst* **2003,** *128* (9), 1123-1130.

35. Satinsky, D.; Solich, P.; Chocholous, P.; Karlicek, R., Monolithic columns--a new concept of separation in the sequential injection technique. *Anal. Chim. Acta* **2003,** *499* (1-2), 205-214.

36. Garcia-Jimenez, J. F.; Valencia, M. C.; Capitan-Vallvey, L. F., Simultaneous determination of antioxidants, preservatives and sweetener additives in food and cosmetics by flow injection analysis coupled to a monolithic column. *Anal. Chim. Acta* **2007,** *594* (2), 226-233.

37. Chocholous, P.; Satinsky, D.; Sladkovsky, R.; Pospisilova, M.; Solich, P., Determination of pesticides fenoxycarb and permethrin by sequential injection chromatography using miniaturized monolithic column. *Talanta* **2008,** *77* (2), 566-570.

38. Welch, C. J.; Gong, X.; Cuff, J.; Dolman, S.; Nyrop, J.; Lin, F.; Rogers, H., Online Analysis of Flowing Streams Using Microflow HPLC. *Org. Process Res. Dev.* **2009,** *13* (5), 1022-1025.

39. Jenkins, T. Real-time monitoring of in-process samples by UPLC. www.waters.com/webassets/cms/library/docs/720002561en.pdf (accessed August 27, 2010).

40. Groton Biosystems ARS Series: Online Sampling systems. http://www.grotonbiosystems.com/products/sampling_ars_overview.cfm (accessed August 27, 2010).

41. Gaddum, J. H., Push-pull cannulae. *J. Physiol.-London* **1961,** *155* (1), 1P-28P.

42. Myers, R. D., Development of push-pull systems for perfusion of anatomically distinct regions of the brain of the awake animal. *Ann. N.Y. Acad. Sci.* **1986,** *473*, 21-41.

43. Arora, A.; Simone, G.; Salieb-Beugelaar, G. B.; Kim, J. T.; Manz, A., Latest Developments in Micro Total Analysis Systems. *Anal. Chem.* **2010,** *82* (12), 4830-4847.

44. Focke, M.; Kosse, D.; Muller, C.; Reinecke, H.; Zengerle, R.; von Stetten, F., Lab-on-a-Foil: microfluidics on thin and flexible films. *Lab Chip* **2010,** *10* (11), 1365-1386.

45. Mark, D.; Haeberle, S.; Roth, G.; von Stetten, F.; Zengerle, R., Microfluidic lab-on-a-chip platforms: requirements, characteristics and applications. *Chem. Soc. Rev.* **2010,** *39* (3), 1153-1182.

46. Zhou, J. W.; Ellis, A. V.; Voelcker, N. H., Recent developments in PDMS surface modification for microfluidic devices. *Electrophoresis* **2010,** *31* (1), 2-16.

47. Lin, W. Y.; Wang, Y. J.; Wang, S. T.; Tseng, H. R., Integrated microfluidic reactors. *Nano Today* **2009,** *4* (6), 470-481.

48. Faure, K., Liquid chromatography on chip. *Electrophoresis* **2010,** *31* (15), 2499-2511.

49. Kleparnik, K.; Bocek, P., Electrophoresis today and tomorrow: helping biologists' dreams come true. *Bioessays* **2010,** *32* (3), 218-226.

50. Tran, N. T.; Ayed, I.; Pallandre, A.; Taverna, M., Recent innovations in protein separation on microchips by electrophoretic methods: An update. *Electrophoresis* **2010,** *31* (1), 147-173.

51. Li, Y.; Lee, M. L., Biocompatible polymeric monoliths for protein and peptide separations. *J. Sep. Sci.* **2009,** *32* (20), 3369-3378.

52. Baker, C. A.; Duong, C. T.; Grimley, A.; Roper, M. G., Recent advances in microfluidic detection systems. *Bioanalysis* **2009,** *1* (5), 967-975.

53. Harel, E., Lab-on-a-chip detection by magnetic resonance methods. *Prog. Nucl. Magn. Reson. Spectrosc.* **2010,** *57* (3), 293-305.

54. Sikanen, T.; Franssila, S.; Kauppila, T. J.; Kostiainen, R.; Kotiaho, T.; Ketola, R. A., Microchip technology in mass spectrometry. *Mass Spectrom. Rev.* **2010,** *29* (3), 351-391.

55. Borecki, M.; Korwin-Pawlowski, M. L.; Beblowska, M.; Szmidt, J.; Jakubowski, A., Optoelectronic Capillary Sensors in Microfluidic and Point-of-Care Instrumentation. *Sensors* **2010,** *10* (4), 3771-3797.

56. Cheong, R.; Paliwal, S.; Levchenko, A., High-content screening in microfluidic devices. *Expert. Opin. Drug Discov.* **2010,** *5* (8), 715-720.

57. Il Park, J.; Saffari, A.; Kumar, S.; Gunther, A.; Kumacheva, E., Microfluidic Synthesis of Polymer and Inorganic Particulate Materials. In *Annual Review of Materials Research, Vol 40*, Annual Reviews: Palo Alto, 2010; Vol. 40, pp 415-443.

58. Clerc, O.; Greub, G., Routine use of point-of-care tests: usefulness and application in clinical microbiology. *Clin. Microbiol. Infect.* **2010,** *16* (8), 1054-1061.

59. Staples, M., Microchips and controlled-release drug reservoirs. *Wiley Interdiscip. Rev.-Nanomed. Nanobiotechnol.* **2010,** *2* (4), 400-417.

60. Liu, K. K.; Wu, R. G.; Chuang, Y. J.; Khoo, H. S.; Huang, S. H.; Tseng, F. G., Microfluidic Systems for Biosensing. *Sensors* **2010,** *10* (7), 6623-6661.

61. Li, L.; Ismagilov, R. F., Protein Crystallization Using Microfluidic Technologies Based on Valves, Droplets and SlipChip. In *Annual Review of Biophysics, Vol 39*, Annual Reviews: Palo Alto, 2010; Vol. 39, pp 139-158.

62. Rosen, Y.; Gurman, P., MEMS and Microfluidics for Diagnostics Devices. *Curr. Pharm. Biotechnol.* **2010,** *11* (4), 366-375.

63. Ng, A. H. C.; Uddayasankar, U.; Wheeler, A. R., Immunoassays in microfluidic systems. *Anal. Bioanal. Chem.* **2010,** *397* (3), 991-1007.

64. Sun, T.; Morgan, H., Single-cell microfluidic impedance cytometry: a review. *Microfluid. Nanofluid.* **2010,** *8* (4), 423-443.

65. Wu, M. H.; Huang, S. B.; Lee, G. B., Microfluidic cell culture systems for drug research. *Lab Chip* **2010,** *10* (8), 939-956.

66. Lee, W. G.; Kim, Y. G.; Chung, B. G.; Demirci, U.; Khademhosseini, A., Nano/Microfluidics for diagnosis of infectious diseases in developing countries. *Adv. Drug Deliv. Rev.* **2010,** *62* (4-5), 449-457.

67. Velve-Casquillas, G.; Le Berre, M.; Piel, M.; Tran, P. T., Microfluidic tools for cell biological research. *Nano Today* **2010,** *5* (1), 28-47.

68. Gijs, M. A. M.; Lacharme, F.; Lehmann, U., Microfluidic Applications of Magnetic Particles for Biological Analysis and Catalysis. *Chem. Rev.* **2010,** *110* (3), 1518-1563.

69. Wang, Y.; Chen, Z. Z.; Li, Q. L., Microfluidic techniques for dynamic single-cell analysis. *Microchim. Acta* **2010,** *168* (3-4), 177-195.

70. Maguire, T. J.; Novik, E.; Chao, P.; Barminko, J.; Nahmias, Y.; Yarmush, M. L.; Cheng, K. C., Design and Application of Microfluidic Systems for In Vitro Pharmacokinetic Evaluation of Drug Candidates. *Curr. Drug Metab.* **2009,** *10* (10), 1192-1199.

71. Young, E. W. K.; Beebe, D. J., Fundamentals of microfluidic cell culture in controlled microenvironments. *Chem. Soc. Rev.* **2010,** *39* (3), 1036-1048.

72. Marre, S.; Jensen, K. F., Synthesis of micro and nanostructures in microfluidic systems. *Chem. Soc. Rev.* **2010,** *39* (3), 1183-1202.

73. Lenshof, A.; Laurell, T., Continuous separation of cells and particles in microfluidic systems. *Chem. Soc. Rev.* **2010,** *39* (3), 1203-1217.

74. Le Gac, S.; van den Berg, A., Single cells as experimentation units in lab-on-a-chip devices. *Trends Biotechnol.* **2010,** *28* (2), 55-62.

75. Perrin, D.; Fremaux, C.; Shutes, A., Capillary microfluidic electrophoretic mobility shift assays: application to enzymatic assays in drug discovery. *Expert. Opin. Drug Discov.* **2010,** *5* (1), 51-63.

76. Sung, J. H.; Shuler, M. L., In vitro microscale systems for systematic drug toxicity study. *Bioprocess. Biosyst. Eng.* **2010,** *33* (1), 5-19.

77. Brody, J. P.; Osborn, T. D.; Forster, F. K.; Yager, P., A planar microfabricated fluid filter. *Sens. Actuator A-Phys.* **1996,** *54* (1-3), 704-708.

78. W. M. Haynes ed., *CRC Handbook of Chemistry and Physics*. 91st Edition (Internet Version 2011) ed.; CRC Press/Taylor: Francis, Boca Raton, FL, 2010.

79. Song, H.; Chen, D. L.; Ismagilov, R. F., Reactions in droplets in microfluidic channels. *Angew. Chem. Int. Ed.* **2006,** *45*, 7336-7356.

80. Gunther, A.; Khan, S. A.; Thalmann, M.; Trachsel, F.; Jensen, K. F., Transport and reaction in microscale segmented gas-liquid flow. *Lab Chip* **2004,** *4* (4), 278-286.

81. Chen, D. L.; Li, L.; Reyes, S.; Adamson, D. N.; Ismagilov, R. F., Using three-phase flow of immiscible liquids to prevent coalescence of droplets in microfluidic channels: criteria to identify the third liquid and validation with protein crystallizations. *Langmuir* **2007,** *23*, 2255-2260.

82. Wang, M.; Slaney, T.; Mabrouk, O.; Kennedy, R. T., Collection of nanoliter microdialysate fractions in plugs for off-line in vivo chemical monitoring with up to 2 s temporal resolution. *J. Neurosci. Methods* **2010,** *190* (1), 39-48.

83. Baroud, C. N.; Gallaire, F.; Dangla, R., Dynamics of microfluidic droplets. *Lab Chip* **2010,** *10* (16), 2032-2045.

84. Teh, S. Y.; Lin, R.; Hung, L. H.; Lee, A. P., Droplet microfluidics. *Lab Chip* **2008,** *8* (2), 198-220.

85. Kralj, J. G.; Sahoo, H. R.; Jensen, K. F., Integrated continuous microfluidic l iquid-liquid extraction. *Lab Chip* **2007,** *7*, 256-264.

86. Castell, O. K.; Allender, C. J.; Barrow, D. A., Liquid-liquid phase separation: characterization of a novel device capable of separating particle carrying multiphase flows. *Lab Chip* **2009**, Advance Article.

87. Roman, G. T.; Wang, M.; Schultz, K. N.; Jennings, C.; Kennedy, R. T., Sampling and electrophoretic analysis of segmented flow streams using virtual walls in a microfluidic device. *Anal. Chem.* **2008,** *80* (21), 8231-8238.

88. Chabert, M.; Dorfman, K. D.; de Cremoux, P.; Roeraade, J.; Viovy, J. L., Automated microdroplet platform for sample manipulation and polymerase chain reaction. *Anal. Chem.* **2006,** *78* (22), 7722-7728.

89. Shackman, J. G.; Watson, C. J.; Kennedy, R. T., High-throughput automated post-processing of separation data. *J. Chromatogr. A* **2004,** *1040* (2), 273-282.

90. Clark, A. M.; Sousa, K. M.; Chisolm, C. N.; MacDougald, O. A.; Kennedy, R. T., Reversibly sealed multilayer microfluidic device for integrated cell perfusion and

on-line chemical analysis of cultured adipocyte secretions. *Anal. Bioanal. Chem.* **2010,** *397* (7), 2939-2947.

91. Clark, A. M.; Sousa, K. M.; Jennings, C.; MacDougald, O. A.; Kennedy, R. T., Continuous-Flow Enzyme Assay on a Microfluidic Chip for Monitoring Glycerol Secretion from Cultured Adipocytes. *Anal. Chem.* **2009,** *81* (6), 2350-2356.

92. Stewart, J. M.; Driedzic, W. R.; Berkelaar, J. A. M., Fatty-acid-binding protein facilitates the diffusion of oleate in a model cytosol system. *Biochem. J.* **1991,** *275*, 569-573.